Chair of Petroleum and Geothermal Energy Recovery

Master's Thesis

Features of thermal and hydraulic calculations in designing of cryogenic pipeline for LNG

Linara Basharova

May 2021

MONTANUNIVERSITÄT LEOBEN
www.unileoben.ac.at

AFFIDAVIT

I declare on oath that I wrote this thesis independently, did not use other than the specified sources and aids, and did not otherwise use any unauthorized aids.

I declare that I have read, understood, and complied with the guidelines of the senate of the Montanuniversität Leoben for "Good Scientific Practice".

Furthermore, I declare that the electronic and printed version of the submitted thesis are identical, both, formally and with regard to content.

Date 12.05.2021

Signature Author
Linara Basharova

Kurzfassung

In der modernen Welt nimmt der Bedarf der Gesellschaft und der Betriebe an Energieressourcen ununterbrochen zu, was den akuten Bedarf an der Vergrößerung der Fördermengen sowie an der Weiterentwicklung der existierenden und der Schaffung neuer Verfahren deren Beförderung zeigt. Da das Gas zum Export in Länder, die Käufer sind, am häufigsten verflüssigt und mit Tankschiffen und Tankcontainern gefördert wird, wie die Welterfahrung zeigt, wird eine Möglichkeit der Einführung der kryogenen Rohrleitung betrachtet. Zur Realisierung des gesetzten Ziels ist es wichtig, ein Paket von Aufgaben gleichzeitig zu lösen. Erstens ist es notwendig, die Analyse der Stoffe durchzuführen, die bei der Arbeit mit Kryomedien verwendet werden können. Zweitens muss die Wärmeisolation die Erhaltung des flüssigen Aggregatzustands des Gases sicherstellen, und dadurch müssen Prozesse des Phasenübergangs und Schaffung der Havariesituationen ausgeschlossen werden. Weiter ist es sehr wichtig, einen Einblick über das Bestehen der Normativbasis zum Entwerfen zu haben, weil sie den Ingenieuren Hauptanforderungen zum sicheren Betrieb der Produktionsobjekte und Basisnormen zum Entwerfen diktiert. Da die Beförderung des verflüssigten Erdgases eine wissentlich gefährliche Maßnahme ist, ermöglicht die Durchführung der hydraulischen Errechnung, sowohl optimale Diameter zur Beförderung vorgegebener Umfänge des Produkts als auch Distanzen einzuschätzen, über die dieses Gas transportiert werden kann.

Abgesehen von Fragen, die mit dem Entwerfen der kryogenen Rohrleitung zur Beförderung des verflüssigten Erdgases verbunden sind, wird die Einführung der Strategie zur Dekarbonisation der in die atmosphärische Luft ausgestoßenen Abgase durch die Beimengung des Wasserstoffs in die Zusammensetzung des verflüssigten Erdgases betrachtet. Zur Sicherstellung des sicheren Betriebs wurde sein Einfluss auf Verbrennungsprozesse und Hydratbildung sowie kritische und physisch-chemische Parameter des Fluidums betrachtet. Die Formulierung dieser Aufgabe wird durch die jährliche Erhöhung der Tarife bedingt, die für Unternehmen festgesetzt werden, die das Erdgas zur Sicherstellung der Arbeitsvorgänge verbrennen. Zudem haben sich die Länder in 2016 verpflichtet, als Ergebnis des Pariser-Abkommens, jährliche Umfänge des Ausstoßes der Treibhausgase zur Minderung der Temperatur der globalen Erwärmung um 3°C zu reduzieren. Die Wasserstoffgewinnung kann durch zwei Hauptprozesse sichergestellt werden: Dampfreformierung des Methans und Elektrolyse.

Die hydraulische Errechnung der kryogenen Rohrleitung wurde im Programmkomplex OLGA von Schlumberege durchgeführt, wo Bedeutungen der Ausgangsdrucke im Bereich sowie erforderliche Dicken der Wärmeisolation gefunden wurden.

Zudem wurde die Errechnung der wirtschaftlichen Effektivität dieses Projekts zur Bildung der Komplexlösung durchgeführt, und eine Reihe von Schlussfolgerungen wurde gezogen, die ermöglichen, die Zweckmäßigkeit der Einführung des Projekts der Beförderung des verflüssigten Erdgases in kryogenen Rohrleitungen einzuschätzen.

Abstract

In the modern world, the society and production needs in energy resources are constantly growing, which shows the urgent necessity to increase production volumes, as well as improve existing ones and create new ways of transportation. Since the exported gas, as world experience shows, is most often liquefied and transported by tankers and tank containers, the possibility of introducing a cryogenic pipeline is being considered. To achieve this goal, it is important to solve several tasks simultaneously. Firstly, it is necessary to analyze a wide range of materials that can be used in cryogenic media without loss of efficiency. Secondly, thermal insulation should ensure the preservation of the liquid aggregate state of the gas, thereby eliminating phase transfer processes and creating emergencies. Further, it is very important to have an understanding of the existence of a regulatory framework for design, as it dictates to engineers the basic requirements for the safe operation of production facilities and the basic standards for design processes. Since LNG transport is a deliberately dangerous activity, carrying out a hydraulic calculation will allow assessing both the optimal diameters for transporting the specified volumes of the substance and the distances to which this gas can be transported.

In addition to issues related to the design of a cryogenic pipeline for LNG transport, the implementation of a strategy to decarbonize exhaust gases into atmospheric air by adding hydrogen to the LNG gas is considered. To ensure reliable operation, its influence on combustion processes and hydrate formation, as well as critical and physicochemical parameters of the fluid, is considered. The setting of this task is due to the annual increase in tariffs that are set for enterprises that burn natural gas to provide work processes. In addition, in 2016, as a result of the Paris Agreement, countries pledged to reduce annual greenhouse gas emissions to reduce global warming temperatures by 3 ° C. The production of hydrogen can be provided by two main processes: steam reforming of methane and electrolysis.

The hydraulic calculation of the cryogenic pipeline was carried out in the program complex OLGA from Schlumberger, where initial pressures in the area were found, as well as the required thermal insulation thicknesses.

In addition, to develop a comprehensive solution, the cost-effectiveness of this project was calculated and many conclusions were drawn to assess the feasibility of implementing the project on LNG transport in cryogenic pipelines.

Table of Content

Page

1 Introduction

British Petroleum conducts an annual study of the global energy market and analyzes changes in imports, exports, consumption, and other parameters. At the moment, fossil energy sources account for about 80-90% of all global consumption, from which the majority is oil, coal, and natural gas. Since the Asian economy is developing rapidly, and therefore a huge amount of fuel is being burned (for example, China uses about 50% of world coal production, and the share of coal in Japan's energy mix is 32%), the process of substitution for a greener type of fuel is gradually taking place - natural gas. This strategy is also typical for other countries, since each year environmental safety requirements are constantly tightened, and production nerds for more energy-efficient fuel are steadily growing.

Thus, according to the results of the annual report, according to the "BP Statistical Review of World Energy 2020," there is an increase in exported and imported LNG fuel, the dynamics of which are shown in Figure 1.

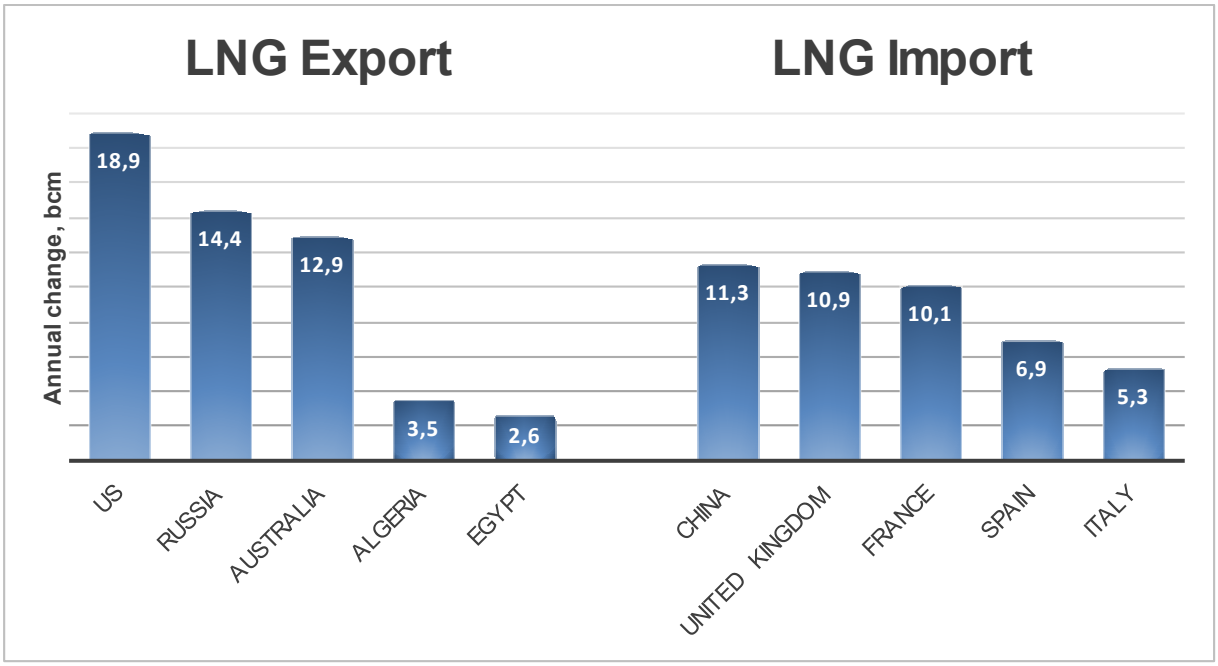

Figure 1: Annual growth of LNG import and export, bln.m

Source: https://www.bp.com/content/dam/bp/business-sites/en/global/corporate/pdfs/energy-economics/statistical-review/bp-stats-review-2020-full-report.pdf, assessed 20.09.2020

Currently, Russia exports gas in several areas. "Nord Stream" ensures the transit of natural gas to Europe through two main lines which capacity is about 27.5 bln.m^3/year of each line. The piping diagram is shown in Figure 2. The length of both lines of gas pipelines exceeds 1200 km. The city of Ust-Luga is the starting point (or entry point) of the pipeline into the Baltic Sea, at the bottom of which it stretches until it reaches the final point - the city of Greifswald. Further, to ensure the uninterrupted supply of gas not only to Germany but also to European countries, the Nord Stream pipeline connects the German NEL and OPAL gas pipelines. The first one delivers blue fuel towards Western and Northern Europe, the second one towards

Central and Southern Europe. The existence of the "Nord Stream" allowed European countries to reduce natural gas production in the above regions, create new jobs for EU citizens, and also receive energy at a relatively lower cost (Zhizin & Timohov, 2019).

Figure 2: Piping scheme of "North Stream-2"

Source: https://www.rubaltic.ru/news/26032020-handelsblatt-poslednee-slovo-v-borbe-za-severnyy-potok-2-ostalos-za-nemetskim-regulyatorom/, assessed 25.09.2020

The second-largest project for the export of blue fuel is the "Turkish Stream", which is intended to supply Europe with natural gas bypassing the territory of Ukraine. It was decided to build two lines of main gas pipelines with a total capacity of 15.75 bln.m^3/year. Mainly, the pipeline will be laid underwater at the bottom of the Black Sea (910 km long). The total length will be 1080 km. This project is still unrealized due to existing political and economic differences. The map of planned pipelines is shown in Figure 3.

Gas projects to Europe and Turkey will not only provide European countries with better conditions for the purchase of gas (compared to the purchase of shale gas from the United States) but also provide the population of Turkey with Russian gas and increase potential channels for the supply of blue fuel to Europe.

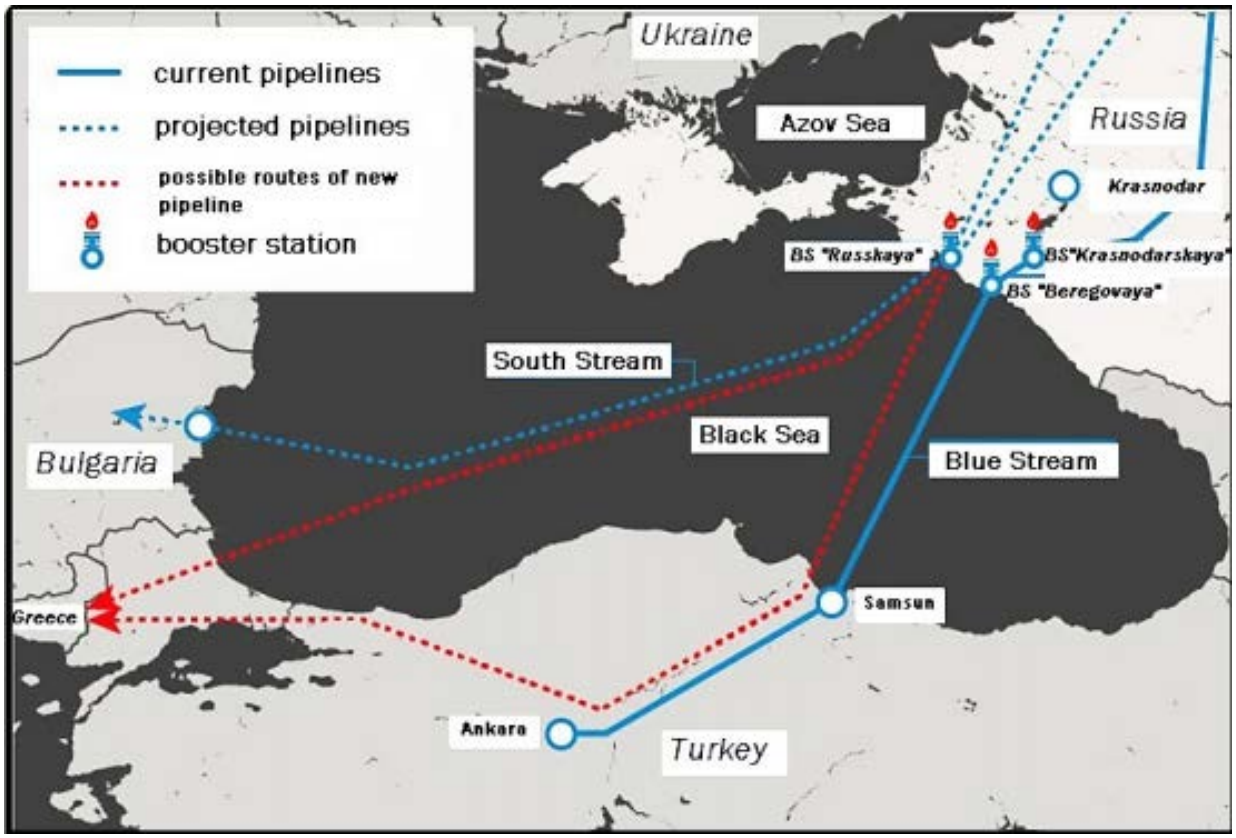

Figure 3: Piping scheme of "Turkish Stream" (Ponomareva et al., 2017)

The "Power of Siberia" project, which is in the final stage of construction, is designed to provide China with natural gas. The construction was divided into 3 stages. At the first stage, a pipeline was laid from the Chayandinskoye field (Yakutia) to Blagoveshchensk bordering China (the length of the site is 2200 km). Then, the second stage provided for the construction of 800 km of a section connecting the Kavyktinskoye deposit (Irkutsk region) with Chayandinsky. The last stage is devoted to the power set of the first section (Kozachenko, 2017). Figure 4 shows the planned pipeline layout "Power of Siberia".

Interest in natural gas is due to several reasons. Firstly, in addition to its broad use in production, the composition of natural gas is valuable for its components used in the production of such products as plastics, glass, rubber, fertilizers, solvents, and much more. Secondly, compared to the burning of oil and coal, natural gas has less detrimental effects on atmospheric air (since combustion produces water vapor and CO_2), and the combustion process is simpler and more reliable.

Figure 4: Planned "Power of Siberia" pipeline scheme

Source: https://www.intellinews.com/gazprom-s-power-of-siberia-gas-pipeline-to-china-is-finished-157956/, assessed 24.09.2020

In addition to the above, one of the most significant advantages of natural gas is its delivery directly to the consumer, in any climate and weather conditions.

Currently, two methods of delivering natural gas to the consumer are widely used:

- Pipeline transport;
- Transportation of LNG in tankers, gas carriers, tank containers, etc.

Transportation of liquefied natural gas is more feasible in areas where pipeline construction is difficult or impossible (for example, in the presence of complex terrain such as mountains, swamps, impassable forests, etc.), as well as in reserves and private land holdings. In addition, the construction of main pipeline lines may be hampered by changes in the political situation. LNG transport is the most economical solution and an advanced method of transferring energy since more than 30% of the produced gas is transported in liquefied form. LNG can be transported both over long distances (during large-capacity transportation) and over short distances with small volumes of the transported product (Tsvetkov & Pritulyak, 2018).

Currently, LNG production is divided into three varieties of natural gas liquefaction complexes: large-tonnage (at the moment, there are two complexes in the Russian Federation within the framework of the Sakhalin 2 and Yamal LNG project, which are designed to export the product by large-tonnage gas carriers and bunkering ships), medium-tonnage (deployed in the northwestern part of Russia), low-tonnage (currently there are 13 industries in Russia) (Gaponova, 2017).

Export of LNG is an extremely priority area of the Russian gas industry. Until recently, the Sakhalin-2 project was the only LNG production project, however, in 2017 the Yamal LNG plant, the largest producer of natural gas with an annual production of 16.6 bln.m^3, went into operation. The implementation of the project is carried out based on the South Tambey field. LNG is shipped in the port of Sabetta (which houses shipping racks with two berths and an ice-class tanker fleet) located near the liquefaction complex. Also, a distinctive feature is the presence of a tanker fleet for Arctic conditions. The port is designed for year-round operation with the possibility of receiving technological and construction cargo. Gas imports under this project are carried out mainly in Asia (11 million tons), India (3 million tons), and Spain (2.5 million tons). A Diagram of LNG delivery in summer and winter time is given in Figure 5. The delivery of liquefied natural gas to the countries of Northeast Asia in the summer period is carried out along the northern sea route, and in the winter - through the LNG transshipment along the western route to ordinary gas carriers after leaving the area characterized by severe weather conditions. Winter transportation is carried out in special tankers of reinforced type Arc7 (20 vessels) and, overcoming the sea route, delivers LNG to the Asia-Pacific region. This reduces transport time by 20% to China, by 32% to South Korea, and by 54% to Japan (Gadinova & Ponomareva, 2015).

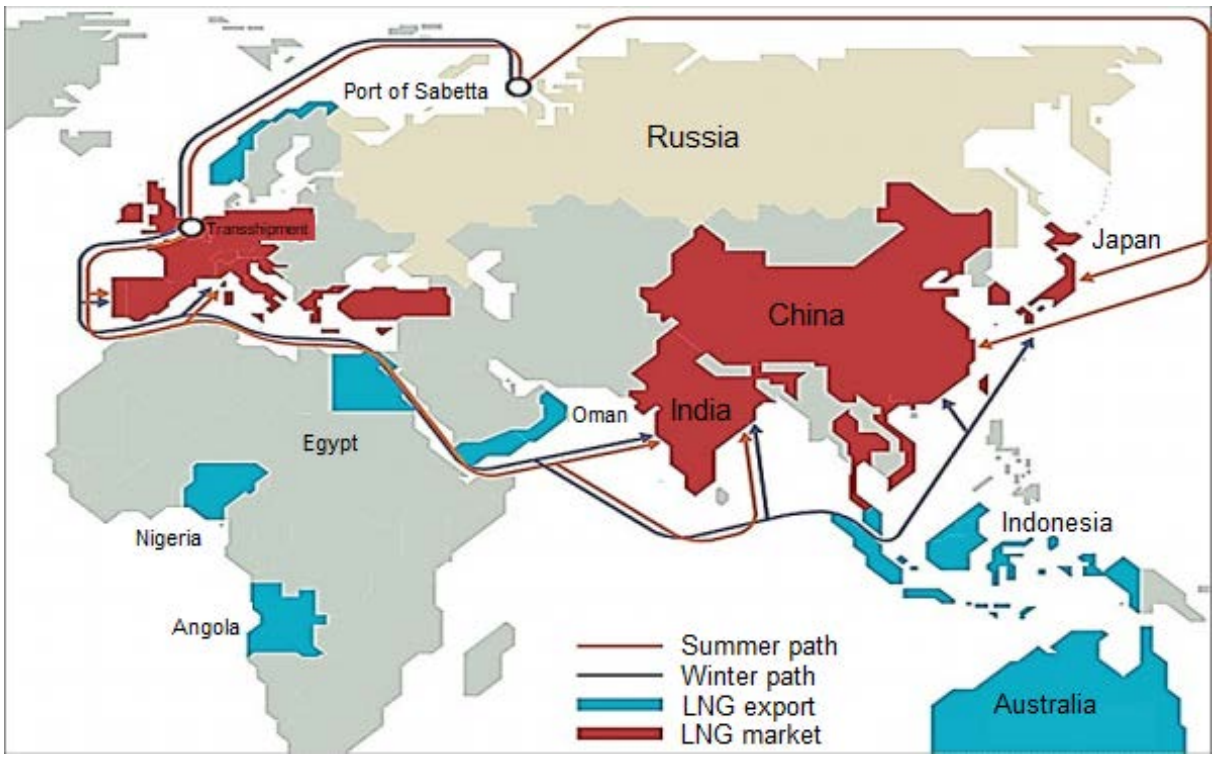

Figure 5: Winter and summer delivery scheme from "Yamal LNG" plant

Source: http://vch.ru/event/view.html?alias=novatek_hochet_postroit_spg-terminal_pod_murmanskom, assessed 25.09.2020

Compared to pipeline construction, LNG transportation requires a large capital cost (since approximately 25% of the natural gas energy is required to carry out the liquefaction process) and infrastructure costs, in addition, the cost of loading and unloading should be taken into

account (Nikolaev & Ganaga, 2011). An approximate ratio of transport costs over different distances is given in Figure 6. Existing experience in operating and transporting natural gas shows that it takes approximately 3,500 routes or 1-3 months to transport equal volumes of product over the same distances.

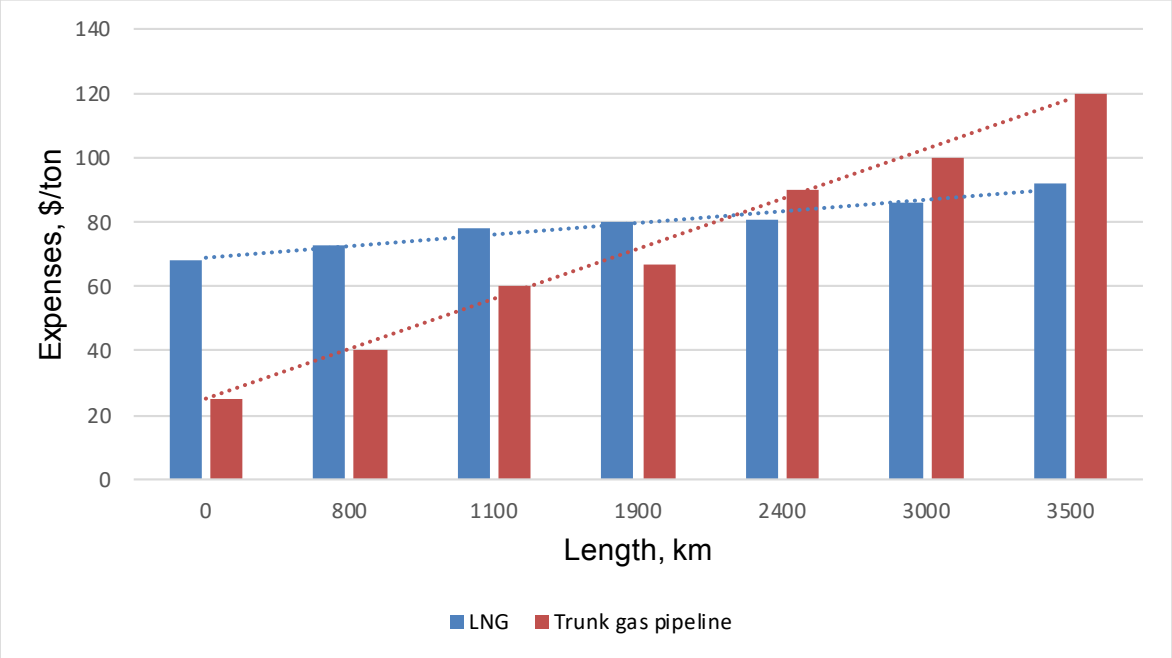

Figure 6: Transportation costs for LNG and pipeline transport (Nikolaev & Dokukin, 2015)

The main advantage of liquefied natural gas is its occupied volume, the value of which is 600 times less than the gaseous state (Nazarova & Voronov, 2017). In addition, one of the most serious disadvantages of gas pipelines is its explosive nature of the transported product, and since combustible gas is inherent exclusively in the gaseous state, the transportation of LNG is more secure if the required modes of transportation and operation are met. Analyzing the advantages of gas pipeline transportation and all known methods of delivering LNG to the consumer, this work considers the feasibility of introducing cryogenic pipelines for LNG transfer to the destination.

The relevance of this topic is because, despite the significant capital costs, the cryogenic pipeline allows transporting LNG without loss of product, to use much smaller diameters at impressive pumping volumes (in comparison with gas pipelines), as well as to exclude economic costs during loading and unloading operations.

The goal of the work is to find another way to deliver liquefied natural gas to places to increase the efficiency of exports of Russian products. Cryogenic piping for LNG transfer can be considered in cases where it is necessary to export gas to places where the laying of the main gas pipeline is impractical or impossible, and transportation of LNG is economically unprofitable.

2 Literature review

2.1 The background of the development of cryogenic liquids transportation

Interest in the construction of a cryogenic LNG pipeline arose already in 1980 of the XX century: the countries of the former USSR, Canada, the USA, and Europe conducted studies on the possibility of transporting LNG by pipeline, however, due to the lack of a regulatory framework, this project has not been implemented since this day. The position of LNG in the global economy is increasing every year, so the search for safe and reliable solutions is increasingly being conducted.

In 1968, a 6-inch pipeline transporting liquefied oxygen from a liquefaction plant to an experimental engine already existed in the United States. The distance between points A and B was 2.2 km.

Since the 1970s, Russia has been interested in LNG trunk transport, studies have been carried out on possible problems that make it difficult to build LNG pipelines (Aleksandrov, 1971), the main parameters of its transfer were considered, and also the most suitable materials were examined (Ivantsov, 1976).

For example, for more than 50 years, several pipelines have been located in the United States that transport cryogenic liquids, such as nitrogen and oxygen. The diameter of each product pipeline is 150 mm with the length of transported section 450 m.

In 1976, a surface 6-mile section of the cryogenic LNG pipeline was built from the Brunei LNG plant, Borneo to the marine LNG tank. Its outer diameter is 18 inches (Deason, 1976).

In 2002, a 9 km underwater LNG pipeline sponsored by Total was successfully tested. The main difference was the location since previously preference was given to laying on artificial overpasses.

By the end of 2004, one of the most interesting hydrocarbon liquid transport projects was the Camisea project, located in Peru. The idea was to combine gas that enters the liquefaction plant from the field, and then, already in a liquefied state, enters the tanker. The capacity of the liquefied gas pipeline is 50,000 barrels per day, and its total length is 540 km (from the Kamisea field to the liquefaction plant near Pisco, located on the Pacific coast). The layout of the field and piping is shown in Figure 7.

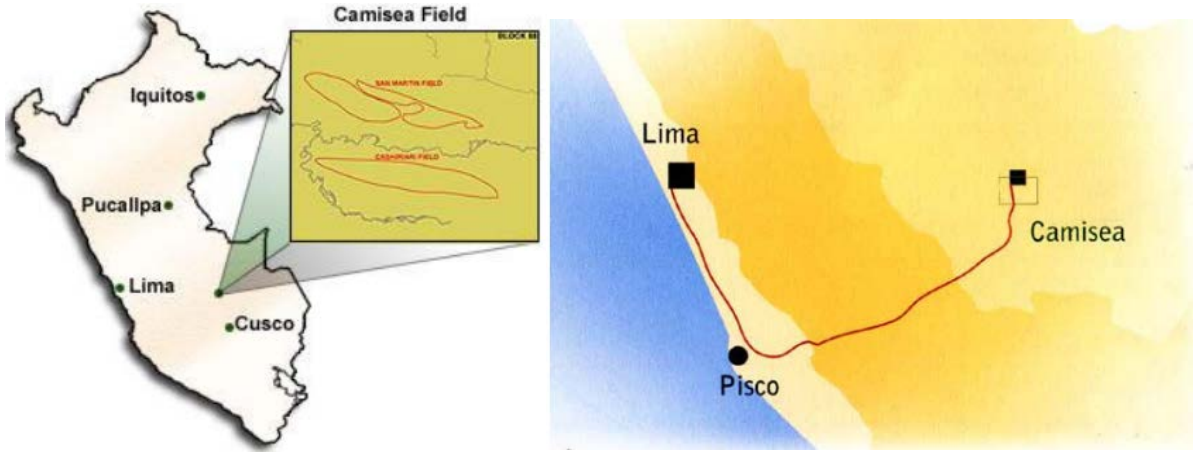

Figure 7: Location of Camisea field and pipeline to the liquefaction plant (Gelder, 2003)

In January 2015, a project describing the construction of a liquefied ethane pipeline with a total length of 486 km and originating in RIL's Dahej Manufacturing Division (DMD) became available. The endpoint is RIL's Nagothane Manufacturing Division (NMD). The pipe profile is shown in Figure 8.

The most developed transport of liquefied hydrocarbons over long distances is located in the United States. One of them is a 1,770 km main pipeline from Houston, Texas, to Danville, Virginia. In addition, there is a 400 km liquefied gas and light oil pipeline originating in the city of Wood River and ending in Chicago.

Pipelines for the transport of liquefied gases have also been laid in Russia. So, the Tuymazy-Ufa gas pipeline was built, which transports liquefied gas for 172 km (with a diameter of 250 mm) and is designed to supply several gas filling stations (gas stations for propane-butane fuel).

The Minnibaevo-Kazan pipeline annually pumps 400 mln.m^3, its length is 300 km (diameter 275 mm) and provides fuel supply from the Gas Processing Plant to the “KazanOrgSynthesis” plant of organic synthesis.

Analyzing the production interest on the example of the considered and existing projects on the transport of cryogenic liquids, one can judge the relevance of LNG pipeline transport, the implementation of which to this day provokes controversy and discussion. It is worth noting that at the time of writing this work, there is no main pipeline transport LNG.

2.2 Requirements for construction of cryogenic fluid pipelines

Even though LNG transport is carried out in many ways (railway transport in tank cars and cars loaded with cylinders; road transport in motor vehicles, tank-containers; sea and river transport in tankers and container vessels, as well as air transport), LNG pipeline transport is possible in terms of feasibility.

Previously, LNG transportation through cryogenic pipelines was used for only one purpose - transportation of liquefied methane for domestic needs, such as:

- Connection of facilities for the production of liquefied oxygen, nitrogen, helium, methane, argon, etc.;
- Connection of cryogenic liquid storages to the vehicle;
- Connection of cryogenic equipment to the consumer.

Cryogenic pipelines can be flexible (for filling vehicles), stationary (with polymer thermal insulation), stationary non-detachable, and detachable (Pavlov & Schippl, 2008). Cryogenic stationary non-disassembly piping with several types of thermal insulation will be considered in this work. LNG transfer flow diagram is given in Figure 9.

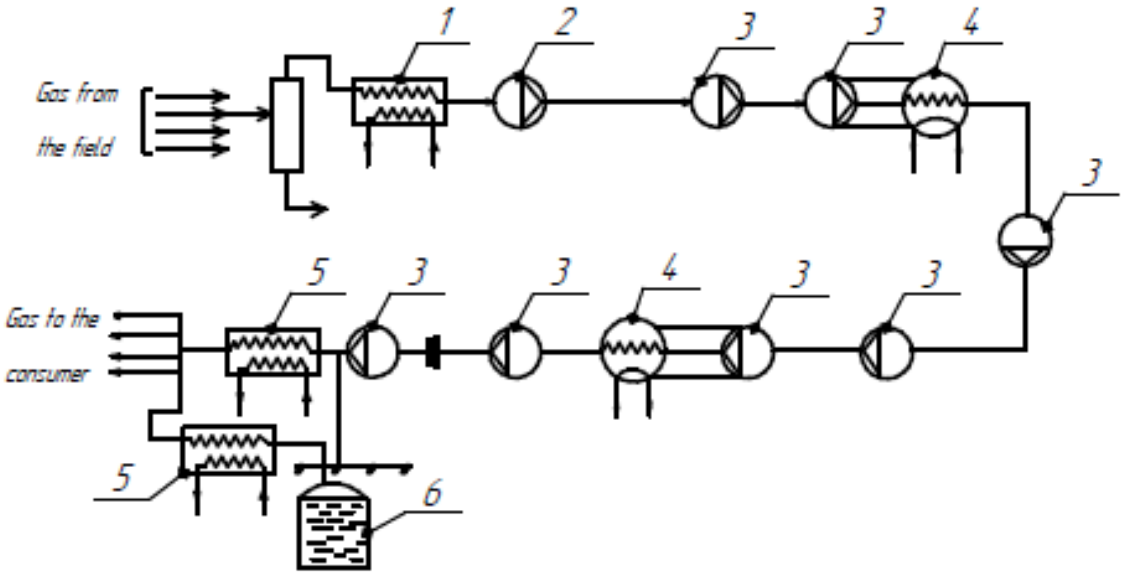

Figure 8: LNG Cryogenic Piping Flow Diagram (Bleyher, 1977)

Where, 1 – Main liquefaction plant, 2 – main pumping station, 3 – booster pumps, 4 – intermediate cooling station, 5 – regasification unit, 6 – low-temperature storage of LNG).
All processes of the proposed scheme (such as liquefaction of natural gas, an increase of LNG pressure in pumping units, transportation through cryogenic pipelines, storage in above-ground or underground storage facilities of different structures, as well as the gasification process) have long been studied and mastered. Transportation of LNG will give an environmental and economic effect. Firstly, compared to conventional gas pipelines, LNG transport will reduce the number of lines of gas pipelines from 4 to 1 LNG line. This means that it is possible to reduce the specific gravity of pipe steel and achieve economic benefits.

Russian Patent No. 2018125984 "Cryogenic Pipeline" presents the design of a cryogenic pipeline with a temperature compensator and monitoring systems (vacuum, temperature, and pressure control). Figure 10 shows a general view of the proposed design.

The supports 5 serve to maintain the coaxial of the pipes and are designed to allow sliding along the axis of the pipe to compensate for thermal changes in length. When liquefied gas enters the annulus, the sorption process occurs due to basket 6.

In the event of an emergency, such as a surface blowhole, a crack, etc., in the space of product line 1, liquefied natural gas enters the interior of casing 3, after which, due to the pressure increase, valve 8 operates to ensure the safety of the external pipe structure and the environment.

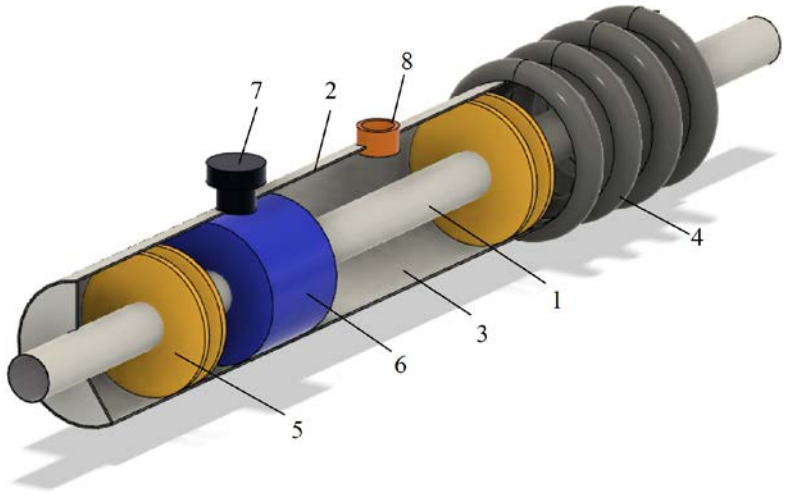

Figure 9: Cryogenic pipeline design (Mnushkin & Nikitin, 2018)

Where, 1 – internal pipe (product line); 2 – external pipe (casing); 3 – vacuum area; 4 – temperature compensator; 5 – supports; 6 – basket with adsorbing agent; 7 – vacuum generator valve; 8 – relieve valve.
The selection of the pipe material must be based on the execution of several characteristics simultaneously:

- Efficiency and stability under conditions of cryogenic temperatures температур (up to 200℃);
- Preservation of characteristics along the entire length of the pipeline sections, reliability, and safety.
- High strength characteristics;
- Eliminating the likelihood of fragile destruction.

At the time of writing, there are 4 most efficient cryogenic pipeline designs (it's material and thermal insulation). A description of the described structures is given in Table 1. The most expensive in terms of capital costs is design type №3, the lowest costs will be in design №1. The operating costs of each design type are at the same level.

Table 1: Most common and effective design structures of the cryogenic pipeline (Voronov & Martynenko, 2017)

Type №	Steel grade	Thermal insulation material
1	12Ch18N10T (or its analogue)	Screen-vacuum
2	Steel according to the standard ASTM A553,	Aerogel
3	36Ni (invar)	Aerogel/ Screen-vacuum
4	Steel according to the standard ASTM A553 / 36Ni (invar)	Polyurethane

The main type of pipe metal is chromium-nickel alloys, which are distinguished by corrosion-resistant properties, as well as possible operation in a wide range of temperatures. The ductility and viscosity of such pipes retain their performance even under cryogenic pumping conditions. Table 2 shows the main disadvantages of these materials and how they can be solved.

For further thermal and hydraulic calculations, it is necessary to know the isobaric heat capacity, thermal conductivity, and density of each pipeline material. The values of the above parameters are given in Table 3.

Table 2: Main disadvantages of nickel-chrome alloys and possible ways to resolve it (Blinov et al., 2003)

The essence of the disadvantage	Possible solution
High costs	Reduction of Ni value due to use of Mn
Low strength	N_2 adding into the material composition in order to improve austenite performance

Table 3: Thermal conductivity, capacity, and density of the pipe materials

	Conductivity, W/(m·°C)	Capacity, J/(kg·°C)	Density, kg/m^3
12Ch18N10T	15	462	7920
Standard ASTM A553	13	470	7800
36Ni (invar)	10,15	515	8050

Since materials comprising Ni are extremely expensive and difficult to access, polymeric materials can be used to make the pipeline. For example, ultra-high molecular weight polyethylene has high specific strength characteristics. Polyethylene pipes are more resistant

to deformation; this is proved by the experience carried out at long-term uniaxial load of the material under conditions of low temperatures (no lower than -80℃). As a result, the yield stress increased proportionally as the temperature decreased (Anoshkin et al., 2014).

Based on the results of the study, it can be concluded that a competent choice of material is an obligatory component in the design of a cryogenic pipeline, however, one of the main problems is high-quality thermal insulation, without which it is impossible to transfer cryogenic liquid.

2.3 Requirements for thermal insulation of cryogenic pipelines

The choice of thermal insulation type should be based on several requirements: be effective in terms of heat loss, reliable and durable, as well as meet fire and environmental safety requirements. There are 4 most effective categories of thermal insulation for cryogenic pipelines, which allows transporting cryogenic liquids without heat losses:

- Screen-vacuum insulation;
- Rigid materials (fiber glass, mineral wool, and so on);
- Powder (perlite, aerogel);
- Foamed polymers (polyurethane foam, foamed rubber) (Rachevskiy, 2009)

Materials used as thermal insulation shall have low thermal conductivity (not higher than 0,232 Вт/(м·К)), shall not absorb moisture. In addition, the thermal insulation density must be as low as possible (e.g. for fibrous thermal insulation types not exceeding 450 kg/m^3, for powders not exceeding 130 kg/m^3) (Kopko, 2002).

2.3.1 Screen-vacuum thermal insulation

The design of screen-vacuum thermal insulation (SVTI) consists of many screens (made of aluminum or copper foil, aluminum mylar), which alternate with layers of fibrous gaskets with low conductivity (glass fiber, nylon mesh, glass paper). All layers are placed in a vacuum that does not exceed 0,0012 Pa (Koshelev et al., 2019). For the SVTI diagram refer to Figure 11. The layer of fibrous material is most often 0.8 mm, and the inner layers of foil are 0.15 mm, and, as a rule, the number of foil layers is usually 40-60. Figure 12 shows the structure of the screen-vacuum thermal insulation layer.

The effectiveness of this type of thermal insulation depends directly on the structure, type, and thickness of the screen materials and the fibrous layers between them. In addition, the importance of vacuum has a huge impact.

One of the main features of the thermal insulation under consideration is that at a certain density of the screen and glass fiber layers, the thermal resistance value of the thermal insulation does not increase.

The disadvantages of SVTI are its extremely high cost (cap. costs), as well as narrow directionality and low resistance to wind loads (which can lead to containment depressurization).

The most important advantages of SVTI are its following characteristics:

- Heat losses are 13-16 times lower (compared to foam and fiberglass thermal insulation). Such savings are equivalent to several million per year. Such low heat losses are associated with a low convection coefficient (close to zero), which is achieved due to the presence of a vacuum;
- Low operation costs;
- Long service life (no need to repair or replace thermal isolation);
- Lightness, compactness, and safety of the structure (due to the presence of a case made from stainless material).

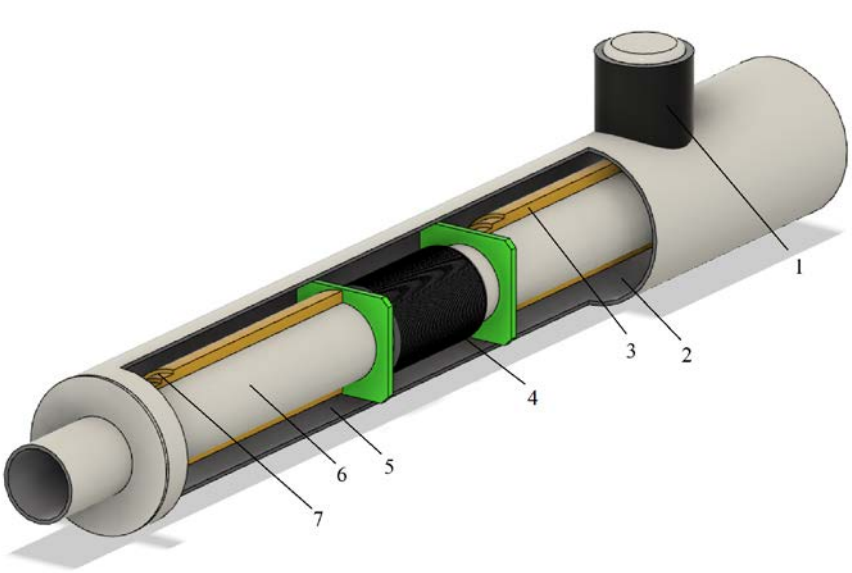

Figure 10: Schematic diagram of screen-vacuum thermal insulation (Motigin, 2015)

Where, 1 – vacuum port, 2 – a cavity in the vacuum insulation, 3 – adsorbents, 4 – bellow valve, 5 – vacuum casing, 6 – production line, 7 – multi-layer screen-vacuum insulation.

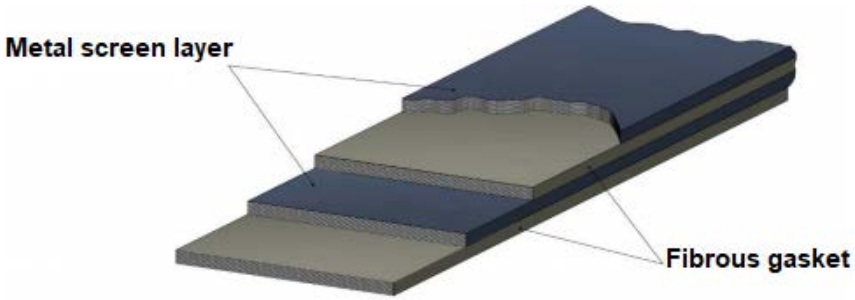

Figure 11: Structure of the screen-vacuum heat insulation layer (Sarkisov et al., 2019)

Since the pipeline, carrying cryogenic liquids, is in extremely unfavorable conditions for insulation material in operating mode, it is necessary to provide a structure that can compensate for the temperature elongations and prevent the vacuum insulation tube from breaking. To solve the problem, it was proposed to install a U-shaped compensator between the product pipeline and the outer casing made of stainless steel, the diagram of which is shown in Figure 13.

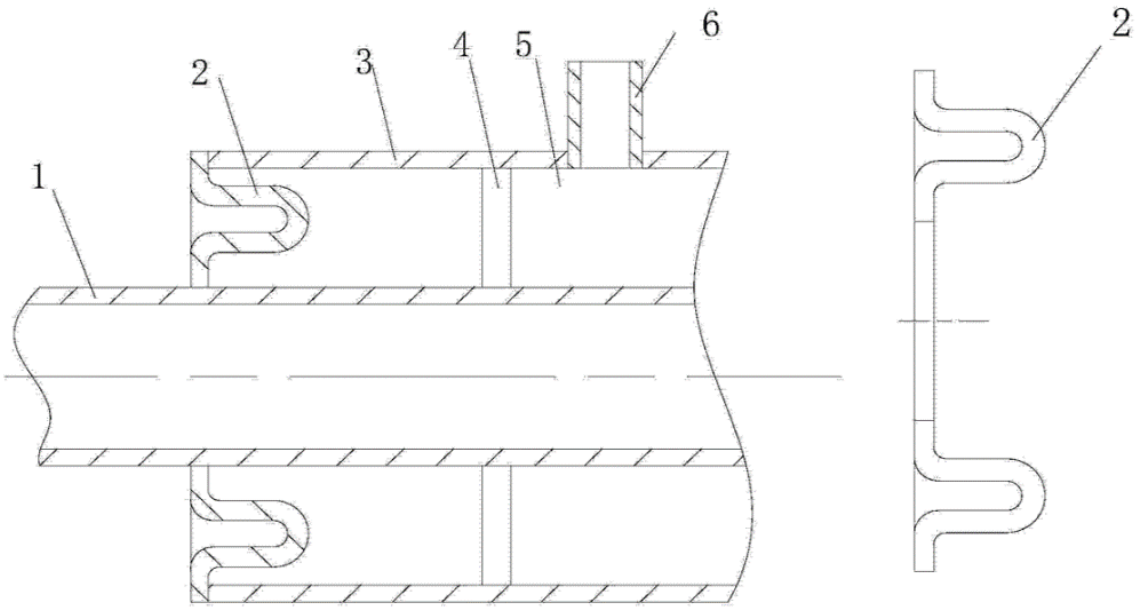

Figure 12: Improved SVTI design (Liang et al., 2015)

Where 1 is the interior pipe, 2 – U-shaped vacuum insulation tube end, 3 - outer pipe, 4 – support, 5 – insulated area, 6 – vacuum nozzle.

2.3.2 Multilayer thermal insulation based on rigid materials

Multilayer construction is the most inexpensive and easy to use. However, its effectiveness is slightly different from SVTI and aerogel. Improved heat efficiency is achieved by improving and modifying existing structures.

Thus, Russian Patent No. 2013108897 "Cryogenic Pipeline" proposes to supplement the existing structure of multilayer thermal insulation with special "holes" that separate the outer layer. Cord made of fibrous heat-insulating material is tightly wound into the "hole". The proposed design is relevant because the layers of cellular thermal insulation (Figure 14), due to the decrease in temperature to cryogenic ones, decrease in diameter, but the presence of fibrous material under them compensates the compression and prevents destruction.

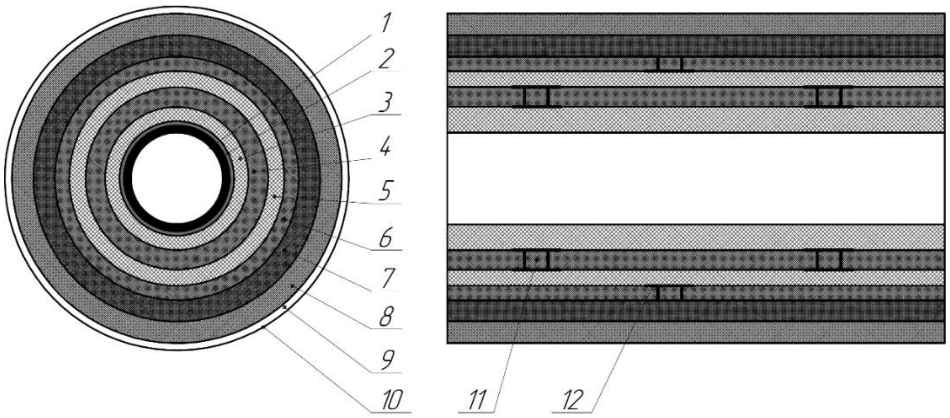

Figure 13: Design diagram of multilayer thermal insulation (Saidal et al., 2013)

Where, 1 - pipeline; 2 - anti-corrosion/anti-abrasive/anti-adhesion layer; 3, 5 are layers of fibrous thermal insulation; 4, 6 are layers of cellular thermal insulation; 7, 8 are additional layers of cellular thermal insulation operating at temperatures close to the environmental ones; 9 - air interlayer; 10 - protective casing; 11 - "holes"; 12 - gas-tight layer.

Layers of fibrous thermal insulation are made of super-thin basalt mats (thermal conductivity coefficient 0.04 W/(m·K)), glass fibers (0.035 W/(m·K)), woolen felt (0.047 W/(m·K)) or slag wool (0.076 W/(m·K)). In fibrous thermal insulation, low mechanical stresses occur while cooling to extremely low temperatures, in addition, it differs in its elastic properties. Because fibrous thermal insulation has high gas permeability, moisture accumulates in the insulation array, deteriorating the thermal insulation properties of the material over time.

The use of cellular insulation eliminates such undesirable effects as water. However, it is strongly compressed and has high values of the coefficient of linear expansion. Made of foam synthetic rubber with thermal conductivity of 0.03 W/(m ·K).

2.3.3 Powder thermal insulation

In terms of powder thermal insulation, perlite and aerogel should be taken into account. Pearlite is produced by thermal treatment of aluminum silicate perlite rock of volcanic origin. Its characteristic feature is the ability to swell during heat treatment (an increase in the volume of 6-20 times from the initial state) (Alekseeva & Natsievskiy, 2002). To obtain a powder structure, pearlite is crushed in crushers, sieved on vibration sieves, dried, and burned in a rotating furnace.

The density of the finished material varies between 40-300 kg/m^3. The efficiency of the thermal insulation properties depends on the radiation parameter. Thus, by increasing the backfill density, the radiant heat exchange value decreases due to the scattering effect. The most rational density limit at which the most efficient thermal conductivity coefficient is achieved is 150-200 kg/m^3 (Kaganer et al., 1962). The main disadvantage is the effect of subsidence, which is inevitable when backfilling a powdered heat insulating material, which, under the influence of its weight and soil vibrations, is compacted. To solve this problem, the pneumatic sealing process can be considered.

Aerogel is a synthetic material with low density, having unique properties, and 99.8% consisting of air. Since the aerogel process is extremely complex and time-consuming, aerogel-based thermal insulation is currently expensive and difficult to access. The process of creating a substance begins with a chemical reaction: the gel (a mixture of silicon, catalyst, and water) polymerizes (molecules with a low molecular weight substance attach to it), then with the help of alcohol (ethanol or methanol) it is necessary to remove as much water as possible from the resulting jelly. The final stage is supercritical drying at high pressures and temperatures. The last stage is the most complex and costly. Due to low porosity, the aerogel has a low coefficient of thermal conductivity. Since a rigid framework in the structure of a substance is required to create a strong and mechanically stable material, tetraethyl silicate (TES), a relatively inexpensive and affordable substance, is most often used (Babashov et el., 2019).

To obtain an aerogel matrix composite, the elastic modulus of which will be high enough, it is necessary to wet woven and non-woven preforms of TES and dry the resulting composition at high pressures and temperatures, the value of which is higher than the critical parameters of alcohol. Then, reaching supercritical parameters, fluid is released from alcohol that behaves simultaneously both as a gas and as a liquid. Thus, the finished sample is rigid and has a high thermal conductivity (Sangeeta & Mukund, 2002).

Similarly, a composite material patented by Hoeschst Actienglessellschaft, Germany, is obtained. After the colloidal solution is prepared and organic or inorganic (mineral wool, glass wool, etc.) fibers are added, the gel-forming step begins. According to the above technology, cracks are controllably created by applying loads in order to give flexibility to the material. The process ends with supercritical drying (Dierk & Andreas, 2005).

Another method of producing an aerogel was described by Aspen Aerogels Company. According to their studies, the fibrous matrix is wetted with TES and immediately dried under supercritical conditions, neglecting the aging processes of the colloidal solution and its gelation. As a result, the resulting material has a structure in which the distribution of the aerogel across the fibrous matrix is more uniform (Jaesoek, 2008). However, the thermal characteristics of the material produced by this technique are significantly lower than those described above.

Further, in 2010, Aspen Aerogels patented material with improved strength characteristics by adding fibrous wool. The execution process is shown in Figure 15. To carry out the process, microfibers (0.1 to 100 μm in diameter) are introduced into the composite by dispersing in TES 1, and then, the fibrous wool 3 is impregnated with the resulting mixture in container 2. After the gelling process, the preform is dried. The building materials in this case areSiO_2, Al_2O_3, TiO_2, ZrO_2, O_2V_5, etc.

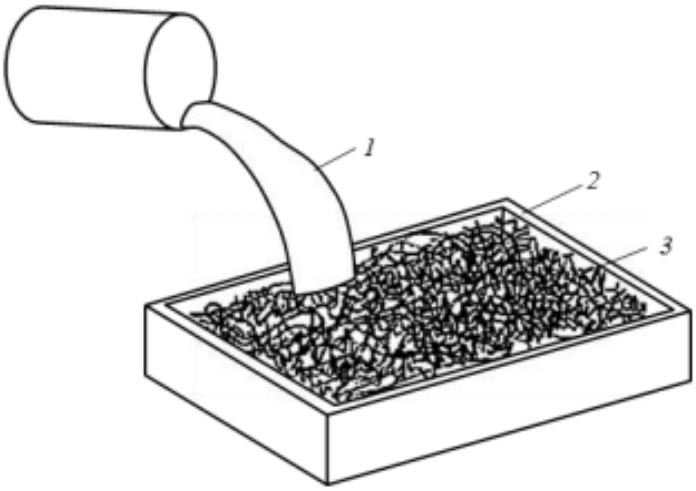

Figure 14: Aspen Aerogels Composite Production Process (Stepanian et el., 2011)

At present, one of the few companies which produce heat-insulating material based on SiO_2 aerogel is Aspen Aerogels. Cryogel Z operates in a wide temperature range from -260 to +90℃. The company's core products and material performance are listed in Figure 16.

	Nominal Thickness		Thermal Conductivity* @ 100F (37.8 C)		Maximum Use Temperature		Typical Applications
	mm	in	mW/m-K	Btu-in/hr-ft²-°F	°C	°F	
Pyrogel® HPS ASTM C1728 compliant	10	0.4	22	0.15	650	1200	Optimized for high temperature hydrocarbon & chemical processing, steam pipes, vessels and equipment, gas and steam turbines, removable blankets
Pyrogel® XTE ASTM C1728 compliant	5 10	0.2 0.4	22	0.15	650	1200	CUI defense, medium to high temperature processes, pipes, vessels and equipment, District Energy steam networks, Aerospace and defense systems
Pyrogel® XTF	10	0.4	22	0.15	650	1200	Passive pool fire and passive jet fire protection for industrial and commercial applications, relief system sizing (API 521)
Cryogel® Z ASTM C1728 compliant	5 10	0.2 0.4	17	0.12	125	257	Sub-ambient and cryogenic pipelines, vessels and equipment, gas liquefaction & re-gasification facilities

Figure 15: The main products based on SiO_2 aerogel of the Aspen Aerogels company and its major characteristics

Source: https://www.aerogel.com/products-and-solutions/product-documents/, assessed 20.10.2020

2.3.4 Foamed thermal insulation

Since rigid types of thermal insulation over time can slightly deteriorate its thermal insulation properties due to the displacement of gases by atmospheric air, the use of thermal insulation based on polyisocyanurate (PIR) is considered. In comparison with the usual polyurethane foam, the technology of creating PIR involves the use of two catalysts. Its structure, which has closed small cells, helps to slow down the diffusion process, thereby increasing its durability and thermal insulation properties. For efficient operation, it is necessary to apply the material

in two layers, and, to reduce losses, glass fiber is used as the sealant. The design of the PIR system is shown in Figure 17.

The thermal conductivity of this material is 0,011 W/m·K. The estimated service life of the material set ISO-C1/2.0 is 50 years. PIR is one of the most affordable thermal insulations.

Thus, today there are already technical solutions to provide reliable and efficient thermal insulation that can ensure the preservation of single-phase flow during LNG pumping through cryogenic pipelines. However, to select a specific type of thermal insulation, it is necessary to carry out a hydraulic and thermal calculation (we will obtain the thickness of the required material), as well as a feasibility study.

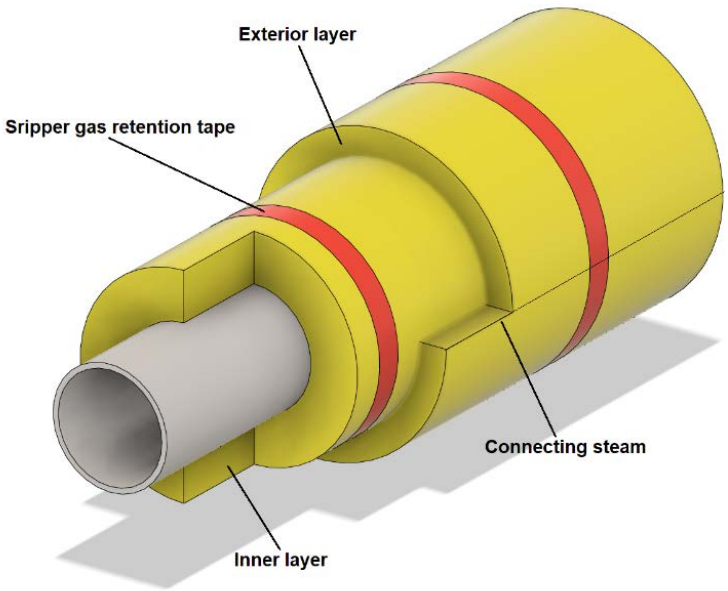

Figure 16: Thermal insulation PIR (Ivanov & Anohin, 2019)

2.4 Features of design and operation of the cryogenic pipeline for LNG transport

In addition to the difficulties that arise at the stage of cryogenic pipeline design (selection of pipe material and insulation, wall thickness, allowable section length, pumping parameters, etc.), there are several factors whose consideration requires special attention.

2.4.1 Analysis of the existing regulatory framework

The absence of a regulatory framework for the design of trunk cryogenic pipelines in the Russian Federation, as well as in Europe, Canada, and the USA is the most serious factor limiting the development and implementation of the suggested idea.

Mechanical strength, structure (material selection, reinforcement, installation, and operation), and industrial safety of pipelines are regulated according to the Safety Guide, as well as GOST 32569-2013 and GOST 32399-2013. Despite the scope of the issues under consideration, these documents do not cover standards for cryogenic pipelines transporting LNG over long distances, do not regulate construction issues at the intersection with railways and roads, as well as public roads and monitoring systems.

By analyzing the regulatory documentation, the purpose of which is to resolve all issues related to the production, storage, and transport of LNG, using the example of VNTP 51-1-88, it can be concluded that they contain requirements only for LNG process pipelines within the production area. Also, the document partially covers the requirements put forward to the master plan of an industrial enterprise, referring to other sources. Product loading and shipping issues are regulated only for the tank truck, requirements for the shipment of fuel to tankers and terminals are not submitted.

The set of rules SP 18.13330.2011 describes the norms for the development of the master plan of the production site. Trunk or process piping issues are not affected.

SP 326.1311500.2017 is devoted to fire safety rules in the design and operation of low-capacity facilities, however, not related to facilities transporting cryogenic liquids. Like the previous source, SP 240.1311500.2015, which guarantees compliance with fire safety requirements of sealed above-ground insulated tanks, is not used for operation with low-tonnage facilities and LNG shipping terminals to tankers.

The closest normative document which is partially covering questions on the design of cryogenic pipelines and having action in the territory of the Russian Federation is industry standard 26-04-1221-75. Although the standard was released in 1992, to this day no updated regulatory bases have been issued. This standard combines a system of requirements in the design of a cryogenic pipeline using screen-vacuum insulation and operating at temperature up to -269 °C and pressure up to 5 MPa. The multi-chapter standard deals with the following issues: regulation of pipe production order (its dimensions and geometry, sequence of strength tests), assembly and welding of sections, insulation application, a requirement for packing, transportation, and storage, as well as thermal insulation (control of its thickness, quality, and sequence of installation).

GOST R 56352-2015 describes the requirements for technological and cryogenic pipelines. Materials used for transportation of cryogenic liquids, as well as structures of pipelines and valves, its placement are considered. Undoubtedly, many issues are covered, but aspects such as the design and equipment of the production site, as well as detailed requirements for the transport of LNG from the tank to the terminal, remain unresolved.

To have a general understanding of the state of the regulatory framework not only in the Russian Federation but also in other countries, an analysis of other sources was carried out. Among them can be distinguished: The United States NFPA standards, the European BS standard, as well as the CSA, which applies in Canada.

The NFPA standard, based on which the Russian GOST 56352-2015 was developed, establishes basic requirements for ensuring the safety of LNG production facilities. It consists of 15 sections and is mandatory for all persons involved in the LNG sector. Its full and identical analog is the standard CSA Z 275-18.

Unlike the standards discussed above, BS EN 1473:2007 is only advisory, but the documents to which it refers are binding. Its scope includes LNG plants, units to cover peak gas demand, and its receiving facilities.

The only existing standard whose scope is to design cryogenic pipelines is ASME B31. One of its sections ASME B31.3 and B31.4 makes recommendations on the most rational design solutions, material selection, stress assessment, etc. It is worth noting that the operation of this standard is limited, this is due to the specifics of the American approach to design, since companies are given wide powers, and the use of project documentation is not limited to the use of one specific document.

Since there is no available regulatory framework for the design of a main cryogenic pipeline, it is necessary to foresee all possible risks arising both during the commissioning phase of the cryogenic pipeline and during its use.

2.4.2 Commissioning of the cryogenic pipeline

2.4.2.1 Blowdown

When putting a cryogenic pipeline into operation, it is important to carry out the process of replacing the air that is located in the interior of the product pipeline with liquefied natural gas. Since this process is explosive and requires particularly careful monitoring and attention, a strategy for its implementation must be envisaged. There are several variants of the procedure for loading liquefied natural gas into the pipeline, which has been widely used in chemical and oil and gas industries:

- Direct mixing of gases (Davidson & Farquharson, 1955);
- Use of separators (plugs) with inert gas.

A differential turbulent diffusion equation can be written to calculate the mixing zones with a relatively small pressure drop and short transfer distances (Nechval & Novoselov, 1965):

$$A\frac{\partial C_B}{\partial \tau} = \frac{\partial^2 C_B}{\partial y^2} \quad \text{(Eq. 1)}$$

$$A = \tilde{\nu} \cdot \left[\widetilde{\mathrm{Pr}}^{-1} + 28,7 \cdot \left(\widetilde{\mathrm{Re}}\sqrt{\overline{\lambda}} \right)^{0,755} \right] \cdot \frac{P_{st.cond.}}{T_{st.cond.}} \cdot T \quad \text{(Eq. 2)}$$

Where A – turbulent diffusion coefficient (m^2/sec); C_B – displacement gas concentration behind the moving coordinate system (m); τ – flow residence time in the pipeline (sec); $\tilde{\nu}$ – average coefficient of kinematic viscosity (N·sec/m^2) of a 50% gas mixture reduced to normal

conditions, Pressure $P_{st.cond.}$ (MPa) and Temperature $T_{st.cond.}$(K); $\widetilde{\Pr}$ – diffusion Prandtl criterion; T – temperature of isothermal flow (K); $\bar{\lambda}$ – coefficient of hydraulic resistance of friction.

$$y = \frac{4}{5} \cdot \frac{P(x)^{5/2} - (P(x)^2 - Ix)^{5/4}}{AI} \quad \text{(Eq. 3)}$$

$$I = \frac{P_1^2 - P_2^2}{L} \quad \text{(Eq. 4)}$$

Where L – the pipeline length (m); P_1 – initial pressure (MPa); P_2 – end pressure (MPa); P(x) – pressure at the origin of the moving coordinate system (MPa).

Since a concentration change occurs at the end of the pipe section, the solution to this equation is:

$$2C_B(L) = 1 + \Phi\left\{\frac{2}{5} \cdot \frac{\left[P_2^2 + \left(P_1^2 - P_2^2\right) \cdot \left(\bar{\tau} - 1\right)\right]^{5/4} - P_2^{5/2}}{P_1^2 - P_2^2} \cdot \sqrt{\frac{WL}{A}}\right\} \quad \text{(Eq.5)}$$

Where Φ – integral of probability $(\Phi(-z) = -\Phi(z)); \bar{\tau} = \frac{\tau}{\tau_0}; \tau_0 = \frac{G_g}{LF\rho_g}$ – time of the filling the pipeline with propellant gas (sec); G_g, ρ_g – mass flow rate and density of the displacing (injected) gas (kg/sec and kg/m^3 respectively); F – the area of the free cross-section of the pipeline (m^2); Wherein, $C_B + C_A = 1$; where C_A – displaced gas concentration; $G_g = G_d$, where, G_d is the displacement gas mass flow behind the moving coordinate system.

Set boundary conditions:

$$\tau < 0;$$
$$C = 0;$$
$$\tau \geq 0;$$
$$x = 0, C = 1;$$
$$x \to \infty, C = 0$$

Based on the conditions of constancy of the average flow rate and diffusion coefficient D_t an analytical solution can be written (Nechval & Yablonskiy, 1964):

$$2c = 1 - erfc\left(\frac{x - Wt}{\sqrt{4D_t\tau}}\right) \quad \text{(Eq.6)}$$

Then, according to the Taylor formula, we find the desired value:

$$D_t = 3{,}51 \cdot WD_{in}\sqrt{\lambda} \quad \text{(Eq.7)}$$

Where D_{in} is the internal diameter of the pipeline (m).

The resulting mathematical model can be used to determine the start time of the explosive mixture and its duration, as well as to determine the volume of the explosive mixture.

Since in practice the opening of the shutoff valves occurs evenly, which affects the process of mixing gases, you can use the "cellular model" method to solve this issue (Sharifullin & Kantukov, 2015):

$$\begin{aligned} &\frac{dC_i}{d\tau} = \frac{n}{\tau} \cdot \left(C_{i-1} - C_i\right); \\ &C(0,\tau) = C_0 = a + b\tau,\ 0 < \tau < T;\ \tau \geq T;\ i = 1,...,n, \end{aligned} \quad \text{(Eq.8)}$$

Where n – number of cells that can be determined from the coupling equation between dimensionless dispersions of the cellular and diffusion models:

$$n = \frac{0{,}283L}{2D_{in}\sqrt{\lambda}} \quad \text{(Eq.9)}$$

2.4.2.2 Equipment cooling

To prevent instantaneous boiling of LNG, it is necessary to ensure that the pipeline is cooled to an intermediate temperature level before it is pumped into the cryogenic pipeline. This will not only prevent explosive processes but also significantly reduce the temperature deformation of the pipe surface.

Assuming that the thermophysical characteristics are constant, the following system of differential equations was used for analysis:

$$\frac{m_1 C_1}{2\pi R_1} \cdot \left(\frac{\partial T_1}{\partial \tau} + W_1 \frac{\partial T_1}{\partial X}\right) = a_1\left[T_2(R_1) - T_1\right] \quad \text{(Eq.10)}$$

$$\begin{cases} \dfrac{\partial T_2}{\partial \tau} = \dfrac{a_2}{r}\dfrac{\partial}{\partial r}\left(r\dfrac{\partial T_2}{\partial r}\right),\ R_1 \leq r \leq R_2, \\ \dfrac{\partial T_3}{\partial \tau} = \dfrac{a_3}{r}\dfrac{\partial}{\partial r}\left(r\dfrac{\partial T_3}{\partial r}\right),\ R_2 \leq r \leq R_3, \end{cases} \quad \text{(Eq.11)}$$

Where, X – axial coordinate (m); r – radial coordinate (m); m – mass per unit length (kg/m); $a = \dfrac{\lambda}{c\rho}$ – thermal diffusivity (m^2/sec), where λ – thermal conductivity (W/(m·K); c – heat capacity (kJ/(kg·K)); 1, 2, 3, “amb” numbers indicates the gas, pipeline wall, thermal insulation, and ambient parameters respectively; “in” indicates the entrance to the pipeline.

The boundary conditions for solving this equation will take the form:

$$\left.\begin{aligned}
&\left(\frac{\partial T_2}{\partial r}\right)_{R_1} = \frac{a_1}{\lambda_2}\left[T_2\left(R_1\right) - T_1\right],\\
&\left(\frac{\partial T_2}{\partial r}\right)_{R_2} = \frac{\lambda_3}{\lambda_2}\left(\frac{\partial T_3}{\partial r}\right)_{R_2},\\
&T_2(R_2) = T_3(R_2),\\
&\left(\frac{\partial T_3}{\partial r}\right)_{R_2} = \frac{a_3}{\lambda_3}\left[T_0 - T_3(R_3)\right],\\
&T_1(0,\tau) = T_{in},\\
&T_i(r,X,0) = T_{amb}
\end{aligned}\right\} \qquad \text{(Eq.12)}$$

The solution to this problem is possible only in an approximate way, using the integral Laplace-Carson transform (Odishariya, 1980). It has been found that when the following conditions are met, the nature of the change in the temperature of the pipeline wall is more affected by its heat capacity (most characteristic of cryogenic pipelines with screen-vacuum thermal insulation).

To simplify the above problem, the thermal conductivity equation of the wall is replaced by the thermal balance equation. Then, the equation takes the form:

$$\left.\begin{aligned}
&-\frac{m_2 c_2}{2\pi R_1}\frac{\partial T_2}{\partial \tau} = a_1(T_2 - T_1),\\
&\frac{m_1 c_1}{2\pi R_1}\left(\frac{\partial T_1}{\partial \tau} + W\frac{\partial T_1}{\partial x}\right) = a_1(T_2 - T_1),\\
&T_1(0,\tau) = T_{in},\, T_2(x,0) = T_{amb.}
\end{aligned}\right\} \qquad \text{(Eq.13)}$$

The solution to such a problem is not unknown, so the equation takes the form (Serov & Korolkov, 1972):

$$\left.\begin{aligned}
&\Theta_2(\chi,t) = M_1(\chi,t) - M_0(\chi,t),\\
&\Theta(\chi,t) = M_1(\chi,t).
\end{aligned}\right\} \qquad \text{(Eq.14)}$$

The description of the obtained components:

$$M_0(\chi,T) = I_0\left(2\sqrt{\chi t}\right)\exp(-\chi - t); \qquad \text{(Eq.15)}$$

$$M_1(\chi,t) = \sum_{n=0}^{\infty}\sum_{k=0}^{n}\frac{t^n \chi^k}{n!k!}\exp(-\chi - t); \qquad \text{(Eq.16)}$$

$$\chi = 4\bar{L}St\bar{x}; \qquad \text{(Eq.17)}$$

$$t = \frac{2a_1 \pi R_1}{m_2 c_2} \tau - \frac{m_1 c_1}{m_2 c_2} \chi; \quad \text{(Eq.18)}$$

$$\bar{L} = \frac{L}{2\pi R_1}; \quad \text{(Eq.19)}$$

$$\bar{x} = \frac{X}{L}; \quad \text{(Eq.20)}$$

$$\Theta_1 = \frac{T_0 - T_i(x)}{T_0 - T_{in}}. \quad \text{(Eq.21)}$$

Where, $St = \frac{a_1 \pi R_1}{G_1 c_1}$ – Stanton criterion; $G_1 = \rho_1 W_1 F_1$ – the mass flow of coolant (kg/sec); $I_i\left(2\sqrt{\chi t}\right)$ – Bessel functions.

Further, representing the modified Bessel function and Eq.14 converging rows, we get:

$$I_0(z) = \sum_{\upsilon=0}^{\infty} (-1)^{\upsilon} \frac{\left(\frac{z}{2}\right)^{2\upsilon}}{(\upsilon!)^2}; \quad \text{(Eq.22)}$$

$$\exp(\nu) = \sum_{\upsilon=0}^{\infty} \frac{\nu^{\upsilon}}{\upsilon!} \quad \text{(Eq.23)}$$

Then, based on Eq. 14, we get the equation that characterizes the change in cooling time:

$$\omega = \frac{\int_0^1 [T_0 - T_2(x,\tau)] d\bar{x}}{\int_0^1 [T_0 - T_2(x,\infty)] d\bar{x}} = \frac{1}{4\bar{L}St} [t - M_2(\chi,t)]_{\chi=4LSt} \quad \text{(Eq.24)}$$

$$M_2(\chi,t) = 4\bar{L}StM_0 + (t-\chi)M_1 + \sqrt{\chi t} \cdot I_1(2\sqrt{\chi t}) \quad \text{(Eq.25)}$$

2.4.2.3 Water-hammer effect

The transient process that occurs when the pipeline is filled with the product can lead to geyser effects, undesirable pressure pulsations, and the water-hammer effect. The most typical reason for the occurrence of the water-hammer effect is the short-term (several seconds) closure of the shutoff valves (for example, in the event of an emergency during the refueling of the tanker). The water-hammer effect is highly undesirable because it may result in depressurization of the structure followed by the release of the cryogenic product.

To be able to analyze the changes in quantitative characteristics, we will use Eq. 26 (Suleymanov & Safonov, 2017):

$$\left.\begin{aligned} &\frac{\partial}{\partial\tau}\left(\frac{P}{\rho}\right)+W\frac{\partial}{\partial x}\cdot\left(\frac{P}{\rho}\right)+C_{sound}^{2}\frac{\partial W}{\partial x}=0,\\ &\frac{\partial W}{\partial\tau}+\frac{\partial}{\partial x}\cdot\left(\frac{P}{\rho}\right)+W\frac{\partial W}{\partial x}+\frac{-}{\lambda}\frac{W|W|}{2d_0}=0\\ &\rho=f(P)_T \end{aligned}\right\} \quad \text{(Eq.26)}$$

Where C_{sound} is the sound velocity (m/sec).

On the left limit, the boundary conditions show the process of collecting liquid from the storage using a centrifugal submersible pump, the diagram of which is shown in Figure 18. The coupling of the hydraulic characteristic of the pipeline and the pressure characteristic of the pump is described by Eq.27. (Safonov, 1977).

$$\Delta P(\tau)=P_{in}(\tau)-P_s=\eta_0+\eta_1 G(\tau)+\eta_2 G^2(\tau), \quad \text{(Eq.27)}$$

Where P_s – suction pressure of the pump (MPa); η_i is the numerical coefficients (for example, if we put $\eta_i=0$, the approximation error will increase to 3%).

At the outlet of the submersible pump, a check valve is installed, selected for a pressure equal to 0.9 of the maximum possible (when the gate valve is closed).

On the right limit, the boundary conditions show the hydraulic resistance of the shutoff valves and closing.

In Figure 18, 1 is a pipeline riser; 2 – blowdown valve; 3 – cylindrical group pump; 4 – reservoir of a submersible pump; 5 – bottom drain valve; 6 – pipeline connecting the pump reservoir with the main reservoir; 7 – valve for fluid supply; 8 – tank for storing liquid; 9 – valve for releasing pressure from the reservoir; 10 – bursting disk; 11 – manometer; 12 – safety valve; 13 – gas pipeline connecting the pump reservoir with the main reservoir.

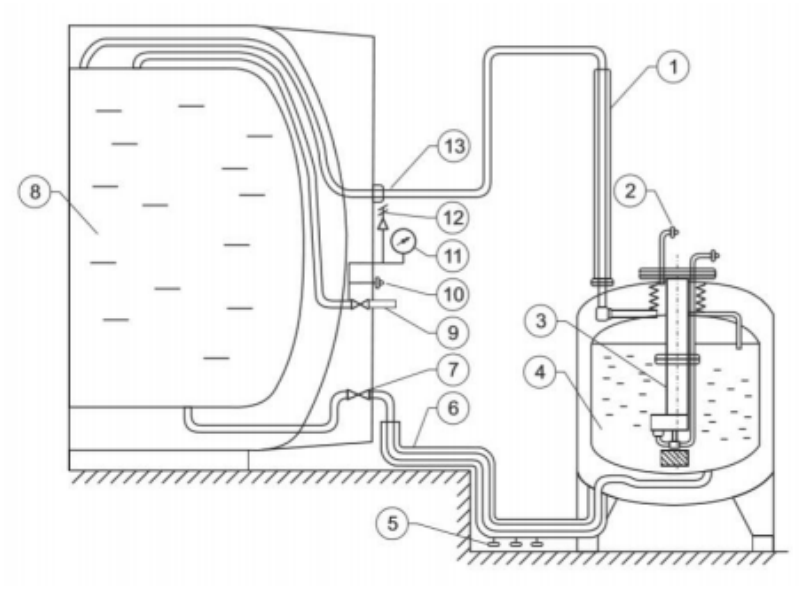

Figure 17: Installation diagram of a centrifugal submersible pump in a tank (Baranov & Sokolova, 2018)

Having solved the system of equations, it can be seen that in the process of the water-hammer effect, the value of waves of pressure amplitude is several times higher than the nominal value. The worst outcome is achieved by abruptly closing the shutoff valves. To reduce pressure pulsations, the best option is to use safety valves and synchronize the signal coming from the actuator of the shut-off device when the pump drive is disconnected (Lyudeke et al., 2015).

2.4.3 Fast phase transition

An equally serious source of danger in the LNG transport is the rapid phase transition (FPT), which causes sharp and explosive evaporation when gas contacts the vapor phase. The volume of the product increases by more than 600 times, and the shock wave has a destructive force and a large radius of damage. FPT is not a chemical phenomenon, since there is no combustion process or accompanying reactions. Most often, LNG loading and shipping terminals, as well as tanker trucks, undergo a fast phase transition.

BFP should be represented as a set of several phenomena:

- Premixing (vapor phase enters liquefied natural gas, but due to different densities, they do not mix, and the resulting steam film leads to a decrease in the level of heat transfer);
- Activation phase, in which the stability of the steam film decreases, which leads to an increase in pressure and an acceleration of heat transfer processes;
- Propagation phase, in which the cold phase absorbs the hot phase;
- The expansion phase, in which the gas-water mixture expands and, counteracting the inertia forces of the surrounding liquid, can lead to huge damage.

The most effective method of forecasting and monitoring is the development of a mathematical model that will allow us to have an idea of the scale of the explosion, its power, and possible damage (Permyakov & Shvets, 2017).

2.5 Features of thermal and hydraulic calculation of cryogenic pipeline

The main difference while pumping liquefied natural gas through cryogenic pipelines is the low product temperature, viscosity, several times less than the viscosity of water, and a high degree of compressibility.

Peculiarities of thermal and hydraulic calculation for low-temperature LNG pipelines include the following parameters:

- Maintain low product temperatures to prevent biphasic flow;
- The choice of piping method depends on the location of the piping (preferably above ground to allow visual inspection of the sections)
- Possible laying in permafrost soils.

Calculation of LNG hydraulic parameters in the software complex from Schlumberger OLGA gives the most accurate values, however, to understand the program calculation sequence, manual calculation of hydraulic parameters during LNG pumping through cryogenic pipelines should be considered.

The main source of inaccuracies in existing calculations is the change in specific volume, mass heat capacity, and other unaccounted values during the calculation. Often, the change in the listed parameters reaches 20-25% (Vladimirov, 1975). The change in heat capacity is more dependent on the initial temperature of the product, since as it approaches the critical point, the fluid parameters change significantly, which leads to a serious change in the properties of the liquefied gas. By analyzing the existing dependencies to determine the final pressure and temperature, it can be concluded that they give a design error of more than 15% (Bleyher et al., 1974).

Assumptions proposed for obtaining more precise dependencies include the following: the value of the total heat transfer coefficient, isobaric heat capacity, thermal expansion coefficient, and isothermal compressibility is unchanged.

It is proposed to carry out the thermohydraulic calculation of cryogenic pipelines based on known calculations of oil and oil products pipelines, however, they do not take into account the properties of compressibility and other thermophysical parameters. To obtain more accurate results, the following calculation method will take into account the main changes in density, heat capacity, viscosity, and other parameters from the most important operating parameters of the system (temperature and pressure).

The Darcy-Weisbach equation calculates the final pressure without taking into account the difference in geodetic elevations (Korshak & Nechval, 2005):

$$P = P_{in} - \lambda_{fr} \cdot \frac{\vartheta^2}{2D_{in}} \rho L, \quad \text{(Eq.28)}$$

Where, ϑ is the average linear flow velocity of liquefied gas (m/sec).

$$\lambda_{fr} = 0,067 \cdot \left(\frac{158}{\mathrm{Re}} + \frac{2\Delta_e}{D} \right)^{0,2}, \quad \text{(Eq.29)}$$

Where, Δ_e – equivalent roughness, which should be determined according to the reference data (mm) (Gurevich & Blinovskiy, 1984), Re – Reynolds number.

$$\mathrm{Re} = \frac{\vartheta D}{\nu}, \quad \text{(Eq.30)}$$

To prevent the formation of a two-phase flow, it is necessary to lay a pressure margin of 0.7 MPa (Preobrachenskiy, 1975).

$$\vartheta = \frac{2G}{\rho \pi D^2} = \frac{4Q_m}{\pi D^2}, \quad \text{(Eq.31)}$$

Q_m is the volume flow rate of the pumping product (m^3/sec).

$$Q_m = \frac{G}{\rho}, \quad \text{(Eq.32)}$$

The final temperature in the pipeline section is calculated using the Shukhov-Leibenzone formula:

$$T_{end} = T_{soil} + u + \left(T_{in} - T_{soil} - u \right) \cdot e^{-III y}, \quad \text{(Eq.33)}$$

Where the correction for heating of the pumped product due to internal friction:

$$u = \frac{g \cdot G \cdot \Delta h}{k \cdot L}, \quad \text{(Eq.34)}$$

And Shukhov parameters:

$$III y = \frac{k \cdot L}{G \cdot c_p}, \quad \text{(Eq.35)}$$

Where the friction head loss is determined by the Darcy Weisbach equation (m):

$$\Delta h = \lambda \cdot \frac{L}{D} \cdot \frac{\vartheta^2}{2 \cdot g}, \quad \text{(Eq.36)}$$

The total heat transfer coefficient from the pumped product in the environment can be calculated by the formula:

$$k = \frac{1}{\frac{1}{\alpha_1} + \frac{D}{2 \cdot \lambda_{metal}} \cdot \ln \frac{D_{out}}{D} + \frac{D}{2 \cdot \lambda_{isolation}} \cdot \ln \frac{D_{isolation}}{D_{out}} + \frac{D}{\alpha_2 \cdot D_{isolation}}}, \quad \text{(Eq.37)}$$

Where, D, D_{out}, $D_{isolation}$ is the internal, external of the pipes and external insulation diameter relatively (m); λ_{metal}, $\lambda_{isolation}$ – the coefficients of thermal conductivity of the metal of the wall and insulation of the pipeline respectively (W/(m·K), α_1, α_2 – internal and external heat transfer coefficients (W/(m^2·K).

$$D_{isolation} = D_{out} + 2 \cdot \delta_{isolation}, \quad \text{(Eq.38)}$$

$$\alpha_2 = \frac{2\lambda_{soil}}{D_{out} \cdot \ln\left(\frac{2h_0}{D_2} + \sqrt{\left(\frac{2h_0}{D_{out}}\right)^2 - 1}\right)}, \quad \text{(Eq.39)}$$

Where the reduced depth of the pipeline axis is calculated by the formula:

- In the absence of snow cover:

$$h_0 = h + \frac{\lambda_{soil}}{\alpha_{air}}, \quad \text{(Eq.40)}$$

- In the presence of snow cover:

$$h_0 = h + \frac{\lambda_{soil}}{\alpha_{air}} + h_{snow} \cdot \frac{\lambda_{soil}}{\lambda_{snow}}, \quad \text{(Eq.41)}$$

Where λ_{soil}, λ_{snow} is the coefficient of thermal conductivity of soil and snow respectively (W/(m·K)), h – average depth of the pipeline axis (m), h_{snow} – average thickness of the snow cover (m).

The heat transfer coefficient from the surface of the soil (snow) into the air α_{air} is determined depending on the wind velocity (Polozov & Zhmakin, 2005).

$$\alpha_1 = \frac{\lambda \cdot Nu}{D_{in}}, \quad \text{(Eq.42)}$$

Where Nu is the Nusselt number (RD-75.180.00-KTN-198.09).

Selection of some physicochemical parameters is carried out according to average temperature:

$$t_{avr} = \frac{t_{out} + t_{wall}}{2}, \quad \text{(Eq.43)}$$

To find the pipe wall temperature, the following equation must be solved by the method of sequential approximations:

$$\alpha_1 \cdot D_{in} \cdot (t_{out} - t_{wall}) = \frac{2\alpha_2 \cdot D_{isolation} \cdot (t_{wall} - t_{in})}{2 + \alpha_2 \cdot D_{isolation} \cdot R} \quad \text{(Eq.44)}$$

Where R is the thermal resistance of the pipe wall.

$$R = \frac{1}{\lambda_{isolation}} \cdot \ln \frac{D_{isolation}}{D_{out}} \quad \text{(Eq.45)}$$

2.6 Prospects for use of cryogenic pipelines for transport of methane-hydrogen mixture and liquid hydrogen

In addition to the medium-term objectives of ensuring gas exports through LNG main pipelines, an important aspect is a study related to the strategic objectives of improving the environmental component of the planet, as well as improving the energy efficiency of existing plants.

The annual changes that occur with climate are extremely important problems that need to be solved by all countries of the world in close cooperation. Since the beginning of the industrial revolution, the increase in the concentration of CO_2 in the atmospheric air has been growing in proportion to the amounts of coal burned. In order to coordinate decisions aimed at combating the destruction of our climate and all the associated negative consequences, 197 countries of our planet adopted the Paris Agreement in 2015. The main goal of the treaty is to reduce the number of global emissions into the atmosphere, as well as to ensure a change in the increase in global temperature over the next 100 years by 2°C. In addition to everything, solutions should be actively sought to reduce the temperature drop up to 1.5°C.

The radical and most effective way is to replace all fossil fuel systems with electricity from alternative sources of energy. The Expert group which studies International Research on Climate Change has developed a possible scenario for increasing/decreasing carbon dioxide emissions into the atmosphere. In Figure 19, the red line RCP8.5 (8,5 W/m^2) is characterized by a scenario of "high emissions," in which the global industry and economy will continue to be associated with fossil fuels without the application of emission reduction measures. Adhering to this strategy, by 2100 the concentration of pollutants will reach 939 ppm. Intermediate scenarios RCP6.0 and RCP4.5 (6 and 4.5 W/m^2 respectively) describe the combination of different emission reduction processes. The most promising and rosy scenario is the RCP2.6 (2.6 W/m^2) scenario, called "low emissions." To implement it, extremely ambitious and long-term actions must be taken to achieve the goal: to reduce greenhouse gases to a minimum (by 2100 the concentration could be approximately 421 ppm). Analyzing

the change in global temperature, its increase will be equal to 16,8℃; 1,4℃; 0,8℃ и 0,1℃ for scenarios RCP8.5; RCP6.0; RCP4.5 and RCP2.6 respectively (Zamolodchikov, 2016).

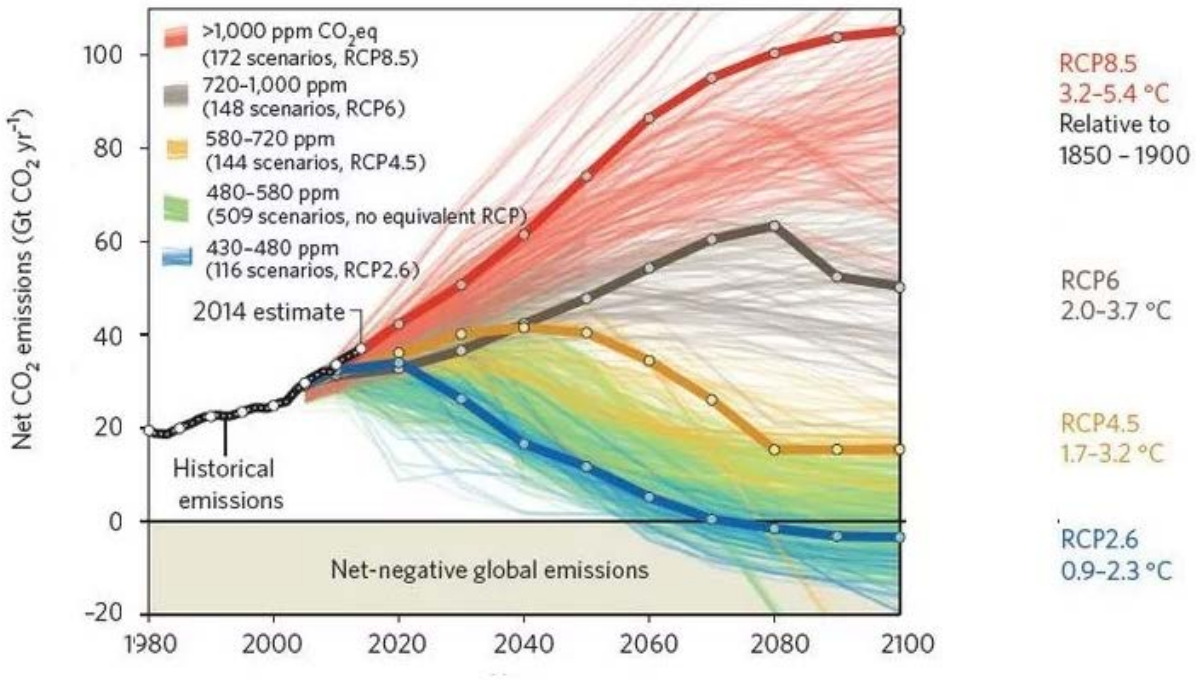

Figure 18: Scenarios for the development of carbon dioxide emissions into the atmosphere

Source: https://neftegaz.ru/tech-library/ekologiya-pozharnaya-bezopasnost-tekhnika-bezopasnosti/521106-dekarbonizatsiya-ekonomiki-i-energeticheskikh-sistem/, assessed 05.12.2020

Unfortunately, under modern conditions, all production processes are tied to the used oil, natural gas, and coal, but according to existing technologies, emissions can be reduced several times, for example, by adding H_2 to the composition of natural gas. Similar experiences will be carried out in this work.

2.7 Potential of methane-hydrogen fuel

Hydrogen technologies attract more and more attention every year. So, the following companies are already working on the creation of an innovative energy model and have already invested more than 1.4 billion euros per year: Anglo American, Air Liquide, BMW GROUP, ENGIE, Royal Dutch Shell, Total, Alstom, Linde Group, Toyota, Daimler, Honda, Hyundai Motor, Kawasaki. This interest is caused by the fact that hydrogen is 100% eco-friendly fuel since only water is formed during the combustion process, without releasing aggressive media such as carbon dioxide and exhaust aerosols. Every year the field of its application is growing and now hydrogen can be used in electrical appliances (up to several thousand kW). For example, in self-contained portable batteries, backup generators, generators that provide a constant supply of heat, and much more. Widespread transition to hydrogen fuel will reduce CO_2 emissions by 65% by 2050.

Currently, there are several methods for producing hydrogen:

- Catalytic reforming;
- Pyrolysis;
- Steam catalytic gas conversion;
- Gasification of oil residues;
- Water electrolysis.

The most widely used steam reforming process (Kalamars & Efstathiou, 2013).

2.7.1 Steam gas reforming

About 95% of all hydrogen is obtained by steam reforming, in which the steam reforming process of methane in combination with the accompanying steam reactions is an effective source of hydrogen, and as a result of the reaction, hydrogen saturated synthesis gas is obtained at a ratio of 3/1. In addition to efficiency and ease of use, this method is also the most profitable from an economic point of view. The purity of the finished product reaches 99.999%.

The steam reforming process includes the following steps and is shown in Figure 20:

- Feedstock preparation by hydrodesulfurization;
- Pre-reforming;
- Steam reforming process;
- Heat recovery (heating of boiler feed water by reaction products);
- Adiabatic CO conversion at high temperatures;
- The purification process of obtained hydrogen in SCAP (short-cycle adsorption process units) (Solodova et al., 2017).

Natural gas enters the compressor, where it is compressed to a pressure of 2.6 MPa, then heated to 300-400℃ and enters the reactors R1 and R2, where a process of purification from sulfur-containing compounds occurs. In an R1 reactor filled with an aluminum-cobalt-molybdenum catalyst, single compounds of sulfur-containing compounds are broken. Reactor 2 adsorbs hydrogen sulfide with a granular absorber to a sulfur concentration of less than 1 ppm. In the mixer, superheated steam is added to the purified natural gas, and the resulting mixture is sent to the furnace. The natural gas is then cooled in the recovery boiler (cooling to 450℃) and fed to the first stage for the conversion process (reactor 3), where the gas is cooled up to 250 ℃. Thereafter, the second conversion stage in reactor 4 begins. The final process at this stage is the cooling of the resulting mixture of hydrogen, carbon dioxide, and steam in the heat exchangers and the first stage of purification in the absorber (elimination of CO_2 with K_2CO_3 solution). The difference in the second purification stage lies in the temperature of the potassium carbonate solution.

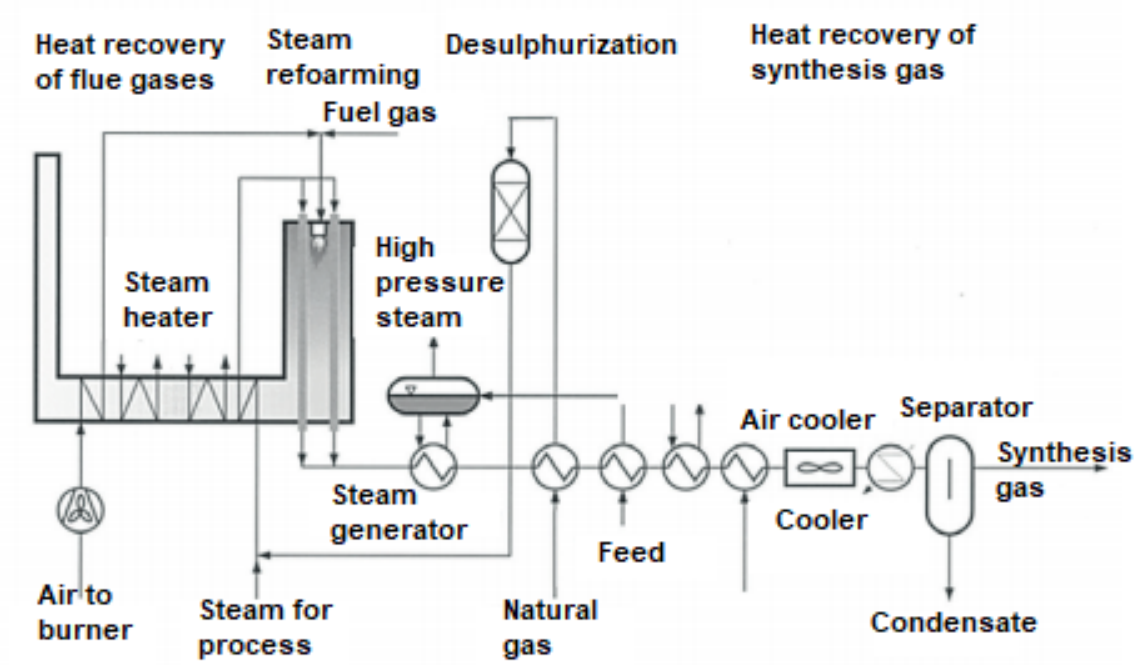

Figure 19: Steam reforming process (Makaryan et al., 2020)

The steam conversion process takes place in nickel catalysts at an operating temperature range of 800-1000℃ and pressure not lower than 2 MPa. In addition to high temperatures, an important parameter is the ratio of steam to carbon, which should be as low as possible. On the other hand, with the reduction of said ratio, there are great risks associated with poisoning of the catalyst material and carbon storage on its surface. The problem is solved by reducing the total activity of the catalyst, or by using a pre-reformer (pre-steam reforming step) to provide smooth and soft conversion. The conversion equation is as follows:

$$C_nH_m + nH_2O \leftrightarrow nCO + (n + 0,5 \cdot m)H - Q_{1,} \quad \text{(Eq.47)}$$

$$CO + H_2O \leftrightarrow CO_2 + H_2 + 42,4\ kJ / mol, \quad \text{(Eq.48)}$$

Where n, m is the number of carbon and hydrogen atoms in the hydrocarbon molecule.

The steam reforming process takes place in tube furnaces, but the designs of the heating schemes may differ in different campaigns. The most important condition is to ensure a uniform temperature profile along the entire length of the tubes. A schematic of the steam reforming furnace is shown in Figure 21. Typically, the tubes are made of steel with 25% chromium and 20% nickel added because such an alloy has good tensile and stretch properties.

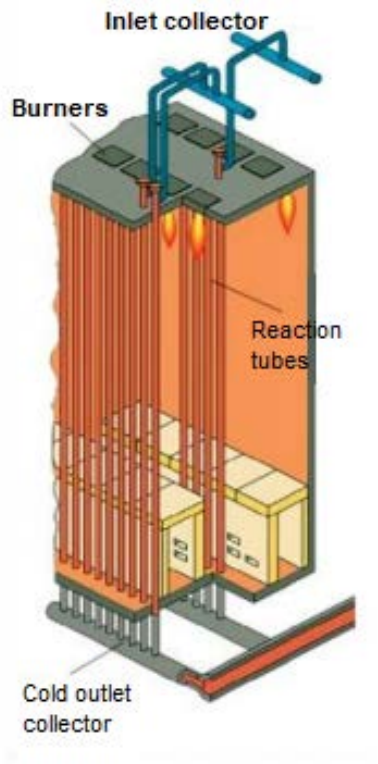

Figure 20: Schematic view of steam reforming furnace

Source: http://newchemistry.ru/letter.php?n_id=7949&cat_id=5&page_id=2, assessed 20.12.2020

Synthesis gas compressors shall be subjected to important processing. Compression leads to significant heating of synthesis gas, and the presence of hydrogen up to 70% obliges to use of special alloys for reformers since they undergo the process of hydrogen wear.

2.7.2 Electrolysis

Electrolysis is a physicochemical process during which a water molecule, under the influence of an electric current in a special device for decomposing solution components (electrolyzer), is divided into hydrogen and oxygen. Two electrodes are placed in a container filled with electrolyte (a positive anode on which oxygen molecules and a negative cathode on which hydrogen are concentrated), after which an electric current is started and the electrolysis process begins. Since hydrogen is 2 times more oxygen in water, therefore, it is produced more. A typical diagram of the electrolysis process is given in Figure 22.

Among a large number of various electrolyzers the greatest distribution was received by the following types:

- Water-alkaline;
- With hard polymer coating (HPC);
- Solid oxide.

Their main characteristics are given in Figure 23, from where it can be seen that the efficiency of solid oxide electrolyzers can reach 1, and the current density of electrolyzers with HPC is 1 A/cm^2, which is large enough for electrochemical systems.

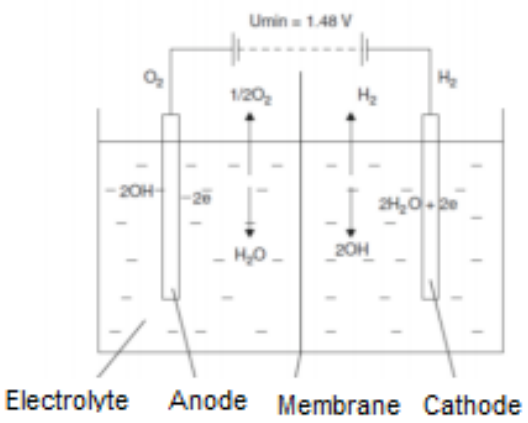

Figure 21: Typical diagram of the electrolysis process (Ugryumov et al., 2018)

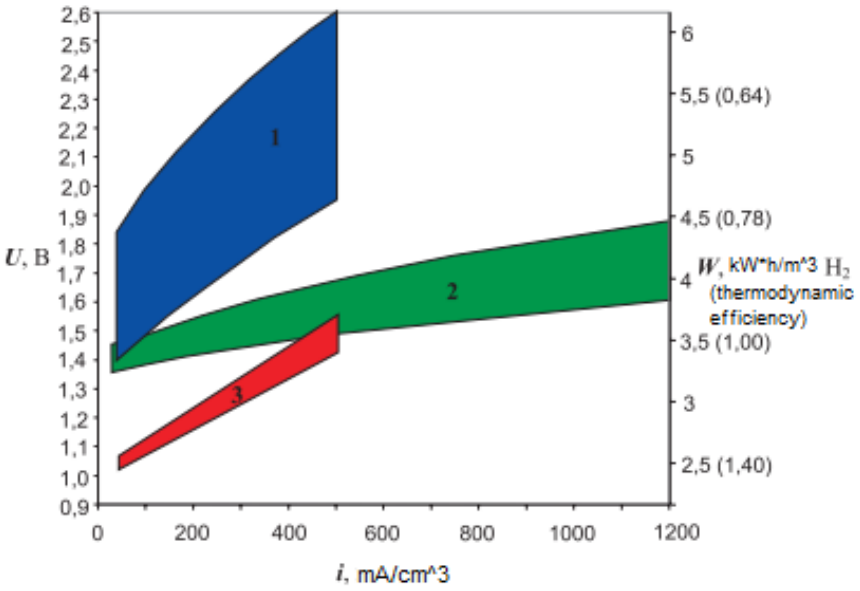

Figure 22: The dependence of cell voltage (U), specific energy consumption (W), and thermodynamic efficiency from the current density for various types of electrolyzers (Grigoriev et al., 2008)

Where, 1 – industrial alkaline electrolyzers (70-95℃); 2 – electrolyzers with HPC (90-110℃); 3 – high-temperature solid oxide electrolyzers with an additional supply of thermal energy (900℃).

The electrolysis process using a water-alkaline electrolysis cell is the main method for producing hydrogen. As the electrolyte, potassium, and sodium solutions are used, and its concentration in the water solution is about 40%. Electrodes are metal steel nets (if necessary, coated with nickel).

It is worth noting that the quality of the released hydrogen is quite low since it contains impurities of oxygen, steam, and alkaline. Also, when conducting the process under pressure, there is a possibility of increased danger, because of the possibility of mixing gases.

The main advantage is the relative cheapness of electrode and diaphragm materials, as well as extensive operating experience and proven technology. The schematic diagram of the water alkaline electrolysis cell is given in Figure 24.

Operating parameters of water-alkaline electrolyzers: current density 0,2-0,3 A/cm^2, power consumption 4,1-4,5 kW·h/nm^3, but it should be in mind that when specific productivity increases, energy consumption will also increase.

The largest producers of water-alkaline electrolyzers are «Norsk Hydro Electrolysers AS» and «Hydrogenics Corporation». In the Russian Federation, «Uralkhimmash» is engaged in the production of water-alkaline electrolyzers.

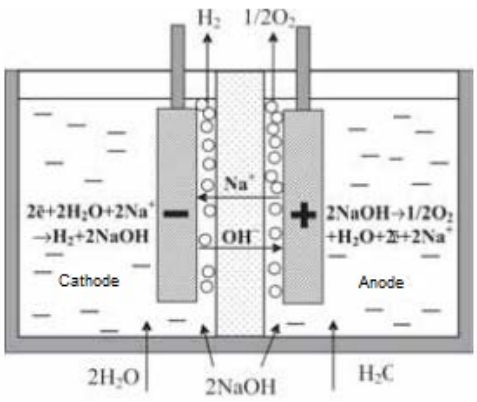

Figure 23: The dependence of cell voltage (U), specific energy consumption (W), and thermodynamic efficiency from the current density for various types of electrolyzers (Semenova, 2010)

The safest and efficient technology for the electrolysis production of hydrogen is the electrolysis of water with a solid polymer electrolyte, the distinguishing feature of which is a material of an ion-exchange membrane made of a perforated polymer. The thickness of the elastic film (membrane) is from several tens to several hundred microns. Uniform and chemically stable membranes can provide several thousands of hours of uninterrupted operation.

The principle of operation is simple: swollen with direct contact with water, the membrane allows hydrogen ions to move in its volume from an electrode to electrode. Its resistivity is much greater than that of water alkaline solutions. Undeniable advantages are the following factors:

- Due to the low permeability of the membrane, higher purity of hydrogen is achieved, the process is safe and reliable;
- Less ohmic loss due to no gap between membrane and electrode;
- Environmental friendliness of the process through the use of deionized water.

Operating parameters of an electrolytic cell with a solid polymer electrolyte: current density 3 A/cm^2, power consumption 3,6-3,9 kW·h/nm^3, as well as the possibility of producing hydrogen under pressure (Grigoriev et al., 2008).

By analyzing the advantages and disadvantages of the two most widely used methods for producing hydrogen, you can summarize the most important analytical parameters into a table for visual comparison. Summary Table 4 shows the main comparative characteristics for alkaline and solid polymer electrolyzers.

Table 4: The comparative characteristics of two popular electrolysis processes

Type of electrolyser	Energy expenses, H_2 m^3/(kW·h)	Temperature, K	Productivity, H_2 m^3/h	Pressure, MPa	Efficiency, %
Alkaline	4,5-5,5	320-370	<500	0,1-5,0	50-70
HPC	3,5-4,5	350-370	<100	0,1-15,0	80-90

The production of green hydrogen by the favorite electrolysis method is the most expensive, however, due to the actively promoted decarbonization strategy, it is a promising method for producing such a valuable substance as hydrogen. Figure 25 shows the cost of producing hydrogen by steam conversion and electrolysis. According to PJSC Gazprom, for the production of 1 m3 of hydrogen, it is necessary to use 0,7-3,3 kW·h of electricity during steam gas conversion; 2,5-8,0 kW·h in electrolysis.

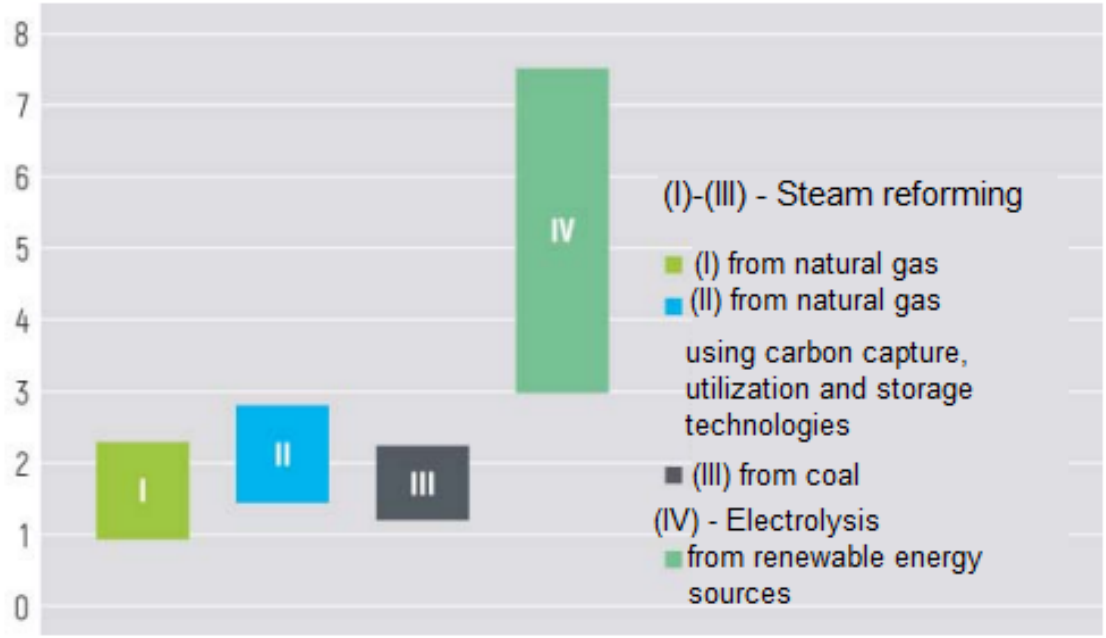

Figure 24: Approximate hydrogen production costs, в $/kg (Sufiyanov, 2016)

2.7.3 Use of methane-hydrogen fuel mixture

Since the universal total transition to hydrogen fuel is not possible in nowadays realities, modern technologies allow you to create processes for the production of methane-hydrogen fuel, with a maximum hydrogen content of 40%. This strategy has great potential, as it will increase the efficiency of thermal engines, reduce toxic emissions to the atmosphere and greenhouse gases, as well as reduce fuel consumption and reduce operational costs of industrial processes.

The new technology of adiabatic methane conversion (AMC) developed in the Russian Federation makes the process of producing methane-hydrogen fuel much easier, to maintain its operational state, additional production of oxygen is not required as well as an extremely expensive electrolysis process. AMC processes take place at lower temperatures (not higher than 680℃) and are spent in large-scale chemical production. The use of this technology is most rational in places where there are few debit deposits, as well as in places where transportation to which is unprofitable. Figure 26 shows the process diagram of the adiabatic conversion of methane.

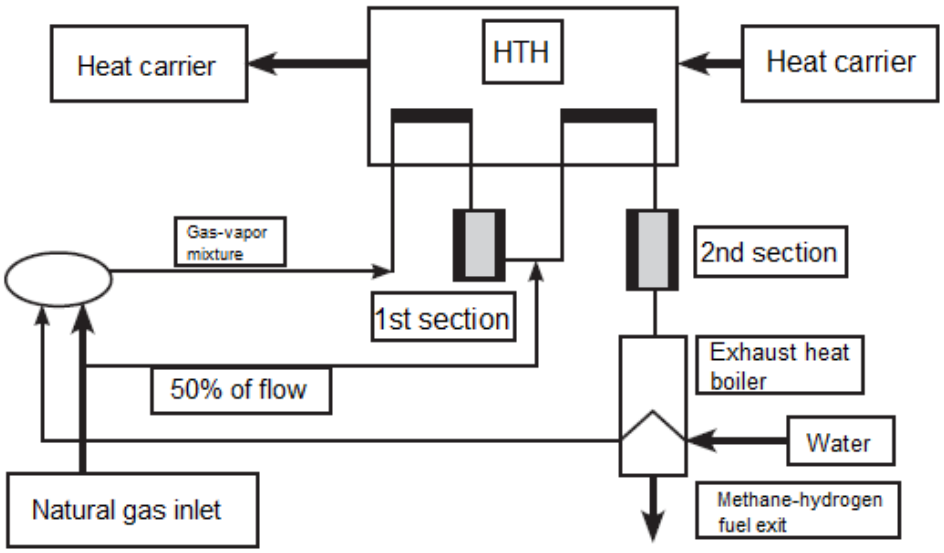

Figure 25: Adiabatic Methane Conversion Flow Chart (Aksyyutin et al., 2017)

The gas, mixed with steam, passes through a high-temperature process heat exchanger, where it reaches temperatures in the range of 640-680℃. Then, it is sent to an adiabatic reactor consisting of two sections and filled with catalyst. After that, it enters the recovery boiler, where moisture is removed and the finished product is released.

Studies have shown that the use of a methane-hydrogen fuel mixture will reduce greenhouse gas emissions by 30%, as well as achieve extremely low values of toxic NO_x emissions. Moreover, such fuel is less expensive than natural gas (without taking into account the capital costs of the plant), as well as, in comparison with electrolysis of water, the energy intensity for the production of 1 $м^3$ of hydrogen is 4-5 times lower (approximately 1 kW·h).

2.8 LNG Eastern market outlook

Natural gas, due to its energy efficiency and environmental friendliness, is developing more and more every year. So, not only for Russia but also for neighboring countries bordering the Russian Federation, natural gas plays a vital role. However, to some countries, such as Japan, Korea, Jamaica, and others, natural gas can only be delivered through LNG. Figure 27 below shows the use of natural gas by the industry sector in Japan. The largest consumption comes from electricity generation (64%) and industry (21%). Japan is one of the largest exporters because it does not have its own natural gas reserves, and due to its geographical location, it cannot be among the countries receiving gas through pipelines (for example, countries provided by the «Nord Stream», the «Southern Stream», the «Power of Siberia»).

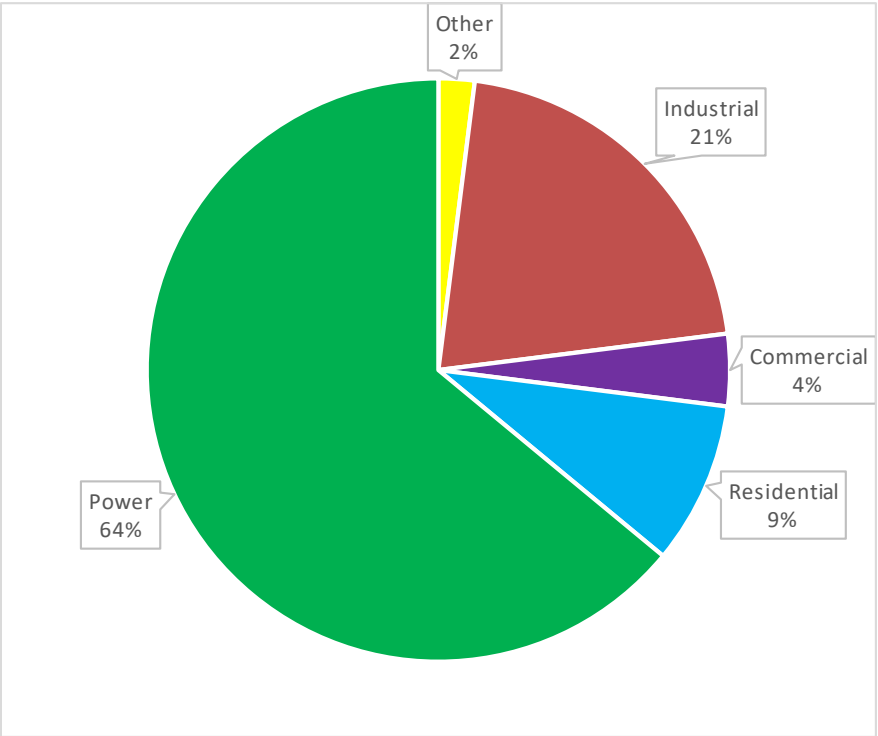

Figure 26: Sectors of natural gas consumption in Japan (Arabadjan, 2015)

The world does not stand in the same place, more and more countries shifting production to renewable energy every year, and only Japan, which accounts for 4% of the world's emissions to the atmosphere, does not just continue to use coal but is building new power plants. Since the tragedy that occurred in 2011 caused enormous damage to both the economic component of the country and the population, the social component of Japan is extremely negative and refuses to use nuclear energy again. Figure 28 shows the distribution of different fuels for power generation.

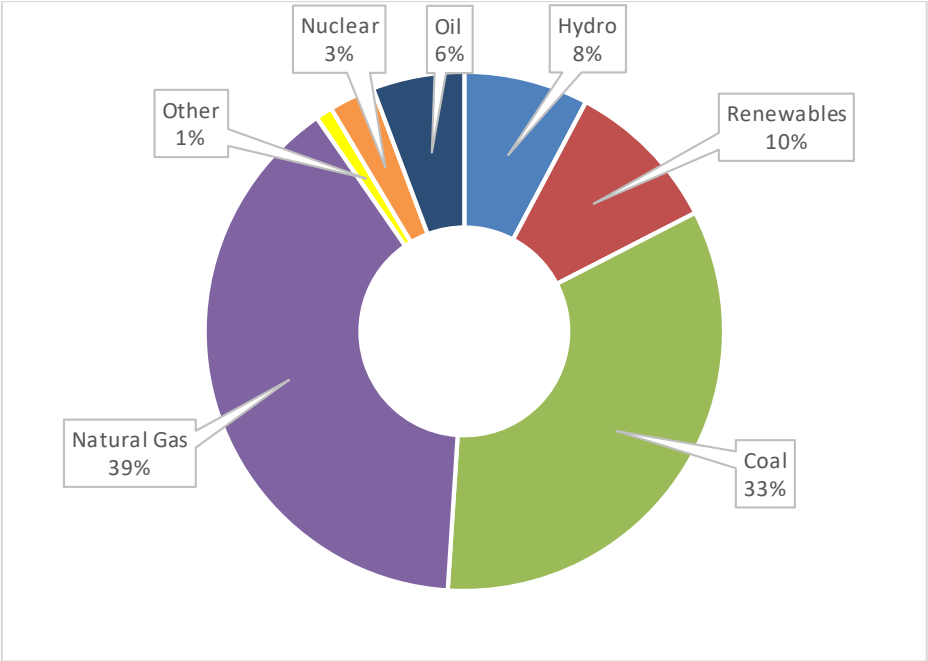

Figure 27: Distribution of different fuels for electricity production

Source: https://www.naturalgasworld.com/japan-future-uncertainty-but-potential-upside-lng-condensed-68811, assessed 10.01.2021

2.8.1 Sakhalin-2 LNH plant «Prigiridnoye»

One of the enterprises producing LNG for export is the Sakhalin-2 LNG plant, which annually produces 11,6 bln.m^3. PC "Prigorodnoye" is located near the city of Korsakov in the southern part of the island. The LNG plant provides reception, preparation, processing, and liquefaction of natural gas from the Lunskoye field and associated gas from the Piltun-Astokhskoye field. The plant consists of two liquefaction process lines, two LNG storage tanks, liquefied natural gas pier (2 parallel loading lines), administrative, process buildings, fire station, workshops, medical station, laboratory and control room, as well as flare area and canteen.

Figure 29 shows the process diagram of the Sakhalin-2 LNG plant. Gas intake and measurement units are used for separation, measurement of raw material flow rate, as well as initial pressure leveling to protect gas pipelines from destruction. The sulfinol circuit (acid gas removal unit) is aimed at separating CO_2 and H_2S from the feed gas and is an adsorber-stripper. The degree of gas purification is carried out to the following values: the amount of CO_2 is not more than 50 ppm, and H_2S is not more than 4 ppm. The experience gained in operating the gas purification system with the presented method gives an idea of some disadvantages, including constant clogging of the heat exchange equipment with products of thermal decomposition of sulfinol, corrosion of the equipment, as well as premature unloading of the adsorbent.

The raw gas drying step is used to reduce the water content to prevent hydrate formation. In the first stage of purification, most of the H_2O is removed in the drip breaker, and then, in the

second stage, it is passed through molecular sieves. The amount of residual water in the gas composition is not more than 1 ppm.

In order to prevent corrosion and protect the aluminum parts of the heat exchange equipment, the gas is removed from mercury in mercury removal plants (reduce its content by about 100 times).

The precooling process then begins. The refrigerant composition of this cycle is a mixture of propane, ethane, and small amounts of methane and butane. After compression, the coolant enters the tube bundle of the heat exchanger. Then, at the outlet it is divided into two flows: the first, passing through the throttling process, returns to the annulus of the heat exchanger, and the second enters the second heat exchanger. Gas cooled in two heat exchangers enters the compressor and passes the second stage of cooling - liquefaction to temperature -160℃.

The composition of the refrigerant of the second cooling cycle is slightly different, it consists of methane, ethane, and a small amount of propane, and nitrogen. In the main cryogenic heat exchanger, natural gas moves from bottom to top is then sent to the LNG storage.

The main advantage of the natural gas liquefaction scheme used is pre-cooling since this makes it possible to control heat loads in a wide range. This possibility is explained by the composition of the mixed coolant (for example, if it is necessary to lower the temperature between the cooling and liquefaction processes, it is enough to increase the amount of propane in the coolant mixture) (Golubeva & Bakanev, 2015).

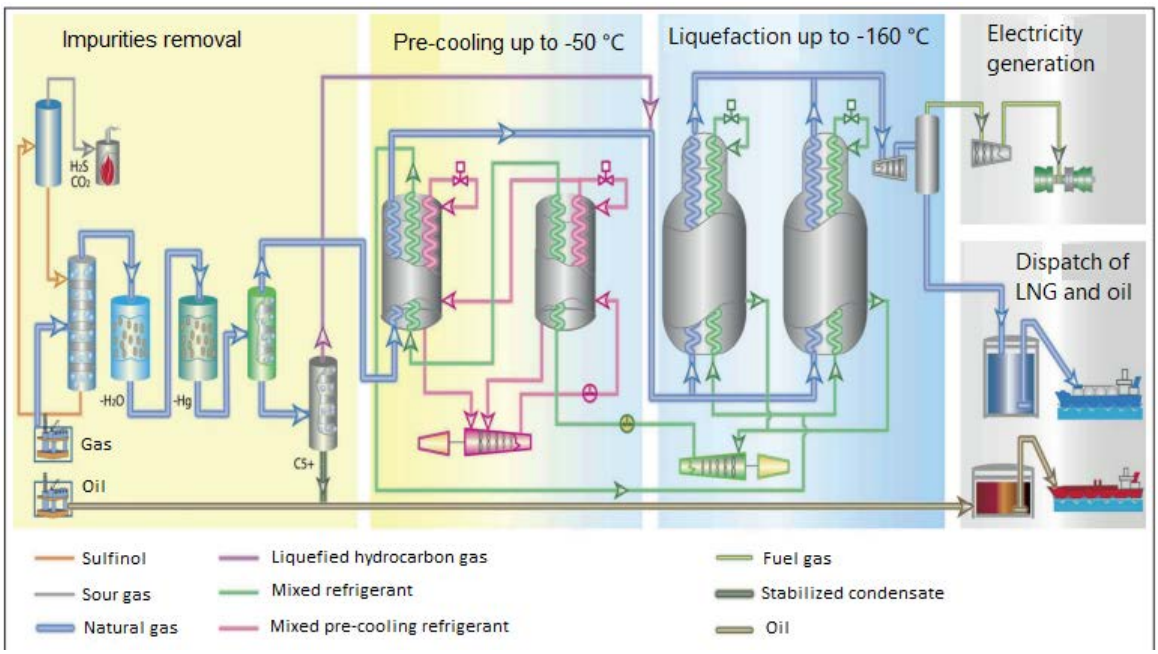

Figure 28: Sakhalin-2 LNG Plant Flow Chart

Source: https://chemtech.ru/razvitie-tehnologij-proizvodstva-szhizhennogo-prirodnogo-gaza/, assessed 11.01.2021

3 Setting the task of the research

As part of this project, the following tasks must be completed:

- Analysis of natural gas composition and influence of hydrogen addition on physical and chemical parameters of the mixture for combustion and pumping processes;
- Propose and justify from a technical and economic point of view options for natural gas transportation;
- Analysis of the environmental impact of pipeline laying on the thermal stability of the environment.

In particular, the following algorithm of actions was carried out:

- Simulated natural gas source fluid for further calculations in the MultiFlash program, appropriate calculation model selected.
- The process of gradual addition of hydrogen to the composition of natural gas within the framework of the maintenance of decarbonization projects was carried out and change of critical parameters was analyzed.
- Analysis of the effect of hydrogen on the hydrate precipitation process and required amount of inhibitor.
- The most important combustion characteristics (Wobbe index) are calculated and conclusions are drawn on the influence of hydrogen on combustion and pumping processes.
- Manual hydraulic calculation of gas pipeline was performed;
- Performed hydraulic calculation of cryogenic pipeline in Schlumberger OLGA software complex for the following cases:
  – Calculation of above-ground section of the cryogenic pipeline using aerogel thermal insulation;
  – Calculation of underground section of the cryogenic pipeline using multilayer thermal insulation;
  – Underwater section calculation using multilayer and aerogel thermal insulation;
- Analysis of the impact of underground laying of the pipeline on the soil in the FemTherm package of the OLGA software complex;
- Project feasibility study.

3.1 Initial data

For the feasibility study, the same pumping lengths and volumes were adopted for both the gaseous state of the fuel and the LNG.

For thermal and hydraulic calculation of the trunk gas pipeline and cryogenic LNG pipeline the following input data will be adopted:

Volume flow – $11{,}6 \cdot 10^3$ mln.m^3/year;

The pipeline with a total length of 159 km is divided into several sections:

- Offshore section of cryogenic pipeline from natural gas liquefaction plant "Prigorodnoye" of Sakhalin-2 LNG project 45 km long;
- Onshore sections (underground and above ground laying) with a total length of 64 km;
- Offshore section to the territory of Japan 49 km long.

The pipelines under consideration for subsequent calculations are given in Figure 30.

Figure 29: Proposed construction site

Source: https://yandex.ru/maps/?l=sat%2Cskl&ll=142.316956%2C45.870919&z=8, assessed 01.02.2021

Component composition of the gas is accepted according to GOST R 56021-2014 Category A. The main difference between gas category A and B is the amount of methane, but the performance of the two products does not differ. The choice of a category depends on the consumer and his needs. Since the work considers the addition of hydrogen and synthesis gas

processes which require as much purified fuel as possible, for further calculations the composition of natural gas of category A is taken, which is given in Table 5.

Table 5: Liquefied natural gas composition, in vol.%

C1	C2	C3	iC4	nC4	neoC5	iC5	nC5	N_2	CO_2
99,097	0,3023	0,0332	0,00932	0,0102	0,00595		0,00414	0,534	0,0039

During the work, the influence of hydrogen on the processes of combustion and precipitation of hydrates will be considered, therefore, the amount of hydrogen is taken 2-20 vol.%.

Physical and chemical properties of pipe material, thermal insulation, and soil required for thermal and hydraulic calculation in the OLGA Schlumberger software complex are given in Table 6.

Table 6: Metal, insulation and soil heat conductivity, heat capacity, and density

	Conductivity, W/(m·℃)	Capacity, J/(kg·℃)	Density, kg/m^3
Pipe material			
12Ch18H10T – LNG pipe	15	462	7920
08Ch18H10 – casing	17	504	7850
Insulation material			
Aerogel	0.038	920	130
Fiberglass	0.04	1050	25
Foamed synthetic rubber	0.039	2052	70
Soil			
Peat-loamy	2.6	1250	1750

The depth of the gas pipeline during underground laying is regulated by SP 62.133330.2011, however, it does not specify the norms for laying cryogenic pipelines. Taking into account the increased category of the hazardous object under consideration, it is proposed to deepen the pipeline by 2 m (McKinnon et al., 2005).

3.1.1 Climatic conditions of the construction area

Sakhalin Island has a monsoon climate; the largest amount of precipitation falls on August-September (about 60%). Winter is long but mild and snowy. The average temperature in the coldest month is 16,2℃, and the minimum is 16,3℃. In summer, constantly blowing winds and

high humidity. The maximum temperature in summer is 19.7 ℃. The climate is quite harsh for its latitude, however, despite this, growth processes on the island are quite intense. Soils are peat-loamy. Data on the maximum distribution of water temperature in Aniva Bay by months are given in Figure 31.

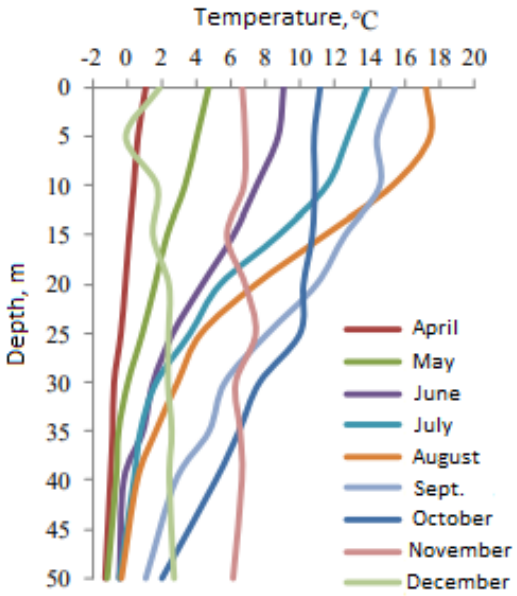

Figure 30: Distribution of maximum temperatures by month in Aniva Bay

Source: http://www.sakhalinenergy.ru/media/library/ru/environmental/impact_assessment/lng/Project_Documentation_LNG_Jetty.pdf, assessed 01.02.2021

4 Studies of the effect of hydrogen on the physicochemical properties of gas

4.1 Creation of fluid in MultiFlash and investigation of critical and physicochemical parameters.

The MultiFlash software complex is designed to simulate the physicochemical properties and phase transformations of substances. The program can be used both independently and in complex with other complexes (for example, OLGA from Schlumberger) and solve such problems as determining thermodynamic properties for engineering projects, calculating the phase diagram, and outputting the corresponding graphs, where phase transformations and critical parameters of a particular substance are clearly shown, as well as modeling the formation of sediments (asphaltenes, kinds of paraffin, hydrates, etc.). In addition, for the convenience of data processing, the function of uploading files to Microsoft Excel is provided.

Starting the task, a component composition of the gas (Table 5) was introduced and the question arose about choosing a model for the program to carry out further calculations. Undoubtedly, the most accurate model for calculating hydrocarbon liquids and gases is the Peng-Robinson model (PR, PRA), which is calculated using the following equation(a modification of the Van der Waals equation of state) (Peng, 1976):

$$p = \frac{R_{un} \cdot T}{V - b} - \frac{a \cdot \alpha}{V^2 + 2b - b^2}, \quad \text{(Eq.46)}$$

Where parameters a, b and α are determined in the following way:

$$a = \frac{0,45724 \cdot R_{un}^2 \cdot T_{cr}^2}{p_{cr}}, \quad \text{(Eq.47)}$$

$$b = \frac{0,778 \cdot R_{un} \cdot T_{cr}}{p_{cr}} \quad \text{(Eq.48)}$$

$$\alpha = \left\{1 + \left[0,37646 + \left(1,542266 \cdot \omega - 0,26992 \cdot \omega^2\right)\right] \cdot \left(1 - T_{cr}^{0,5}\right)\right\}^2 \quad \text{(Eq.49)}$$

Where a,b is the Van-der-Waals constants, R_{un} – universal gas constant (J/(mol·K)), p_c, T_c is the critical pressure and temperature respectively (MPa, K), ω – Pitzer acentric factor.

In the software complex MultiFlash, the cubic Peng-Robinson equation (PR and PRA) is used to create hydrocarbon fluids with a small content of waxes, paraffin, and asphaltenes. A key difference between the conventional version (PR) and the extended one (PRA) is the ability to be used in the calculation of a fluid with a larger content of water and steam. Most of the fluids studied are calculated from these models.

However, since the work will analyze the impact of adding hydrogen to the composition of natural gas, it is necessary to select a model that will take into account the individual content in the substance H_2.

The Redlich-Kwong equation (RK) is another modification of the Van der Waals equation and has the following form (Brusilovskiy, 2002):

$$p = \frac{R_{un} \cdot T}{V - b} - \frac{a}{T^{0,5} \cdot V \cdot (V + b)}, \quad \text{(Eq.50)}$$

$$a = \frac{0,42748 \cdot R_{un}^2 \cdot T_{cr}^{2,5}}{p_{cr}}, \quad \text{(Eq.51)}$$

$$b = \frac{0,08664 \cdot R_{un} \cdot T_{cr}}{p_{cr}} \quad \text{(Eq.52)}$$

Typically, the cubic RK model is used in simulating the liquid phase using an activity factor. In addition, RKS models are based on the above equations (an extended version of the RK model, which allows combining the stored volume of liquid with saturated vapors) and the RKS API version, which, in turn, is suitable for creating a system of a mixture of hydrocarbon and individual hydrogen. Therefore, further calculations will be carried out based on the RKS API version model, since the reliability of determining critical parameters of the hydrocarbon mixture will affect the reliability of the description of the phase behavior of the hydrocarbon mixture.

Firstly, a pure fluid without hydrogen was created. Then, hydrogen from 2% up to 20% vol was gradually added. The change in composition leads to an increase in the total number (the total amount of substances exceeds 100%), so the program automatically and performs the normalization of the data to ensure 100% content of substances.

By activating the PT Flash command, the program calculates and displays in the summary table all calculated fluid parameters under normal conditions (P=0,101325 MPa, t=20°C). Then, to display the results graphically, create a phase envelope. A graphical representation of the calculation result for pure LNG without adding hydrogen is given in Figure 32. Figure 33 shows the calculation results for pure hydrogen and all test mixtures in Figures 34-41.

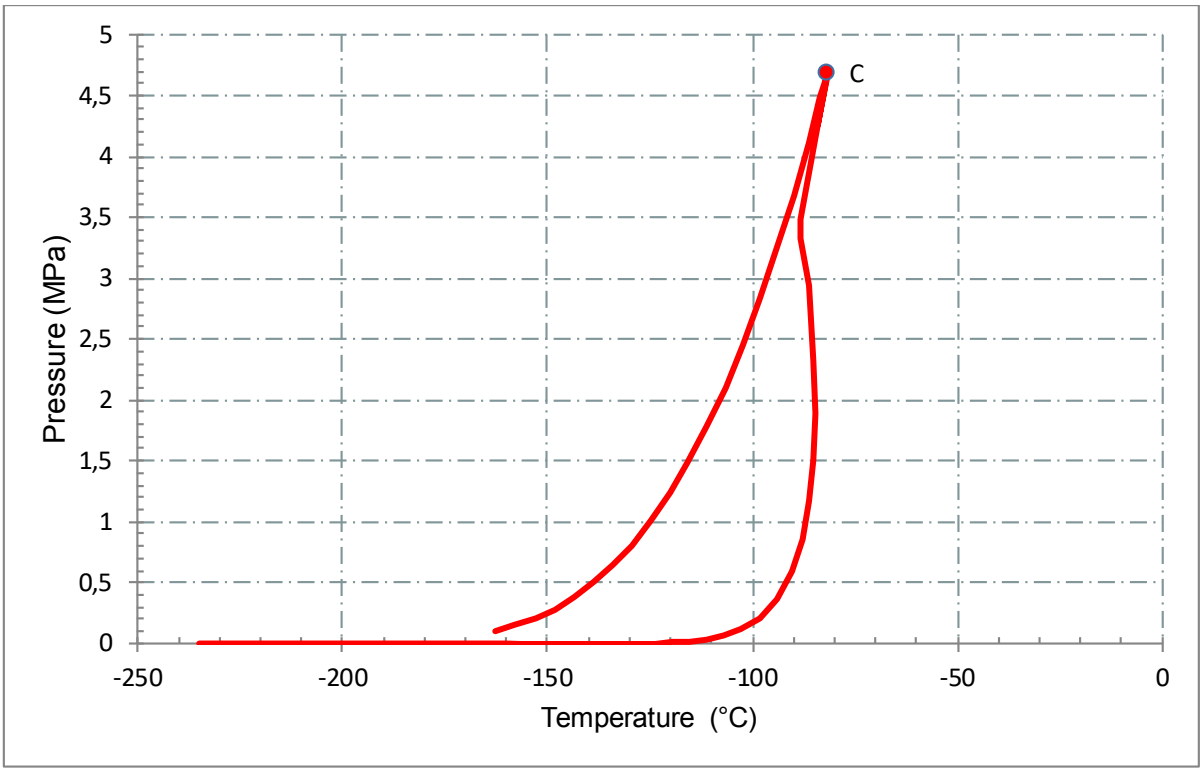

Figure 31: LNG phase envelope

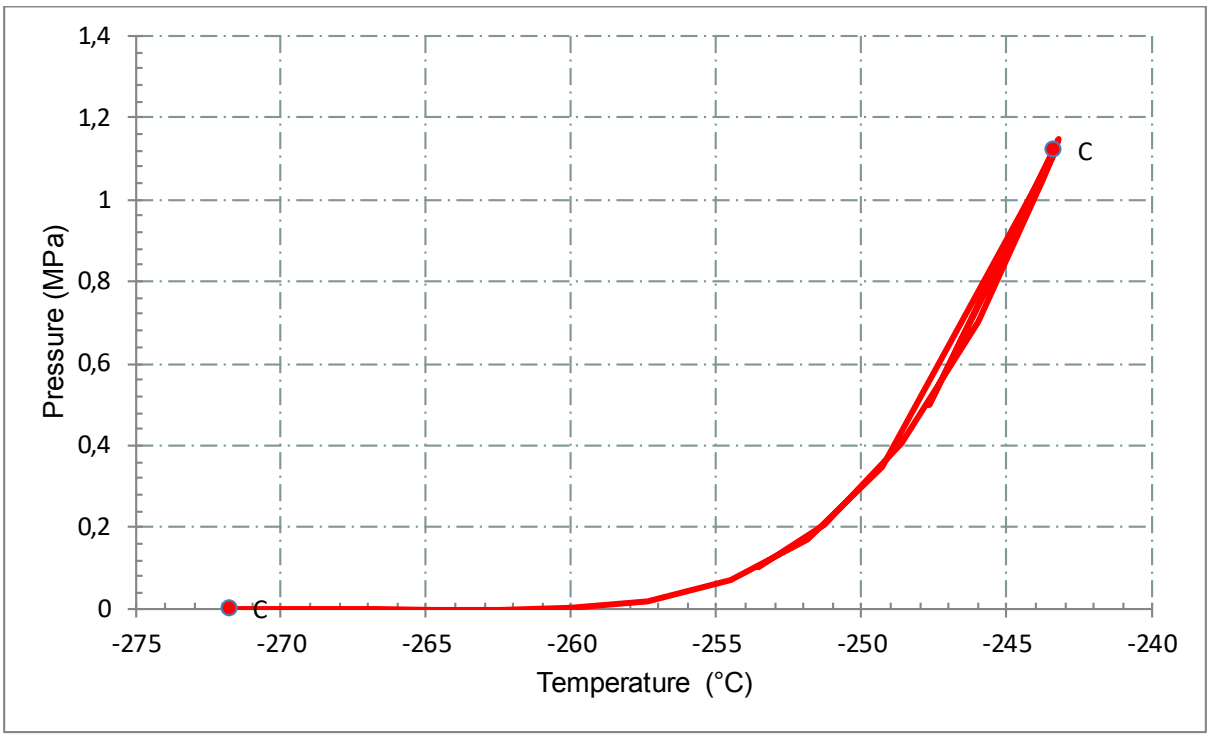

Figure 32: Hydrogen phase envelope

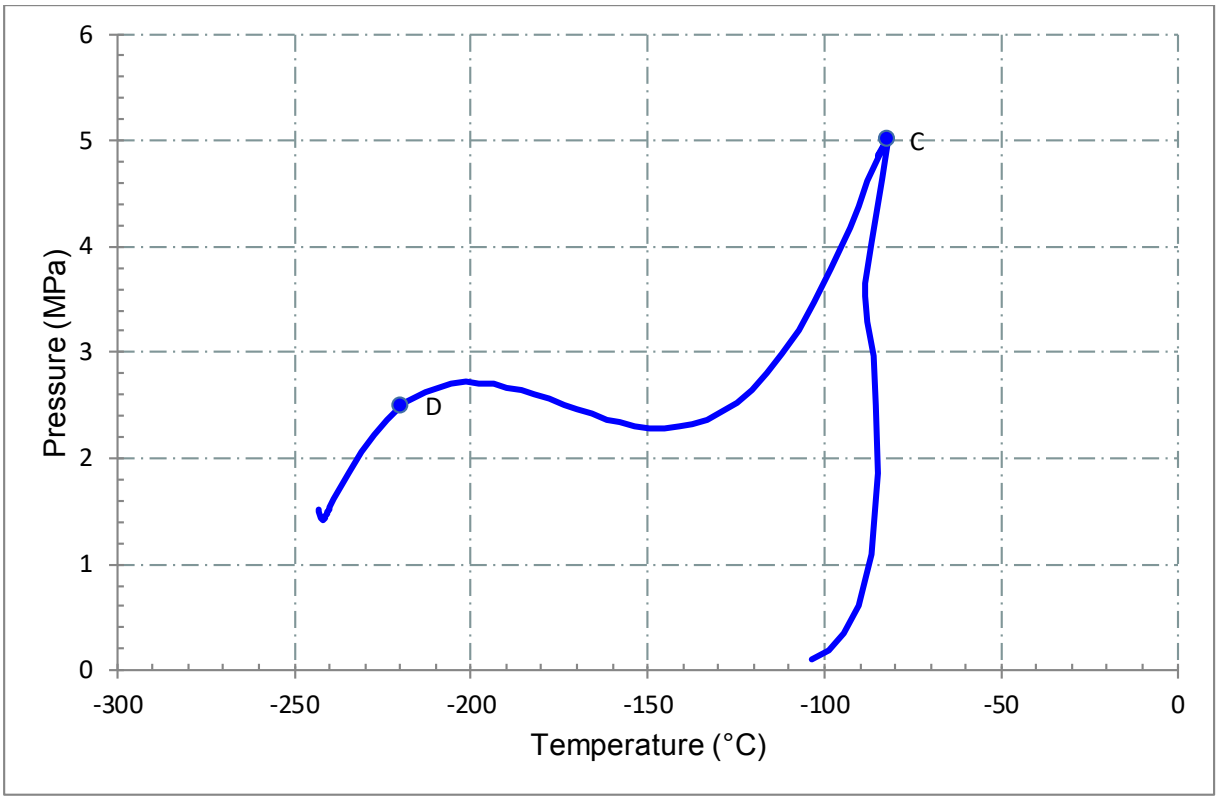

Figure 33: LNG phase envelope (with 2% of Hydrogen)

The right side of the loop in Figure 34 tends to be pure LNG. The left part of it can be explained by looking at the phase curve of hydrogen, the critical point of which is reached at P=1,14 MPa, t=–243,5℃. Based on this, by comparing the coordinates of the left side of the loop in Figure 34, it is possible to draw appropriate conclusions about its origin, since the mixture shows both the properties of hydrogen and LNG.

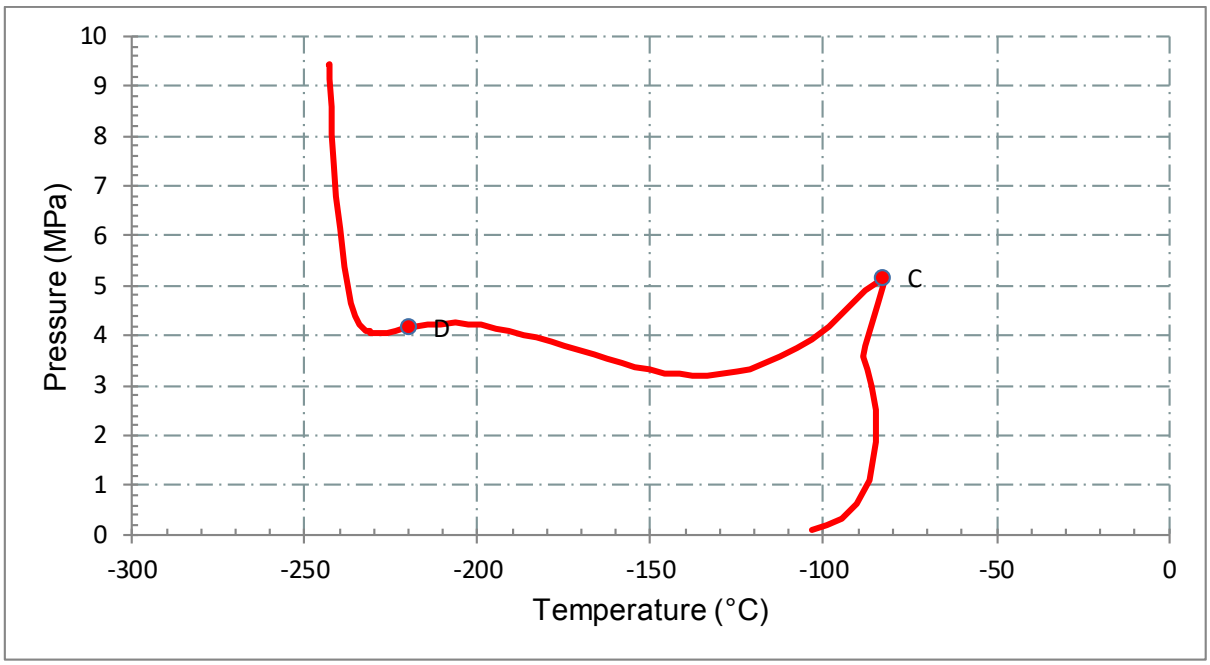

Figure 34: LNG phase envelope (with 3% of Hydrogen)

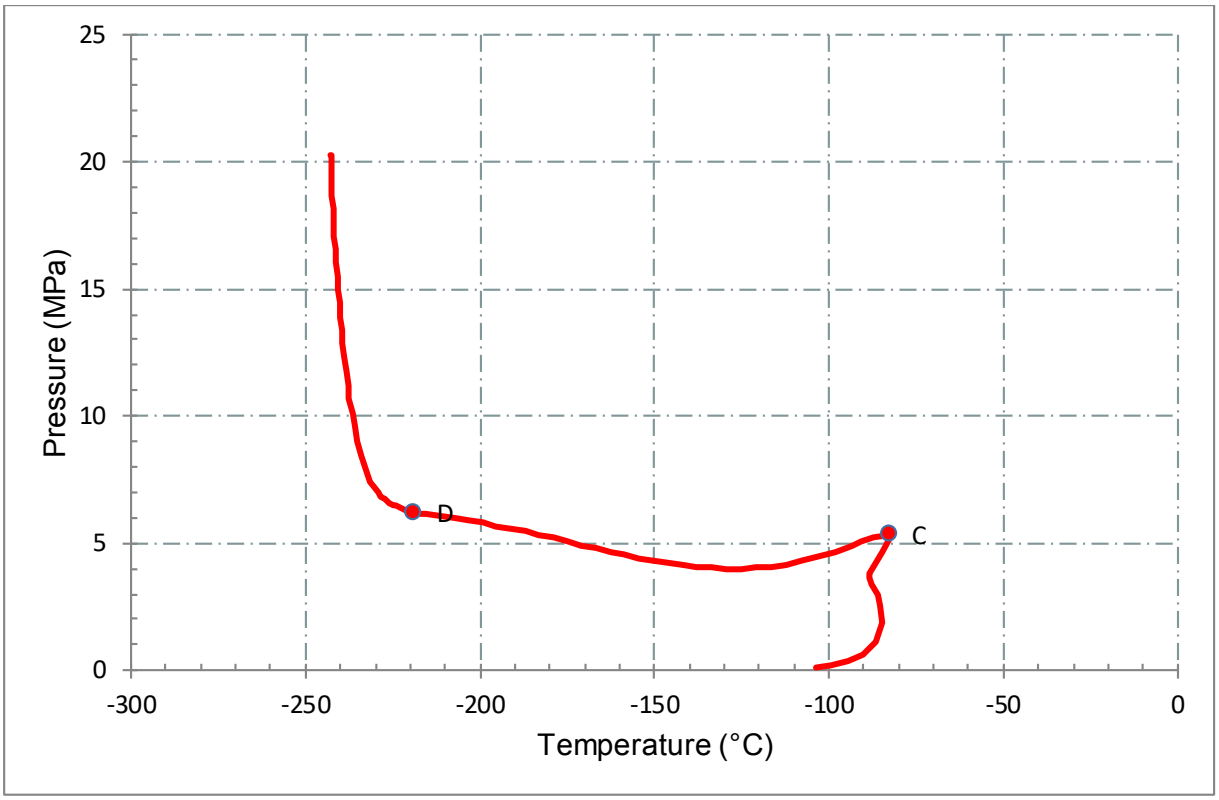

Figure 35: LNG phase envelope (with 4% of Hydrogen)

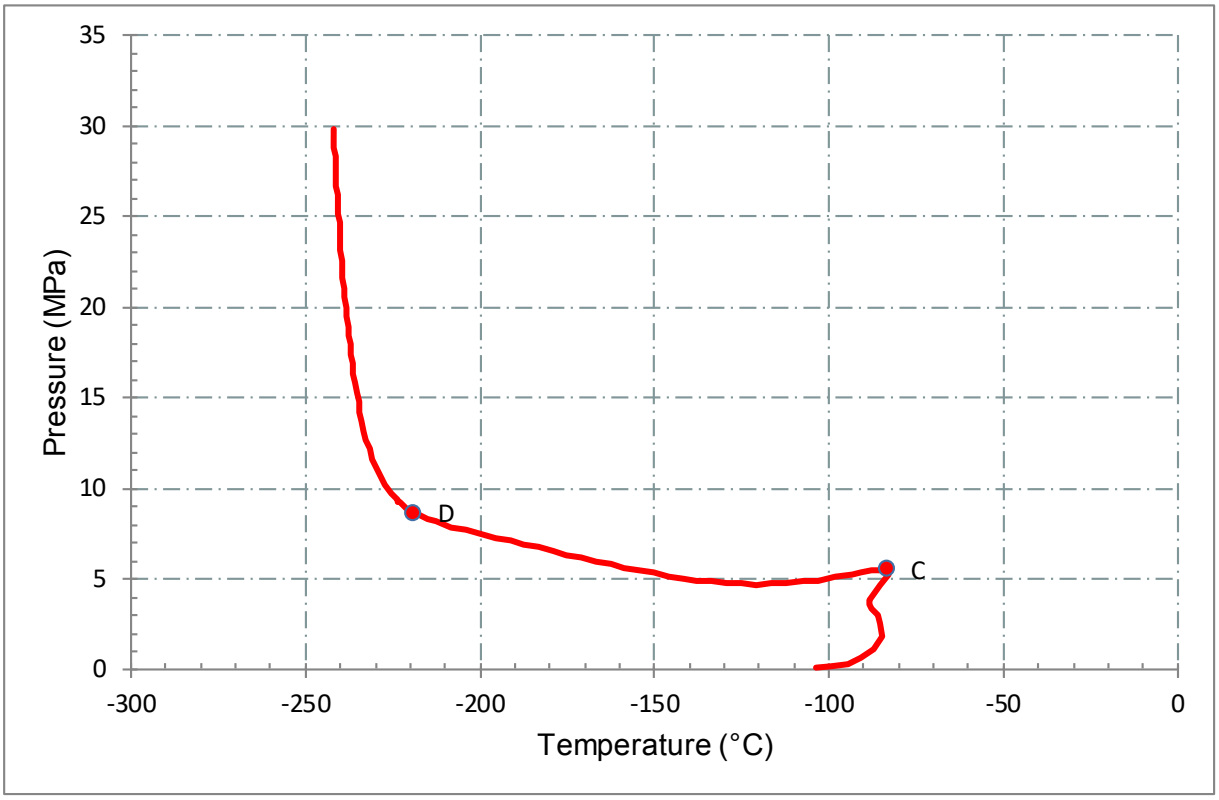

Figure 36: LNG phase envelope (with 5% of Hydrogen)

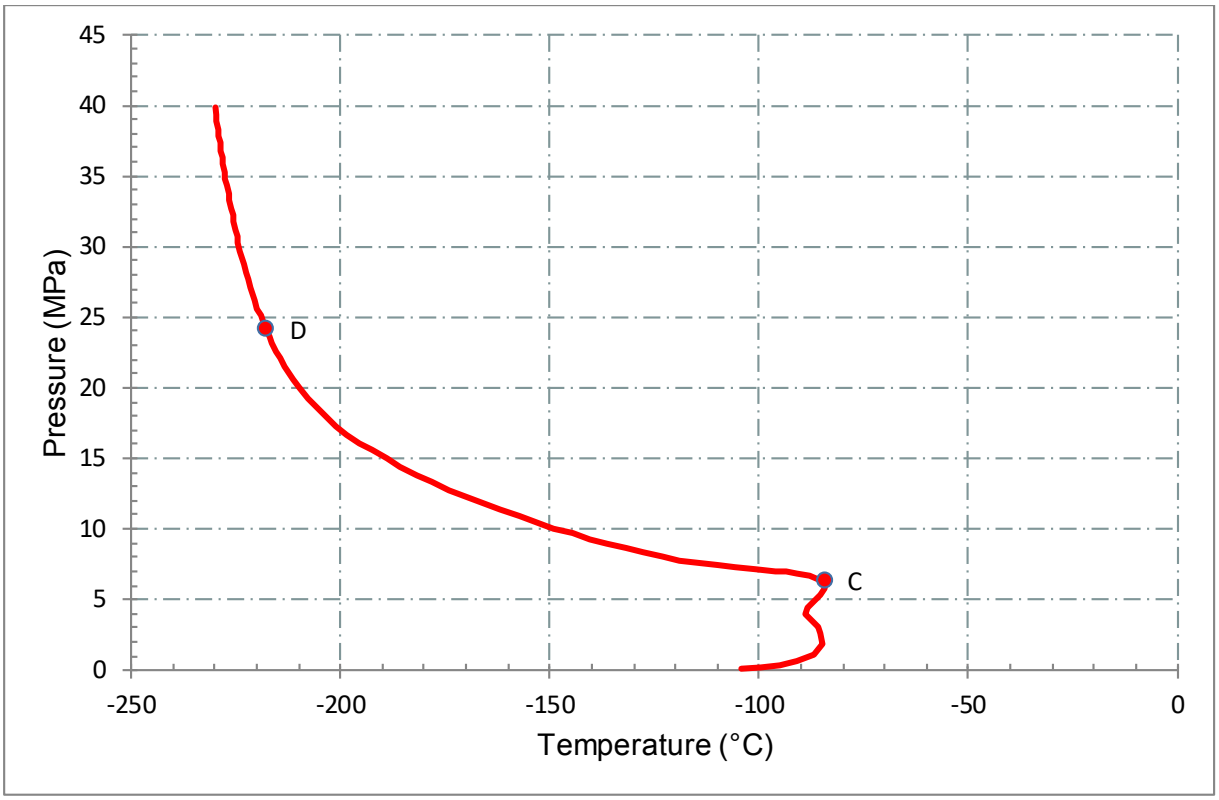

Figure 37: LNG phase envelope (with 10% of Hydrogen)

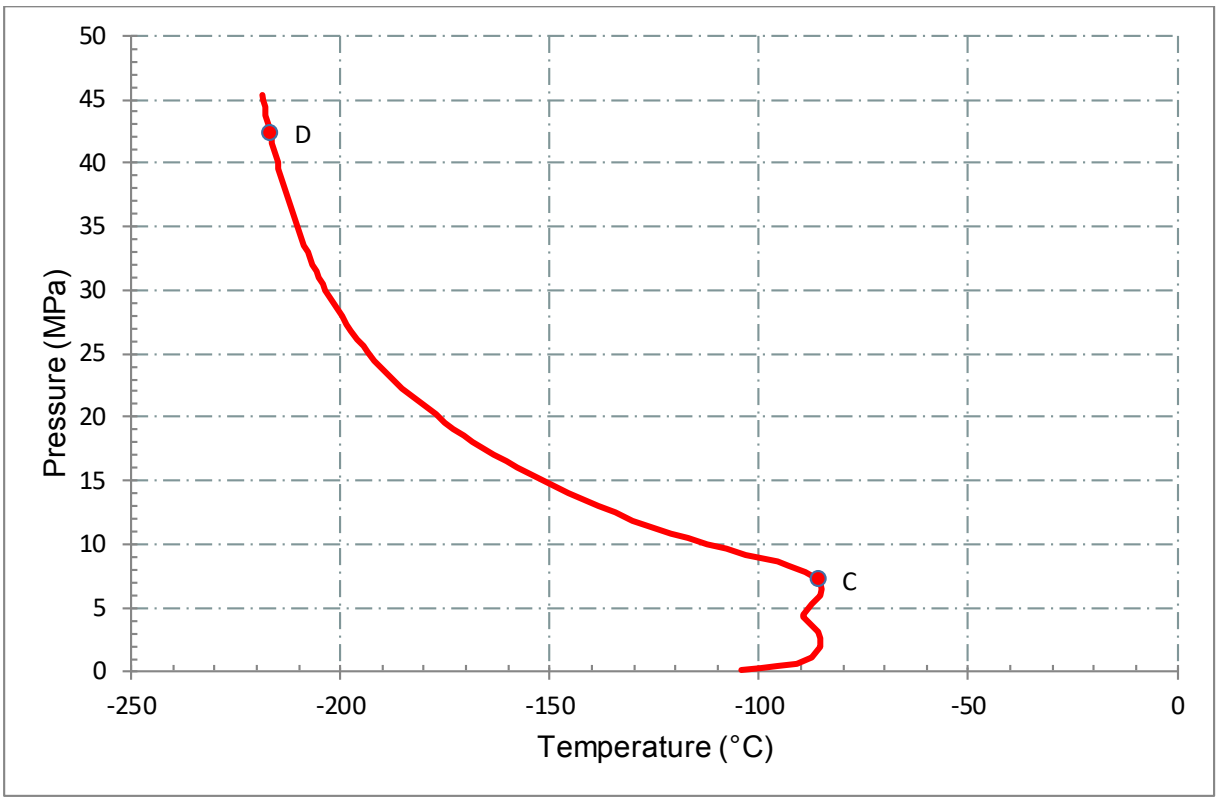

Figure 38: LNG phase envelope (with 15% of Hydrogen)

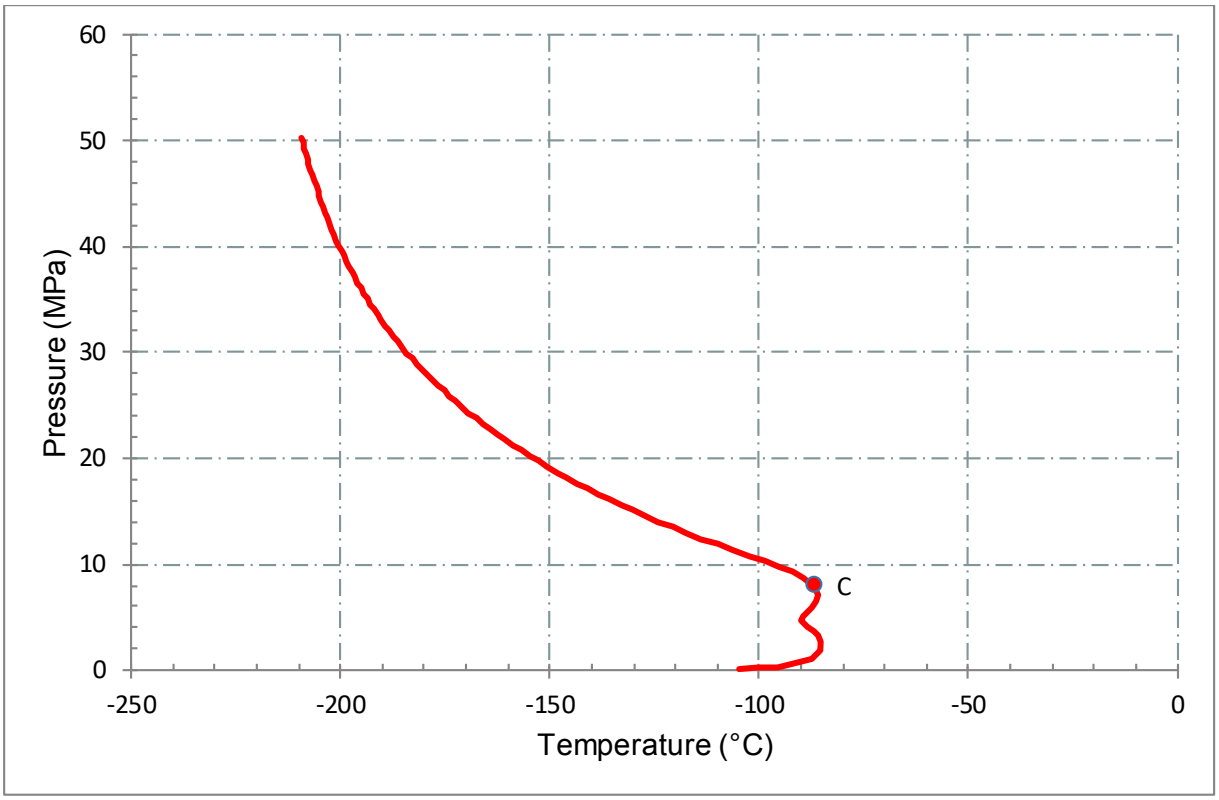

Figure 39: LNG phase envelope (with 20% of Hydrogen)

Phase diagrams have a loop-like appearance. The two-phase flow state is within the loop (liquid and gas). To the left, behind the evaporation start curve, is the liquid state region of the substance, and to the right of the condensation, the start curve is the vapor state region of the mixture. Critical point C characterizes the beginning of the supercritical state of the fluid in which the gas acquires the characteristic features of the liquid (or vice versa).

The criticality of the change in physicochemical parameters can be judged based on the calculations carried out in the program (density, viscosity, heat capacity, thermal conductivity)., which are given in Table 7.

According to the results of Table 7, it can be concluded that the physicochemical parameters change, but not significantly, so adding 20% hydrogen to the composition of natural gas will not require radically new burner technologies. The critical amount of hydrogen in the mixture is 25% of the LNG volume (Stetsenko et al., 2019).

Table 7: Change of physicochemical parameters at the change of hydrogen content in mixture under standard conditions

	Density, kg/m^3	Viscosity, Pa·sec	Thermal conductivity, W/(m·K)	Heat capacity, kJ/(kg·K)
LNG	0.67351032	1.0884e-5	0.033877902688	2.207924
LNG+2% H_2	0.66197994	1.087193e-5	0.03451542785985	2.2376527
LNG+3% H_2	0.65638253	1.086589e-5	0.0348347551065	2.252463
LNG+4% H_2	0.65638253	1.086589e-5	0.03483475511	2.252463
LNG+5% H_2	0.64550729	1.08539e-5	0.0354738927282	2.2819758
LNG+10% H_2	0.62004766	1.082476e-5	0.037069505741	2.3551359
LNG+15% H_2	0.59679942	1.07965e-5	0.03865334411371	2.4274187
LNG+20% H_2	0.57548599	1.07693e-5	0.040217545983	2.4988389

Based on the results of the obtained phase states, the change in the position of the critical point is given in Table 8.

Table 8: Change of critical point C parameters with an increase of hydrogen quantity in natural gas

	0% H_2	2% H_2	3% H_2	4% H_2	5% H_2	10% H_2	15% H_2	20% H_2
Pcr, MPa	4,68	5	5,16	5,3	5,48	6,3	7,13	7,99
Tcr, °C	-81,65	-82,16	-82,41	-82,83	-83	-84,24	-85,57	-86,88

The change in critical temperature and pressure parameters is not excessively high, however, to conclude the possibility of adding 20% hydrogen to the composition of natural gas, it is necessary to check the influence on the combustion processes and hydrate formation during gas transportation through gas pipelines.

4.2 Analysis of the effect of hydrogen on the combustion processes

The accumulated foreign experience shows that the idea of reducing the number of harmful emissions into the atmosphere is attractive not only from the point of view of production but also for ordinary consumers. So, in 2007, as part of a pilot group, 14 families living in the Netherlands, on the island of Ameland, agreed to add hydrogen to gas distribution networks. Initially, hydrogen was injected by cylinders, and then, as the project developed, an electrolysis

plant was commissioned, and electric energy was received from solar panels. After several years of successful operation, it was concluded that mixing with hydrogen does not affect boiler equipment, including burners (Kippers et al., 2012). However, in order to check the constancy of the heat flow generated during gas combustion, a calculation of the Wobbe index was carried out according to the formula:

$$W_{index} = \frac{Q_l}{\sqrt{SG}}, \quad \text{(Eq.53)}$$

Where Q_l is the lower heating value, kJ/kg, SG is the specific gravity, that can be determined in the following way:

$$SG = \frac{\rho_{gas}}{\rho_{air}}. \quad \text{(Eq.54)}$$

Where ρ_{gas} is the gas mixture density, (kg/m³); ρ_{air} is the air density equal to 1,2754 kg/m³.

The lower heating value of combustion is calculated according to the following formula:

$$Q_l = 10{,}8 \cdot H_2 + 35{,}8 \cdot C_1 + 63{,}4 \cdot C_2 + 91 \cdot C_3 + 120 \cdot C_4 + 144 \cdot C_5, \quad \text{(Eq.55)}$$

Gas densities at different hydrogen content are accepted according to results of phase calculations in MultiFlash and are listed in Table 9. Also in the table is shown the results of calculations.

Table 9: Wobbe index calculation results

	ρ, kg/m³	Ql, MJ/m³	SG	W_{index}, MJ/m³
LNG	0,707568	37,57115	0,554781	50,4422
LNG+2% H_2	0,695268	37,07115	0,545137	50,2092
LNG+3% H_2	0,689298	36,82115	0,540457	50,0861
LNG+4% H_2	0,683445	36,57115	0,535867	49,9586
LNG+5% H_2	0,677703	36,32115	0,531365	49,8268
LNG+10% H_2	0,650574	35,07115	0,510094	49,10491
LNG+15% H_2	0,625819	33,82115	0,490684	48,28223
LNG+20% H_2	0,603139	32,57115	0,472902	47,36392

To assess whether the obtained values do not violate the permissible limits, according to GOST 5542-2014 the range of the permissible value of the Wobbe number is determined, and an error of ± 5% of the obtained values is also accepted since this value allows deviation from

the normalized value of the Wobbe index. The diagram of the obtained values is given in Figure 41.

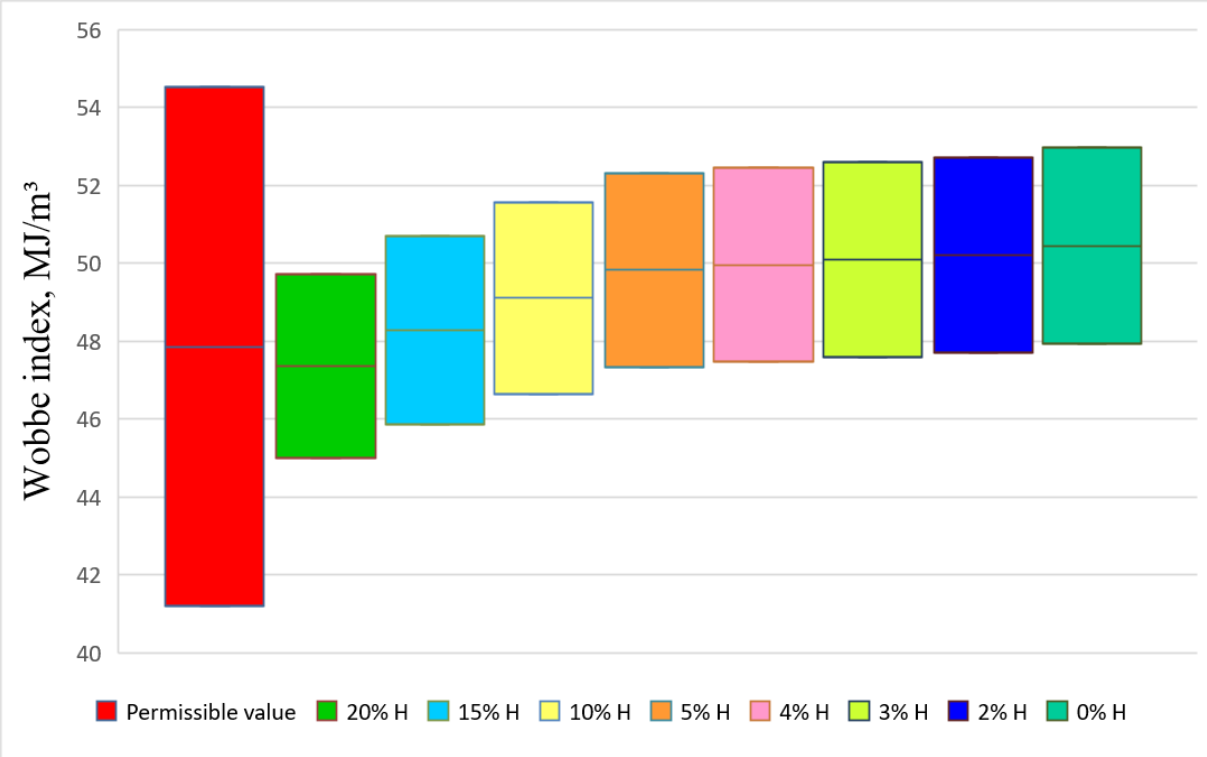

Figure 40: Wobbe index calculation results

The diagram shows that even with a volume hydrogen content of 20%, the permissible limits are not exceeded. Therefore, at the moment of the study, there is no reason to use a mixture with a lower content H_2.

4.3 Analysis of the effect of hydrogen on hydrate formation

Hydrate formation takes place in the presence of water in the composition of natural gas and represents as s solid crystalline substances that exist even at high temperatures.

Since LNG gas provides for a high degree of drying and cooling but analyzing the effect of hydrogen on the hydrate formation process is quite serious, it was decided to artificially simulate the situation by adding 1% and 2.5% water to the study composition using a program MultiFlash.

To add hydrates, it is necessary to first add water to the list of components and indicate its amount. Then add the lines in the Phase Envelope graph sequentially. Start with gas and water loops. After that, the previously selected RKS API version simulation model must be replaced with the CPA Infochem model, which is used to quickly calculate type 1 and type 2 hydrates and hydrate dissociation, as well as to match the amount of inhibitor required. After selecting the model, you must perform the PT Flash calculation again and apply the resulting hydrate line to the phase curve plot. The resulting hydrate curves for different amounts of hydrogen are shown in Figure 42.

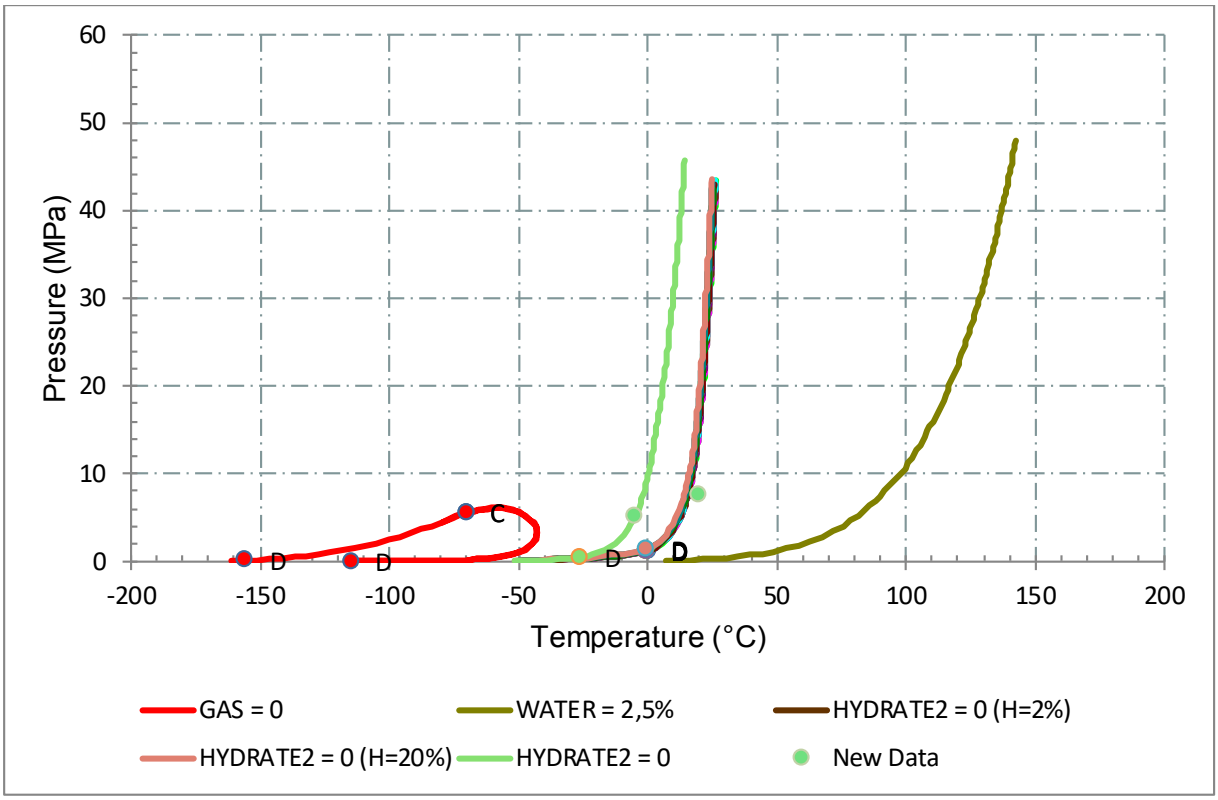

Figure 41: Change of hydrate line position at different amount of hydrogen (water content 2.5%)

From the results obtained, it can be concluded that, due to the position of hydrate curves on each other, hydrogen does not affect the hydrate formation process, and even more, so does not aggravate. "New data" in the graph shows the initial and final parameters for gas pumping through gas pipelines (P_{in}=7,48 MPa, t_{in}=20°C, P_{out}=5,1 MPa, t_{out}=– 5°C), which were created to find the amount of inhibitor (methanol) at a given amount of water. The results of the inhibitor amount calculations are given in Table 10. As a result, it can be concluded that the dose of the inhibitor is proportional to the amount of water, and the addition of hydrogen does not affect the hydrate formation processes.

Table 10: Inhibitor dosage for 1% and 2,5% of water

	1% H_2O	2,5% H_2O
Inhibitor dosage, kg of methanol/1000 kg of gas	5,39	12,1565

Having analyzed the most serious factors by which the effect of hydrogen addition on the combustion and pumping parameters can be judged, it can be concluded that a composition including a 20% H_2 content will be used for further calculations.

Since the MultiFlash does not provide for the calculation of dynamic currents characteristic of pipeline transport and its characteristics, further calculations will be carried out in the OLGA program from Schlumberger. Importing files is provided by developers. To generate a simulation file, you must specify a file name, fluid ID and create a matrix of values that will be

used for further calculations. The starting point was t_1= -230 °C and pressure P_1= 0,1 MPa, and the final parameters t_2=50° and P_2=25 MPa. The number of design points of each edge condition should be at least 100 (in this case, 120 design points were set for high accuracy). After you create the matrix, the program creates a tab. file and outputs graphs of various parameters gradient distribution from temperature and pressure. Some of them are listed in Figures 43-45.

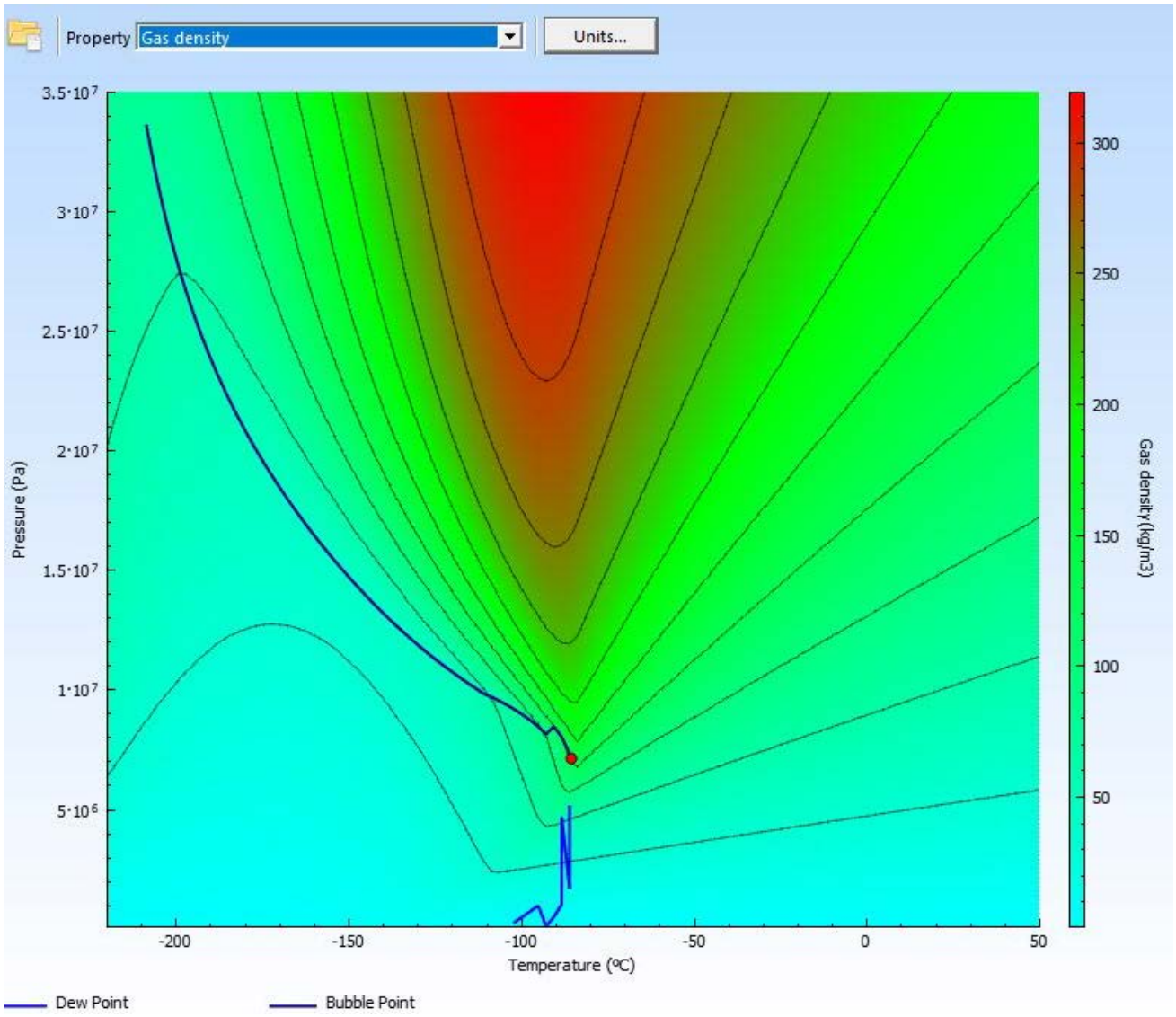

Figure 42: Density gradient

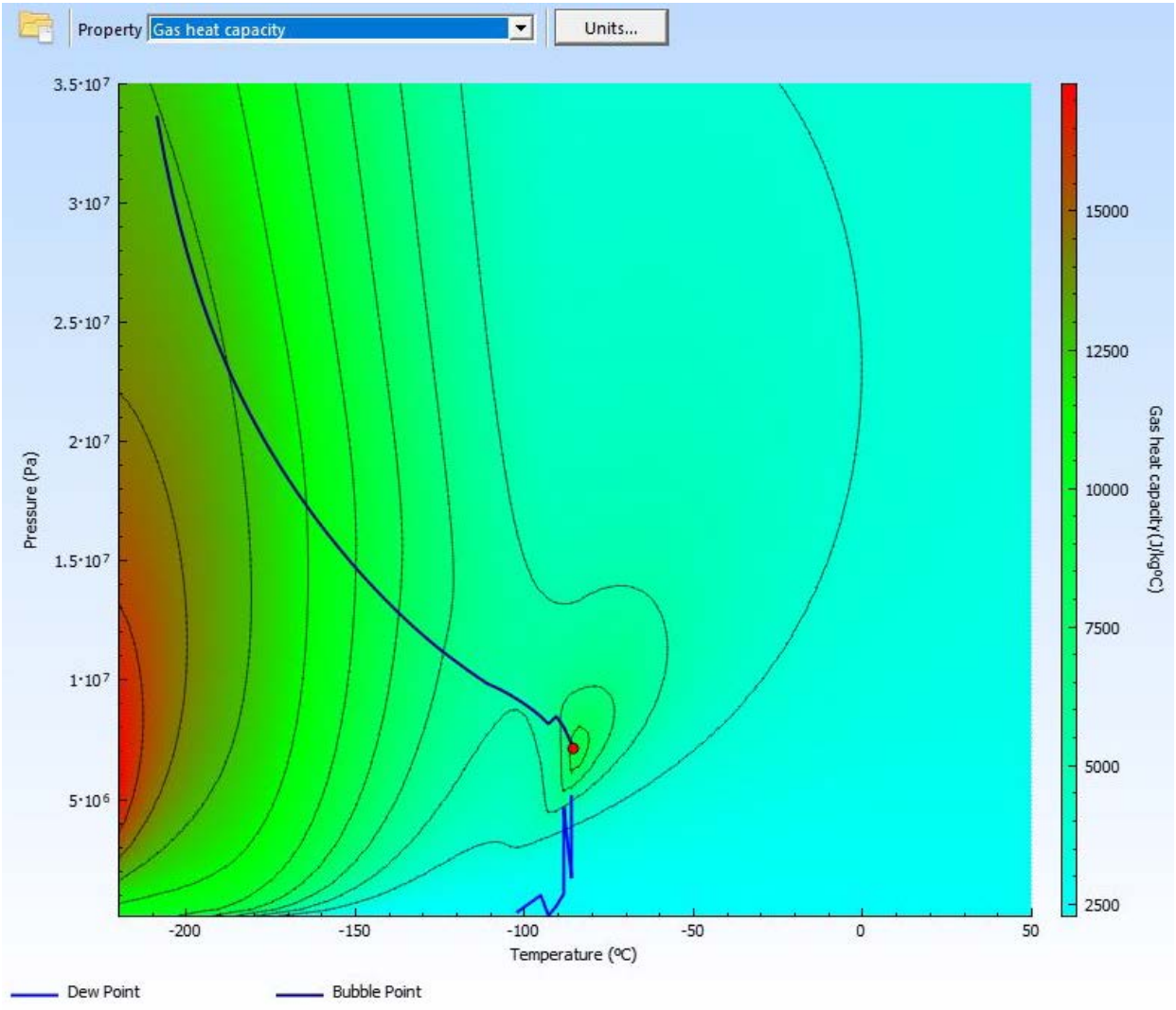

Figure 43: Gas heat capacity gradient

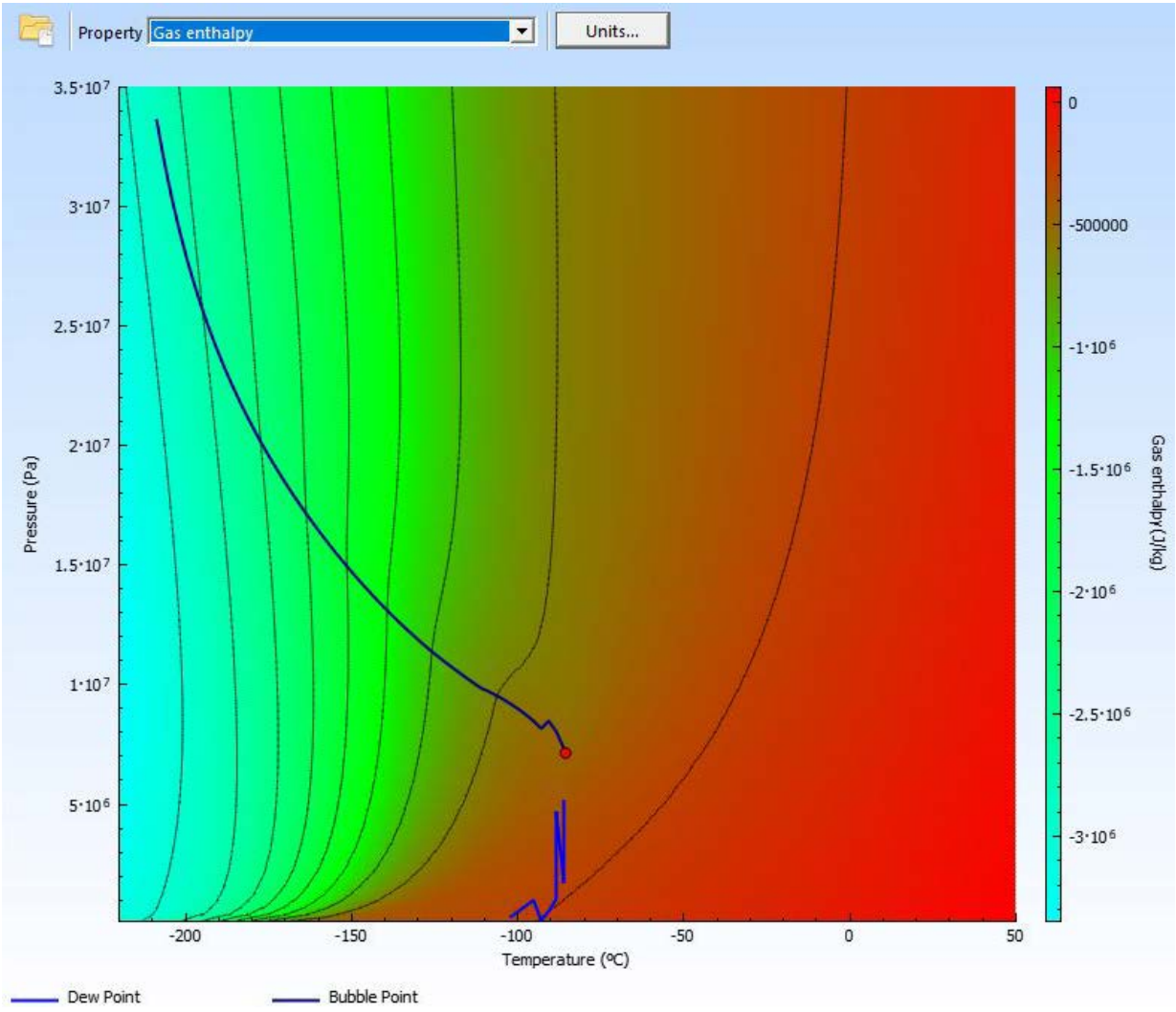

Figure 44: Gas enthalpy gradient

5 Hydraulic calculation of cryogenic pipeline

Since MultiFlash performs calculations exclusively for static objects (for example, when examining the parameters of the mixture in tanks, finding and graphically constructing phase curves and hydrate formation curves, finding the amount of inhibitor required, etc.), then for hydraulic dynamic calculation (selection of optimal values of temperature and pressure, required insulation thickness to prevent the phenomenon of fast phase transition, etc.), the OLGA software package is used, the licensor of which is Schlumberger.

OLGA is a dynamic simulator of multiphase flows and is used in the modeling of unspecified flow modes. The calculation is carried out according to system parameters versus time and the use of this software complex allows to model both production processes and product transportation with high accuracy.

After creating an empty case, which serves as the basis for further calculations, you need to build a dynamic model, the general view of which is shown in Figure 47.

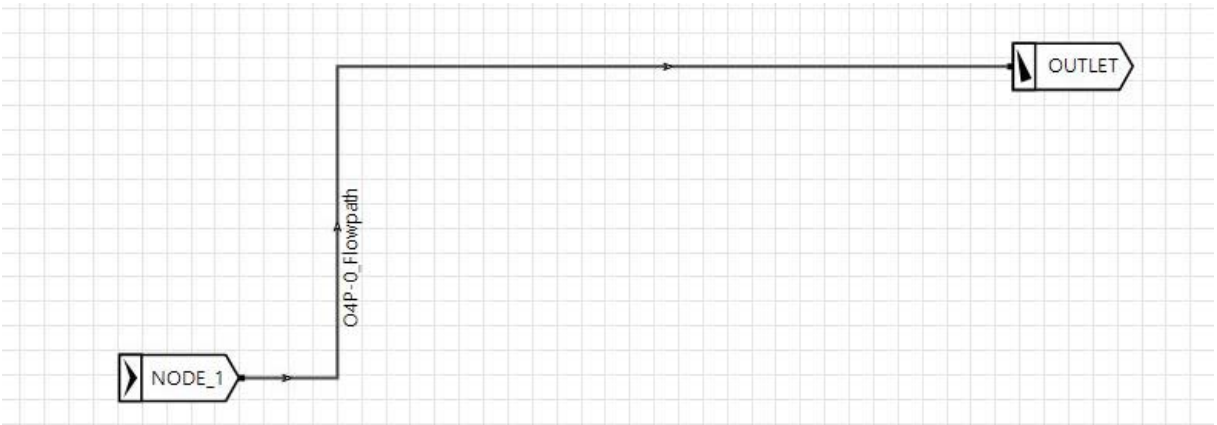

Figure 45: Dynamic scheme of the LNG transfer

Next, on the «Case Definition» tab, you must load the simulation file that was previously imported from the MultiFlash in tab. format into «Files». The process of creating a pipeline profile is then started, as the LNG transfer scheme must be described as fully as possible to obtain the correct results.

Then it is important to specify the pipe material: the thermal conductivity, isobaric heat capacity, and density values in the Library→Material column. All necessary data are given in Chapter 3 (Table 6). To create an object (in this case a pipeline), use the same dialog box to do the following: Library→Add→Wall. When creating a wall, you must specify its thickness. The specifics of the calculation rules of the program obliges you to create a Wall according to the following rule: each subsequent layer must be 2-3 times larger than the previous one (but not exceed the value by 4 times larger). This means that by creating a 10 mm thick pipe wall, the next layer (e.g. thermal insulation) should be at least 20 mm. Since sometimes you need to add a layer with a lower thickness than the previous one to solve the problem, you can use the split rule. For example, the pipe wall layer is 10 mm and the thermal insulation is 6 mm. Then,

to perform the calculation, you need to split the pipe layer into 5 (5:2 mm) and then the general view of the pipe wall setting takes the form (Table 11).

Table 11: General view when defining a pipe wall

Material 1 (pipe)	Material 1 (pipe)	Material 1 (pipe)	Material 1 (pipe)	Material 1 (pipe)	Material 2 (isolation)
2 mm	2 mm	2 mm	2 mm	2 mm	6 mm

The split rule cannot be neglected and in all subsequent calculations, the wall will be set according to the rule.

To create a pipeline profile, each line must be divided into several sections, then set the lengths of each section and the corresponding elevation relative to the surface (ground, seabed, etc.). Then, to ensure accurate calculations, you must activate the «Discretize Geometry» command, which will divide each section into a specified number of subsections and the calculation will be carried out for each of them (in this work, the calculation will be carried out for each 100 m length). Design profiles of pipelines are given in Figures 48-51. According to the task, the total number of lines is 4. Each of them is described in Chapter 3 of this report.

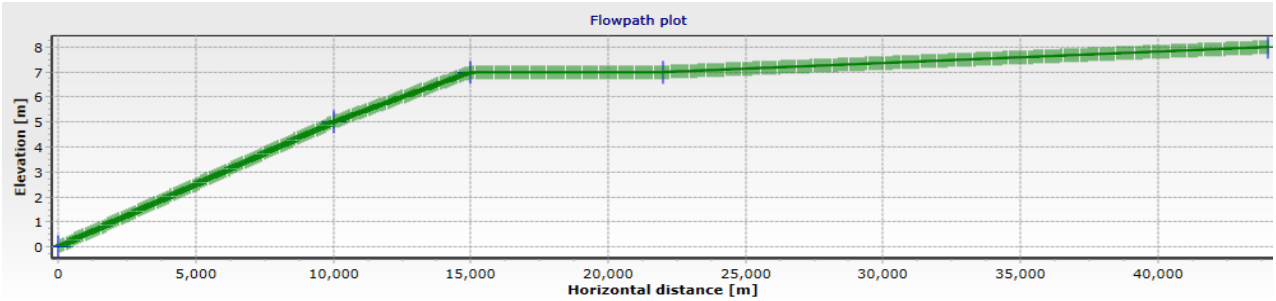

Figure 46: 1st line of the pipeline (offshore)

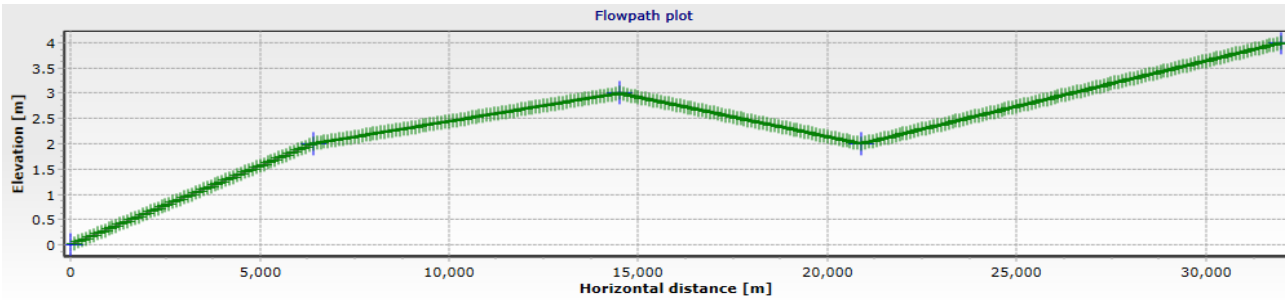

Figure 47: 2nd line of the pipeline (onshore)

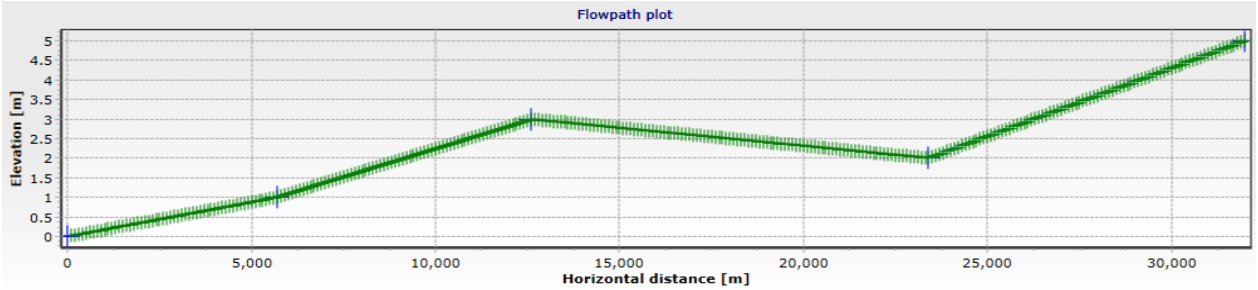

Figure 48: 3rd line of the pipeline (onshore)

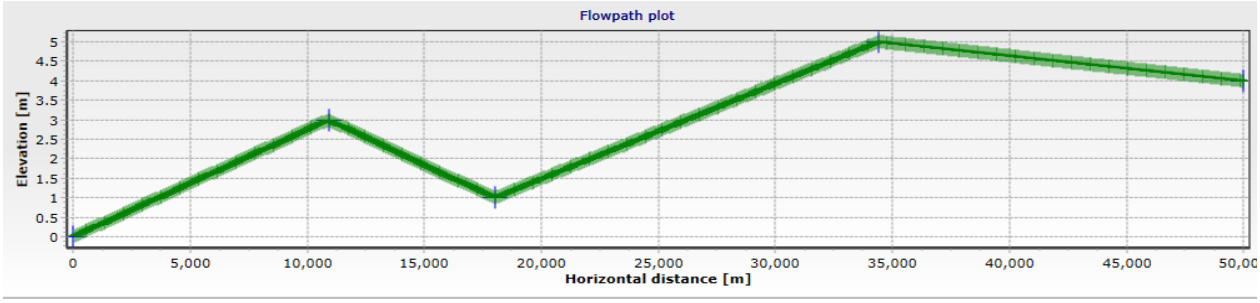

Figure 49: 4th line of the pipeline (offshore)

Further, the flow rate specified in Chapter 3 shall be specified in order to carry out a parametric study to find optimal values of diameter, initial and final pressure.

The parametric study process then begins. The first step is to select the optimal diameter for the given flow rate. The selection was carried out in a number of diameters: 60 mm, 75.5 mm, 88.5 mm, 101.3 mm, 114 mm, 140 mm. As a result, a diameter of 75.5 mm with a wall thickness of 10 mm will be adopted as the most suitable outer diameter for further calculations.

Similarly, a parametric study of the optimal value of the initial and final pressure was carried out, which was selected in the range from 4 to 30 MPa with a step of 0.5 MPa. So, as a result of the study, the value of the final pressure is 6 MPa, since at this value, LNG will be kept in a liquefied state, and the initial pressure will be calculated by the program individually for each case, but will not exceed the values of 12 MPa to ensure normal pumping.

To display the graphs, you must add the test parameters in the TRENDDATA tab. The choice was made in favor of the following parameters reflected in Table 12.

Table 12: Selected Trend Data

Trend Data abbreviation	Description
PT	Pressure
TM	Fluid temperature
GG	Gas mass flow
GL	Liquid bulk mass flow
Geometry	Representation of geometry
ID	Flow regime (1 – Stratified, 2 – Annular, 3 – Slug, 4 – Bubble)

5.1 Results of hydraulic calculation of cryogenic pipeline without thermal insulation

Since 4 lines are considered in the work, therefore, for each of them it is necessary to track the change in phase flow along the length. Hydraulic calculation results are given in Figures 52-55. It can be seen that to estimate the total pressure drop and temperature change, it is necessary to carry out a similar calculation with the addition of thermal insulation on the outer surface of the pipe.

It is important to take into account that since the program allows assessing heat exchange with the environment, and when calculating the cryogenic pipeline, the task of preventing heat inflows from the outside is paramount, all further calculations will be carried out not for average temperatures of water, soil, and air, but the maximum over the past 10 years. This is due to the fact that LNG pumping is a safe process until the fast phase transition phenomenon begins. That is why, assuming that the pipeline operation will be carried out in the summer period as well, all further calculations are carried out for the most unfavorable operating conditions. In the «HeatTransfer» dialog box, you must specify the medium (water, air, gas) and its temperature.

The 1st line calculation was made based on the maximum water temperature at the depth of the pipeline (in Aniva Bay the pipeline will be laid at 50 m), which is 7°C (Figure 31).

2nd and 3rd lines will be calculated at the maximum possible outside air temperature in the warmest period of the year, which for South Sakhalin is 19,7°C for the above-ground laying method. During underground laying, the calculation of these lines of the cryogenic pipeline will be carried out according to the soil temperature at a depth of 2 m, which is the warmest month of the year is 9,4°C.

4th line is also underwater and at a depth of 40 m, the design temperature will be 4°C.

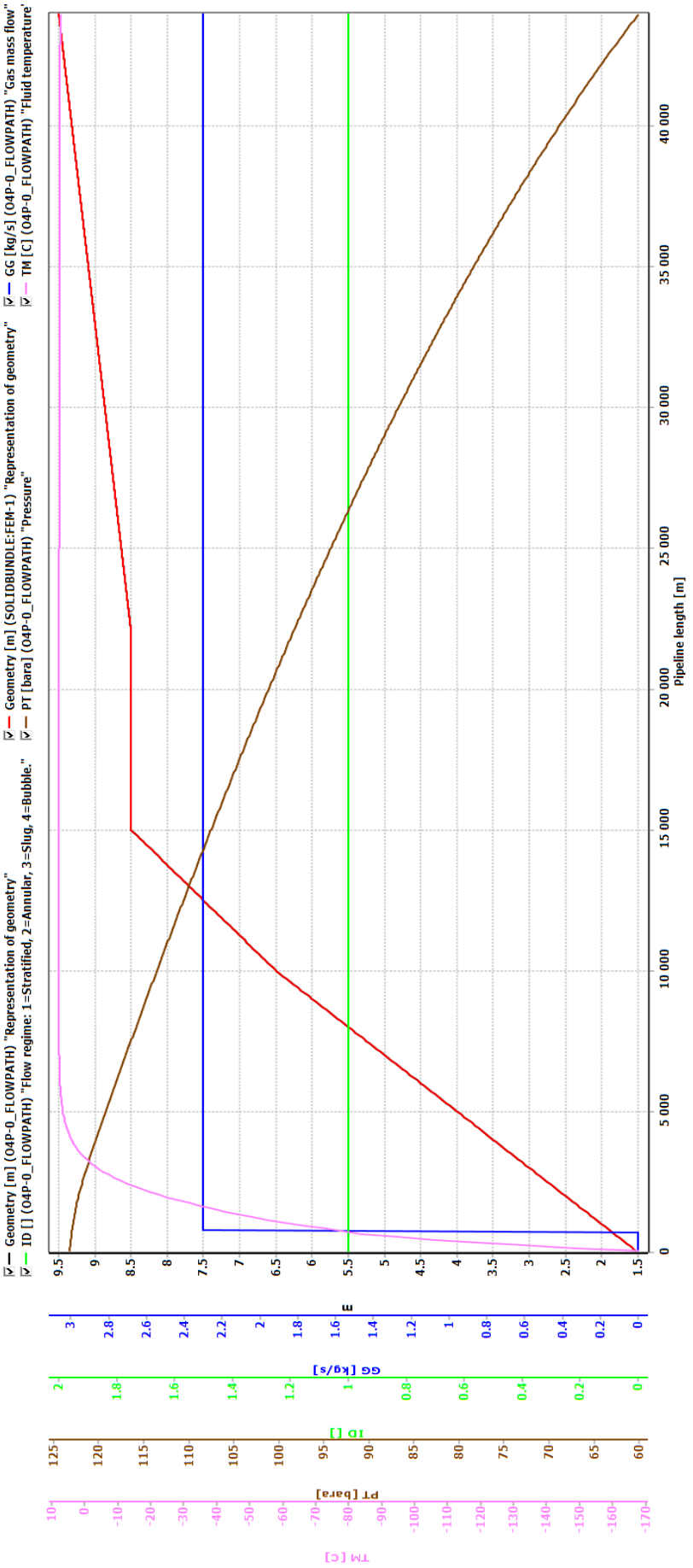

Figure 50: 1st section cryogenic pipeline without isolation

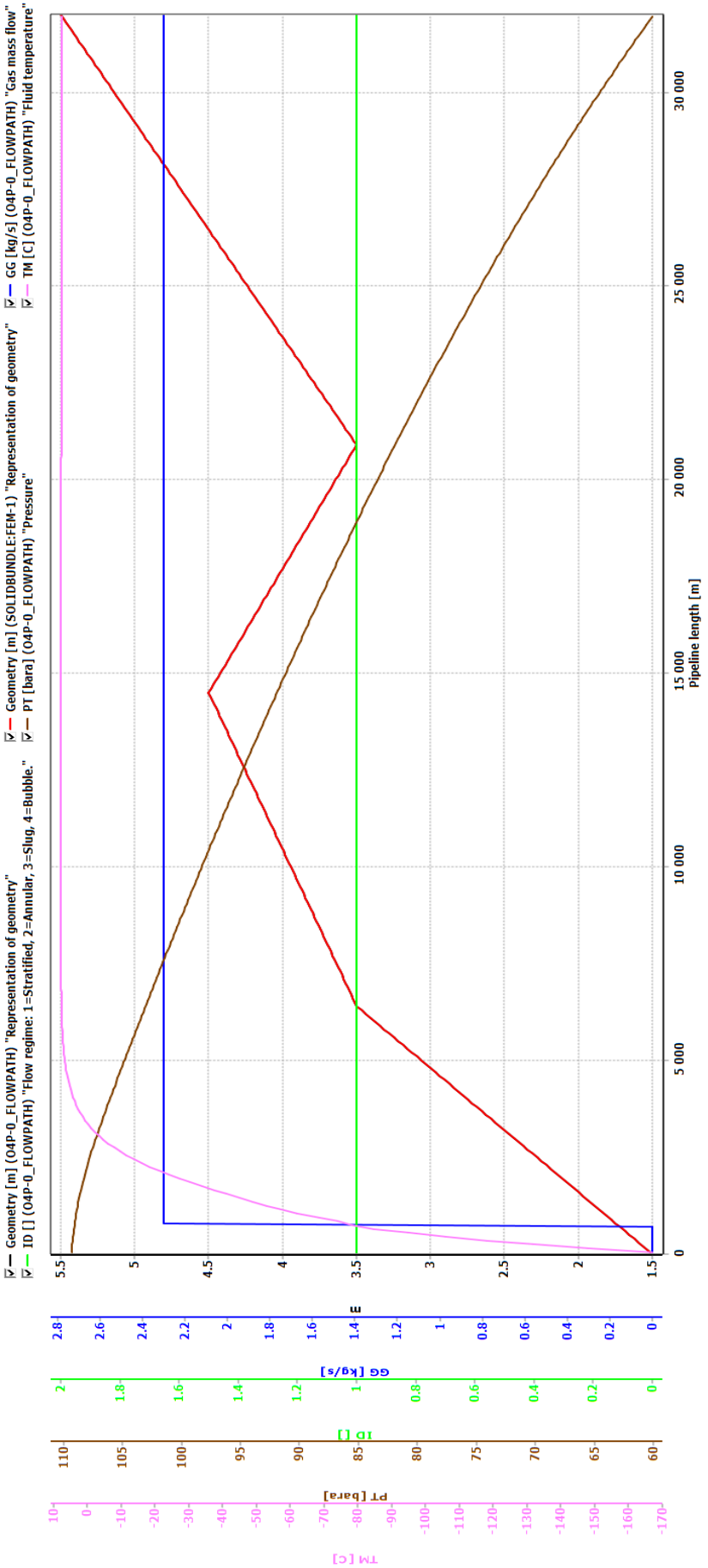

Figure 51: 2nd section of the cryogenic pipeline without isolation

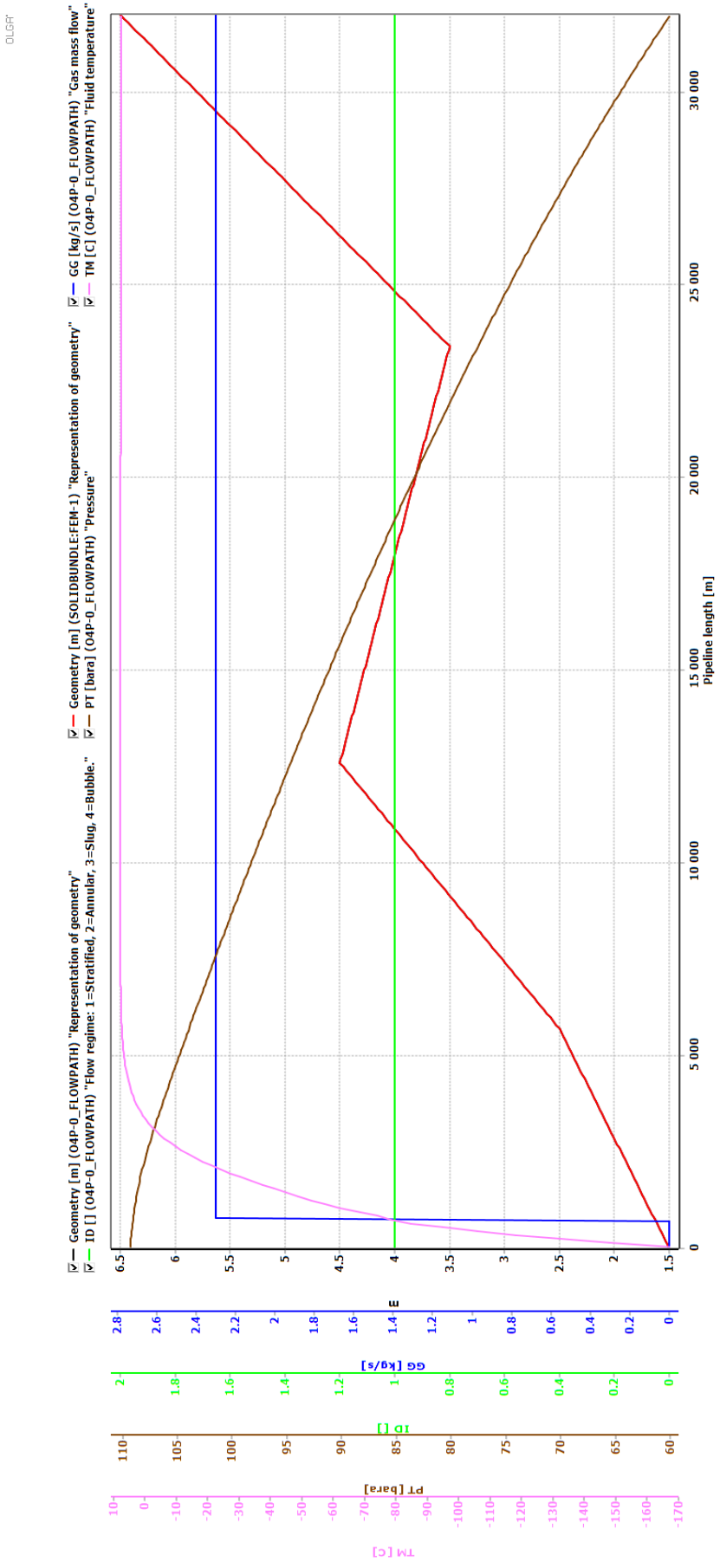

Figure 52: 3rd section of the cryogenic pipeline without isolation

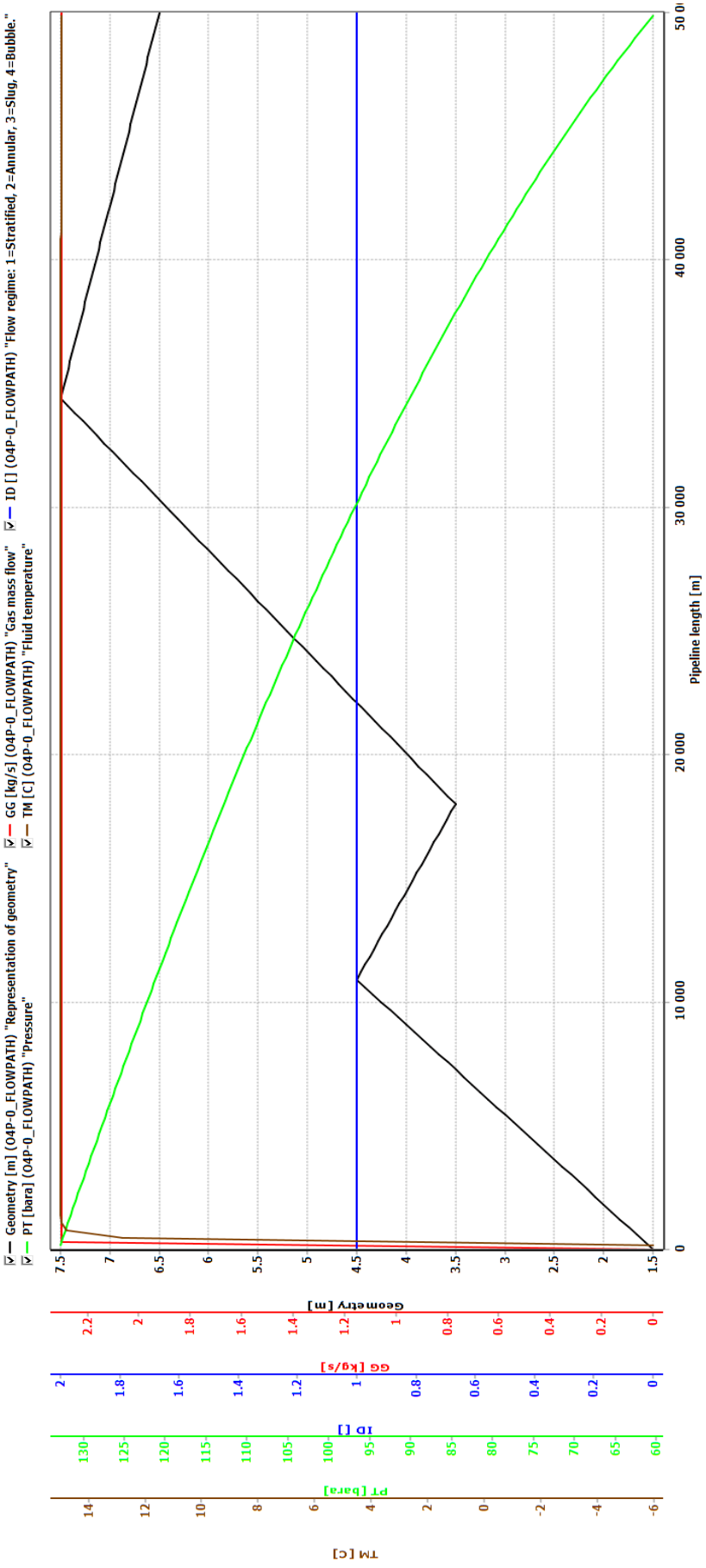

Figure 53: 4th section of the cryogenic pipeline without isolation

As a result, analyzing the change in the parameter GG, it can be concluded that its value is zero only at the very beginning of pumping, then the FPT of LNG from the liquefied state goes into gas and expands, increasing the temperature and creating an emergency. Despite the use of cold-resistant steel, long-distance pumping of LNG through cryogenic pipelines can be carried out exclusively using thermal insulation. The following points of calculation will consider the use of thermal aerogel insulation with a protective steel stainless casing for the above-ground laying, as well as multilayer thermal insulation from fiber and cellular thermal insulation for the underground laying at a depth of 2 m.

5.2 Hydraulic calculation of underwater and above-ground lines of the cryogenic pipeline using aerogel thermal insulation

As part of the work, two versions of the cryogenic pipeline design will be considered. In this case, all lines of the pipeline will be made with the application of powder thermal insulation based on aerogel.

To add thermal insulation, do the same as when creating a pipe wall. In the Library→Add→Material enter the aerogel characteristics (Table 6) and add the desired thickness in the «Wall» line.

The calculation was carried out in stages, it was first decided to add 5 mm of insulating material, and then, analyzing the state according to the resulting schedules, increase the thickness as necessary until there was no gas phase over the entire length of the area under investigation.

For an underwater section with a total length of 45 km, 5 calculations were made for 5 different thicknesses of thermal insulation. The 5 mm step was selected based on the manufacturer's proposed size of the product supplied. Cryogel Z produces thermal insulation based on the aerogel with mats, 5 and 10 mm thick. The results of the studies are given in Figures 56-60. In addition, for protection of material of thermal isolation the installation of the protection cover from stainless steel 08H18N10 4 mm thick is provided.

It can be seen that when using a 5 mm aerogel, the maximum possible distance by which it is possible to pump cryogenic liquid is less than 10 km. Therefore, it is necessary to continue the calculation.

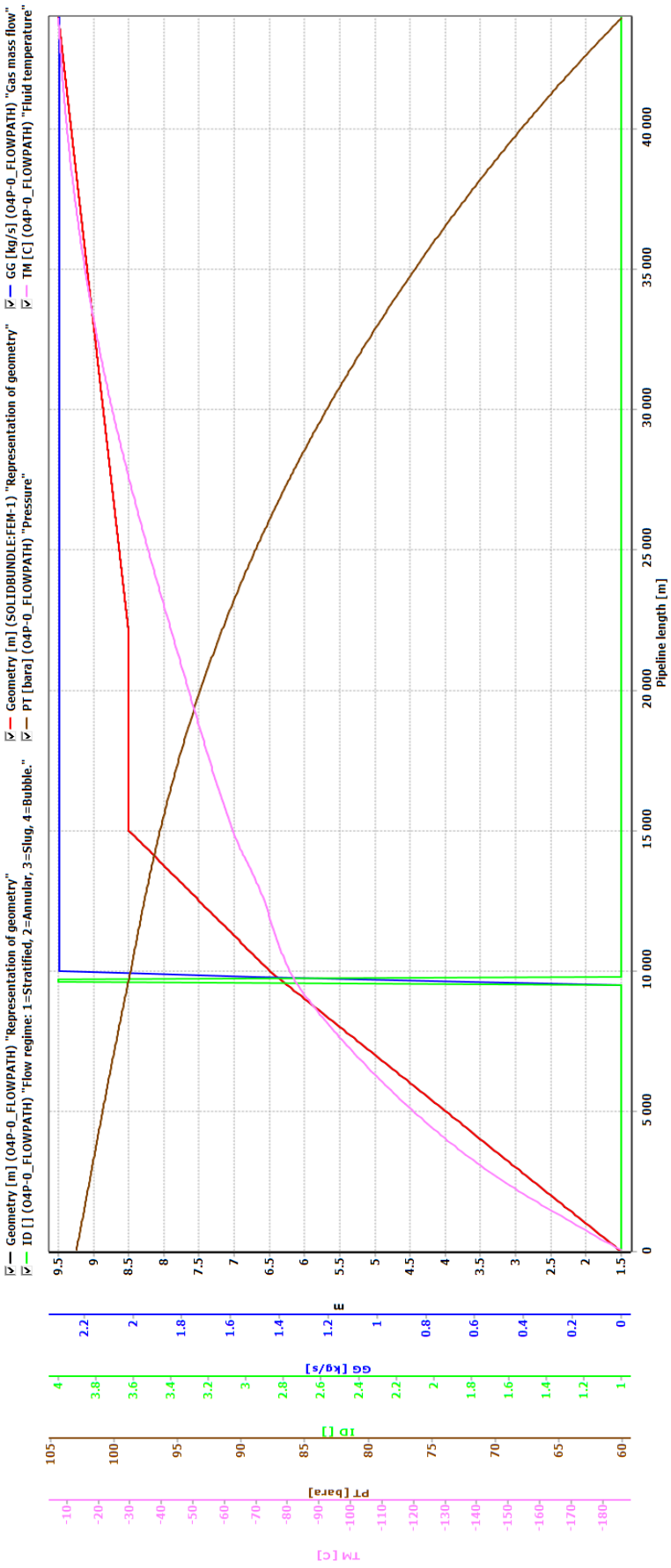

Figure 54: Results of hydraulic calculation with aerogel thermal insulation thickness 5 mm for 1st line of LNG cryogenic pipeline

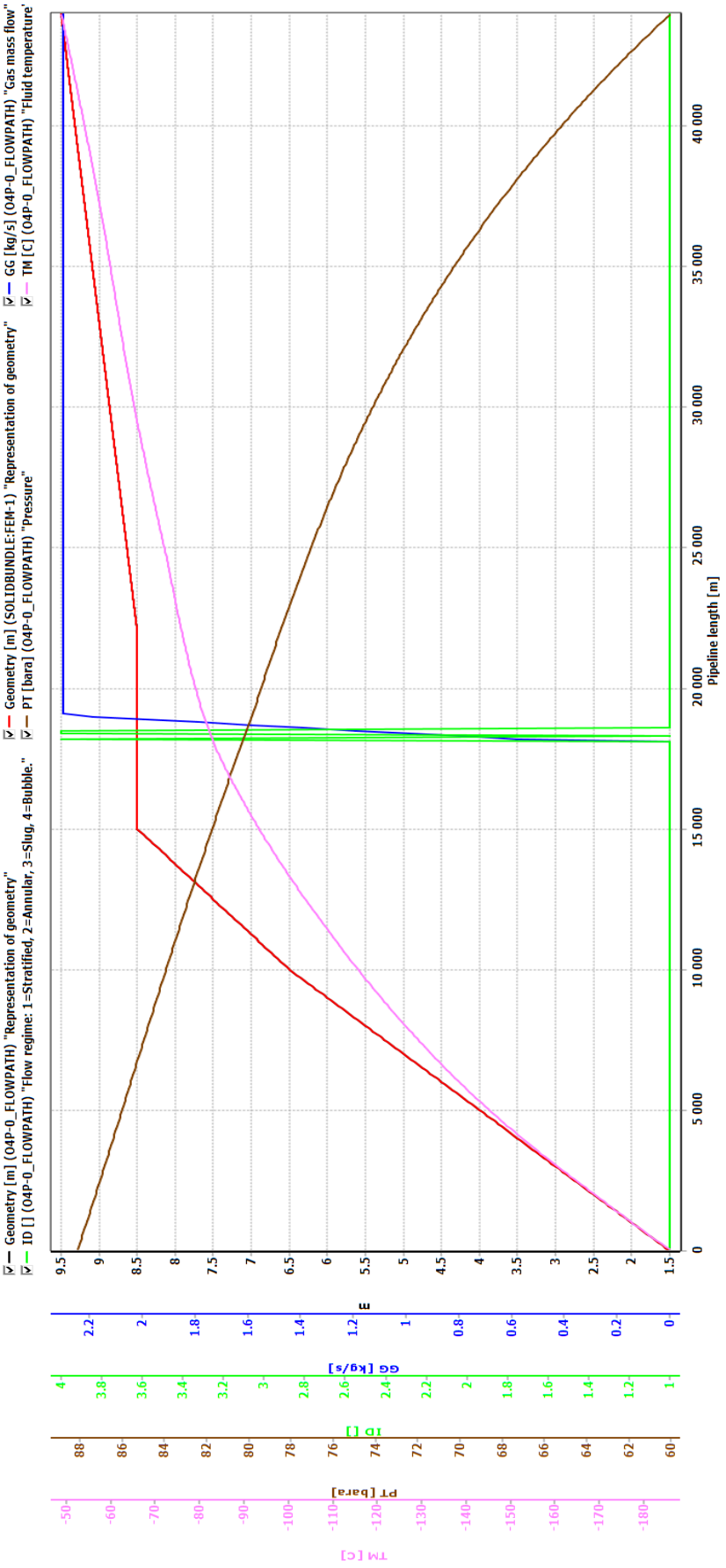

Figure 55: Results of hydraulic calculation with aerogel thermal insulation thickness 10 mm for 1st line of LNG cryogenic pipeline

According to the graphical result, it can be concluded that 10 mm is also insufficient and a further gradual increase in the thickness of the thermal insulation is required.

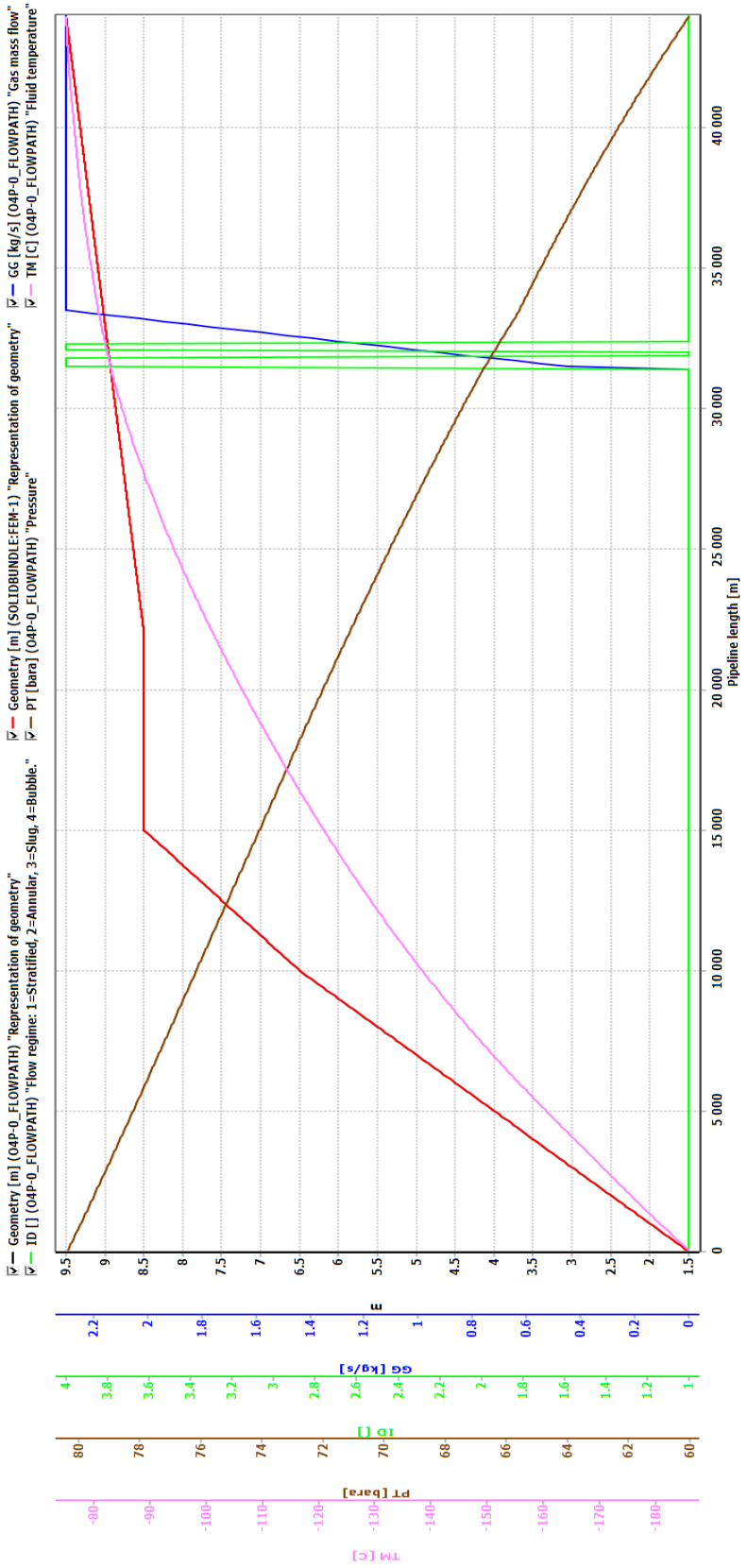

Figure 56: Results of hydraulic calculation with aerogel thermal insulation thickness 15 mm for 1st line of LNG cryogenic pipeline

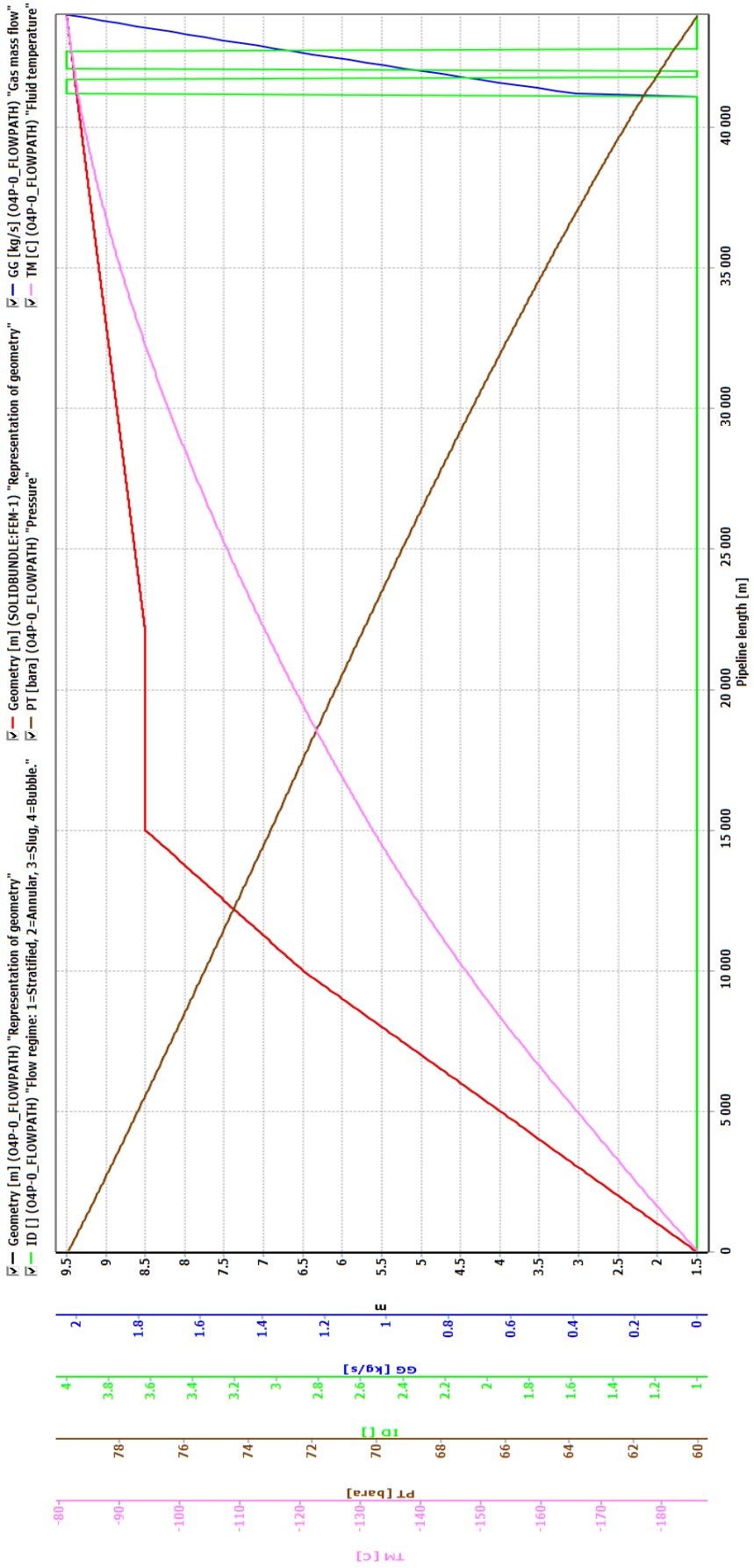

Figure 57: Results of hydraulic calculation with aerogel thermal insulation thickness 20 mm for 1st line of LNG cryogenic pipeline

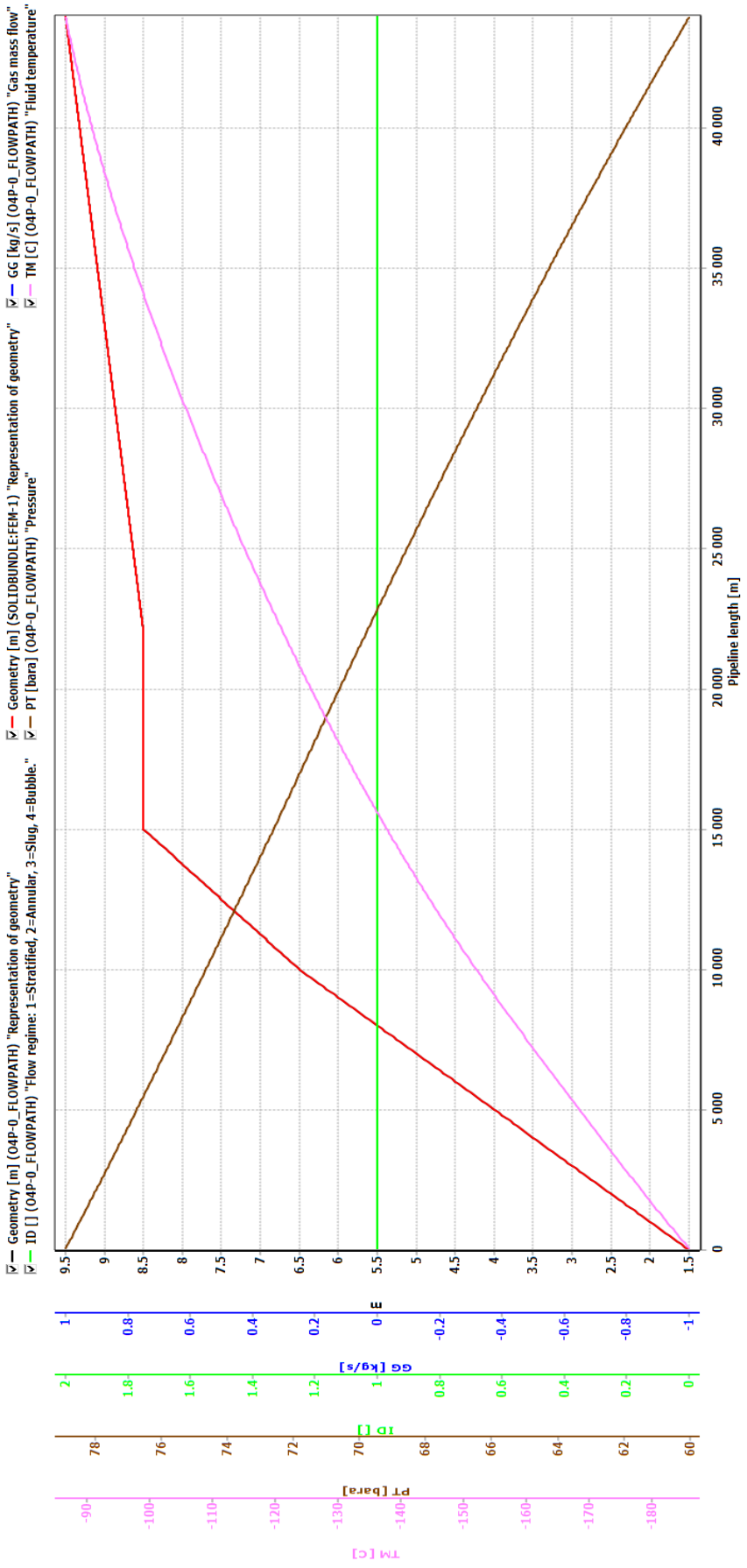

Figure 58: Results of hydraulic calculation with aerogel thermal insulation thickness 25 mm for 1st line of LNG cryogenic pipeline

It can be seen that 25 mm aerogel thermal insulation will be required to ensure flow integrity. The initial pressure in the 1st line is 7,889 MPa, the final pressure is 6 MPa. The temperature at the beginning of the line section is -185,893°C, and at the end -90°C.

Two subsequent sections will be laid above ground. The choice of this method of laying is due to the possibility of visual inspection of the integrity of the structure. Results of 2nd line section calculations are given in Figures 61-64.

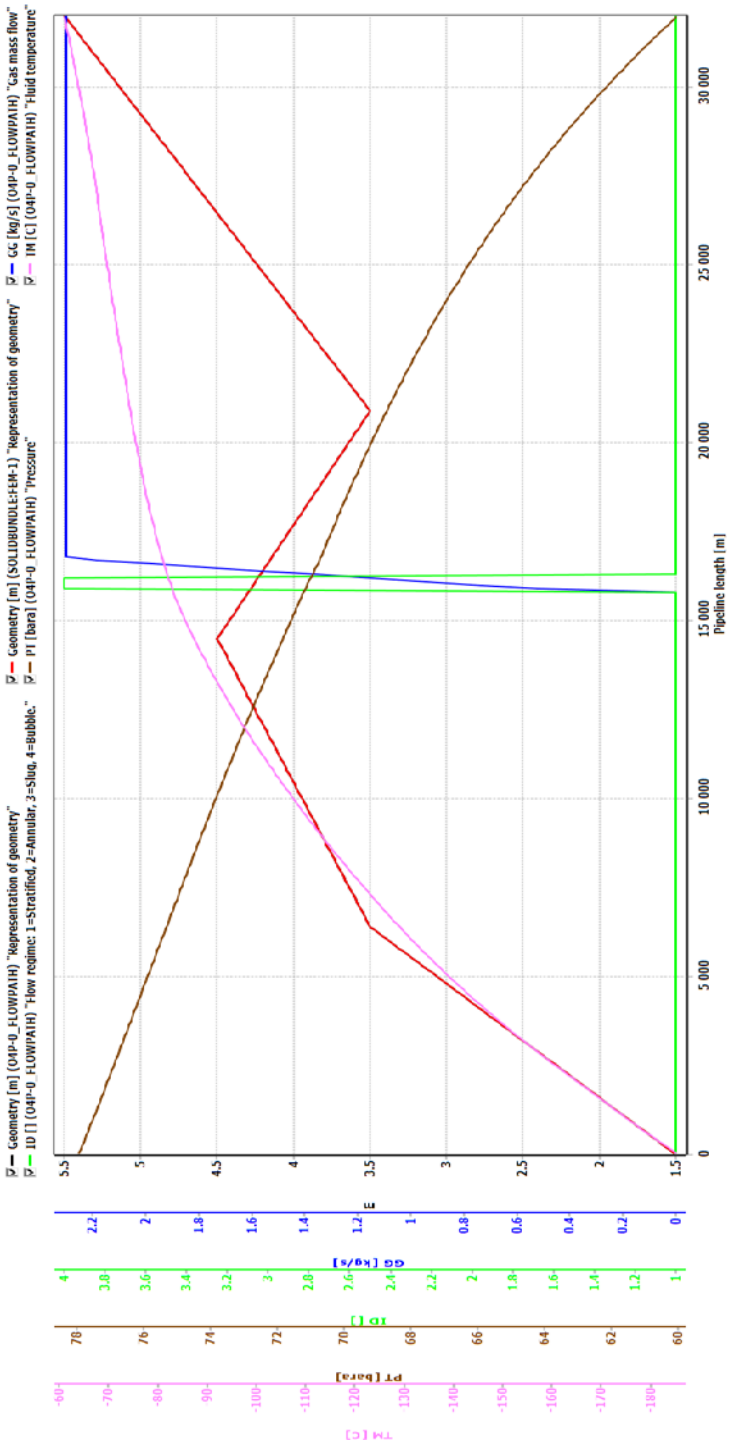

Figure 59: Results of hydraulic calculation with aerogel thermal insulation thickness 5 mm for 2nd above-ground line of LNG cryogenic pipeline

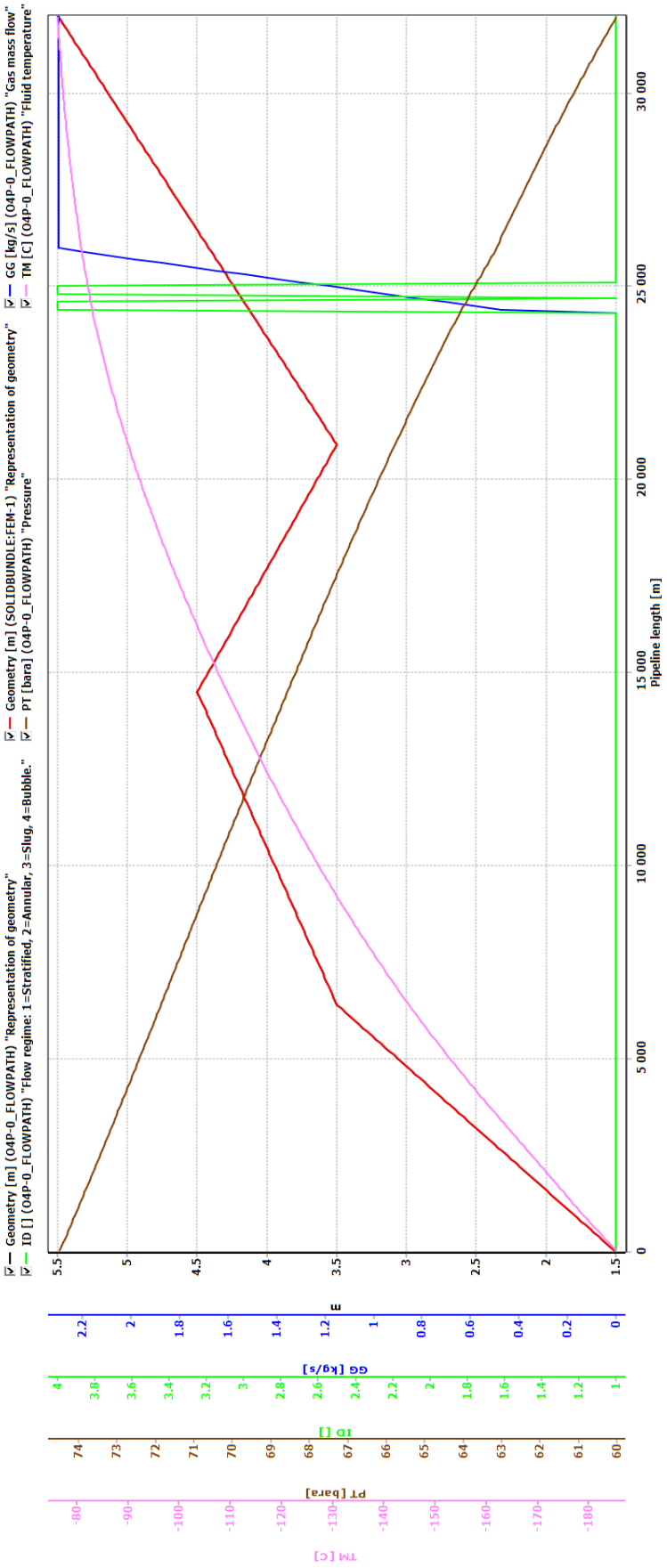

Figure 60: Results of hydraulic calculation with aerogel thermal insulation thickness 10 mm for 2nd above-ground line of LNG cryogenic pipeline

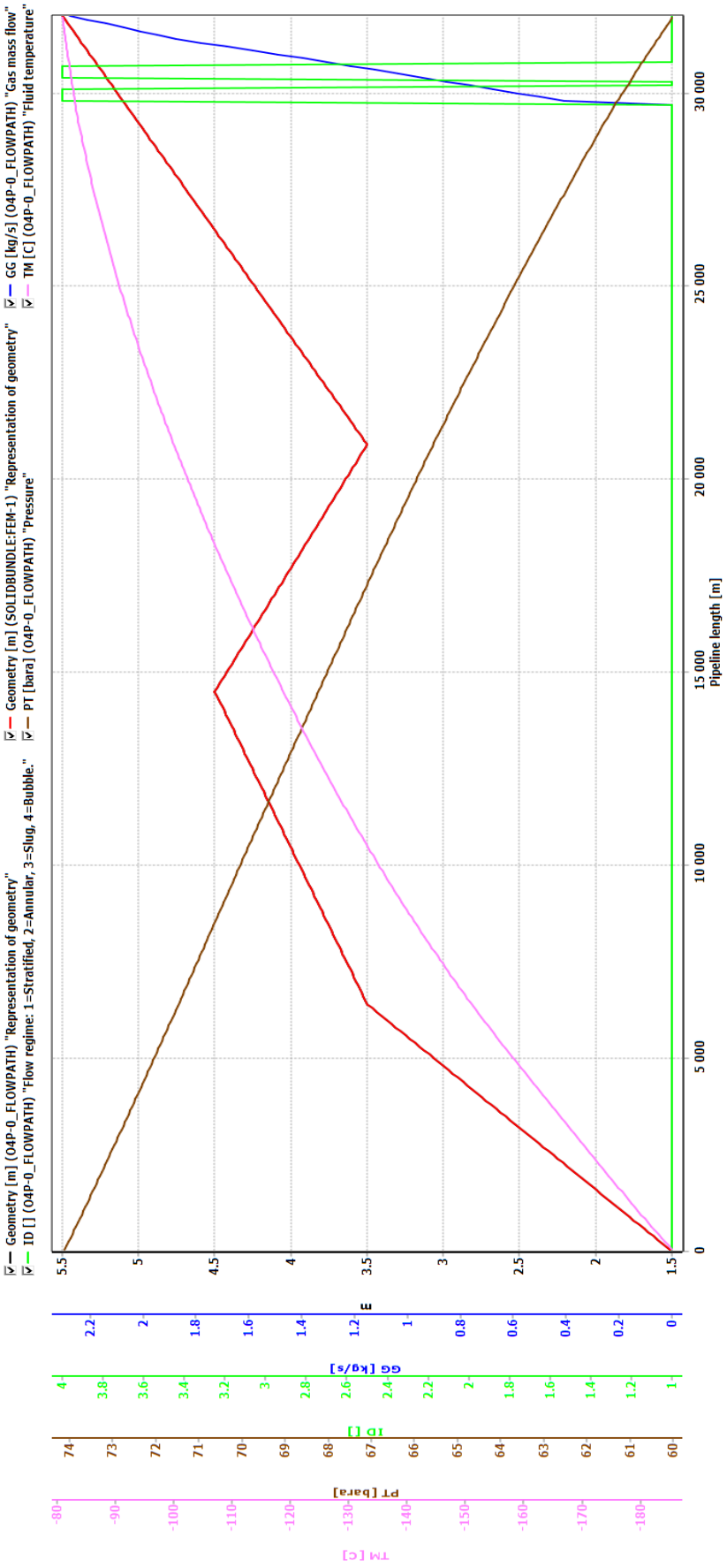

Figure 61: Results of hydraulic calculation with aerogel thermal insulation thickness 15 mm for 2nd above-ground line of LNG cryogenic pipeline

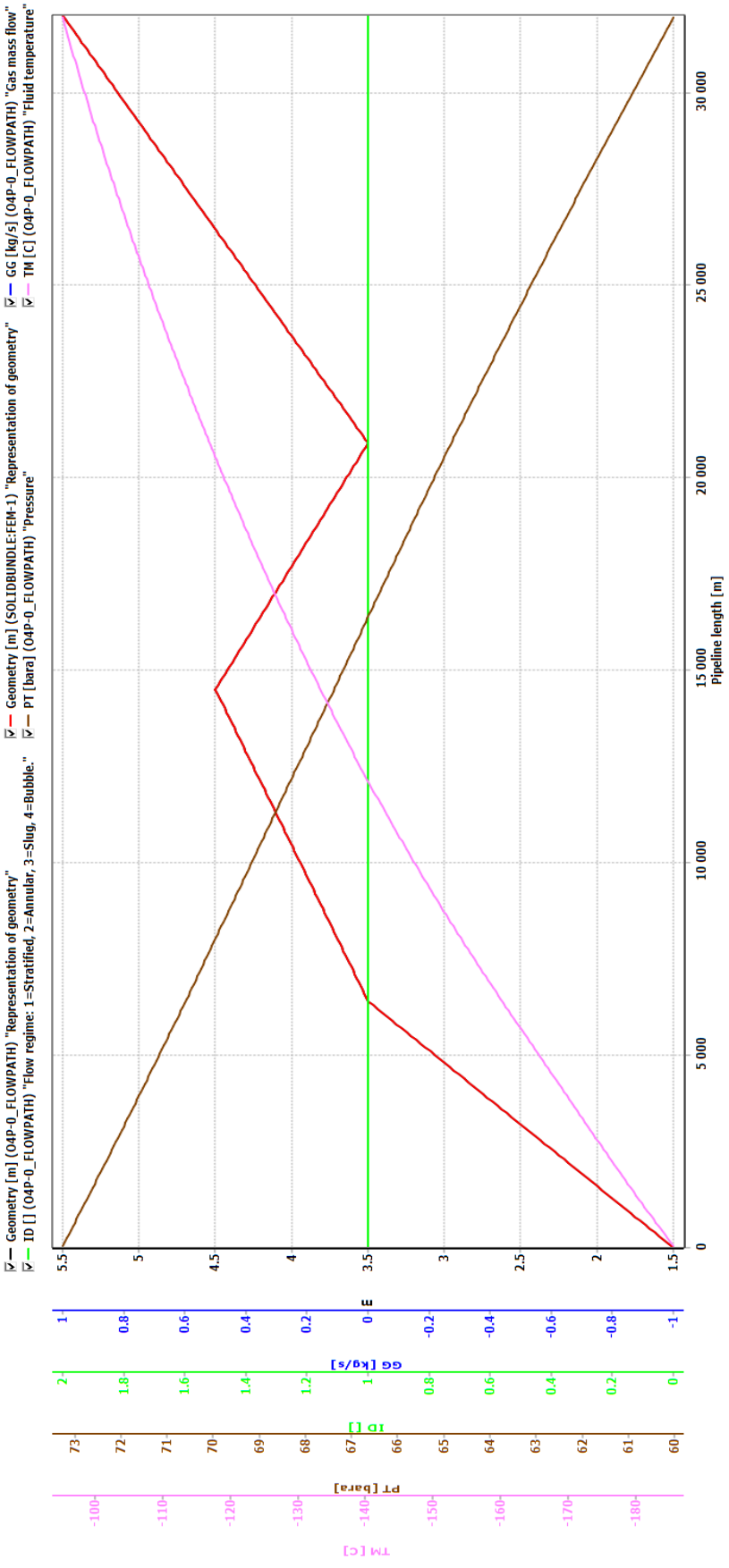

Figure 62: Results of hydraulic calculation with aerogel thermal insulation thickness 20 mm for 2nd above-ground line of LNG cryogenic pipeline

In this case, the initial and final parameters are P_1=7,326 MPa, t_{in}=-185,549°C, P_2=6 MPa, t_{out}=–90°C with thermal insulation thickness of 20 mm.

A similar calculation was made for the 3rd above-ground area, the results of which are given in Figures 65-68.

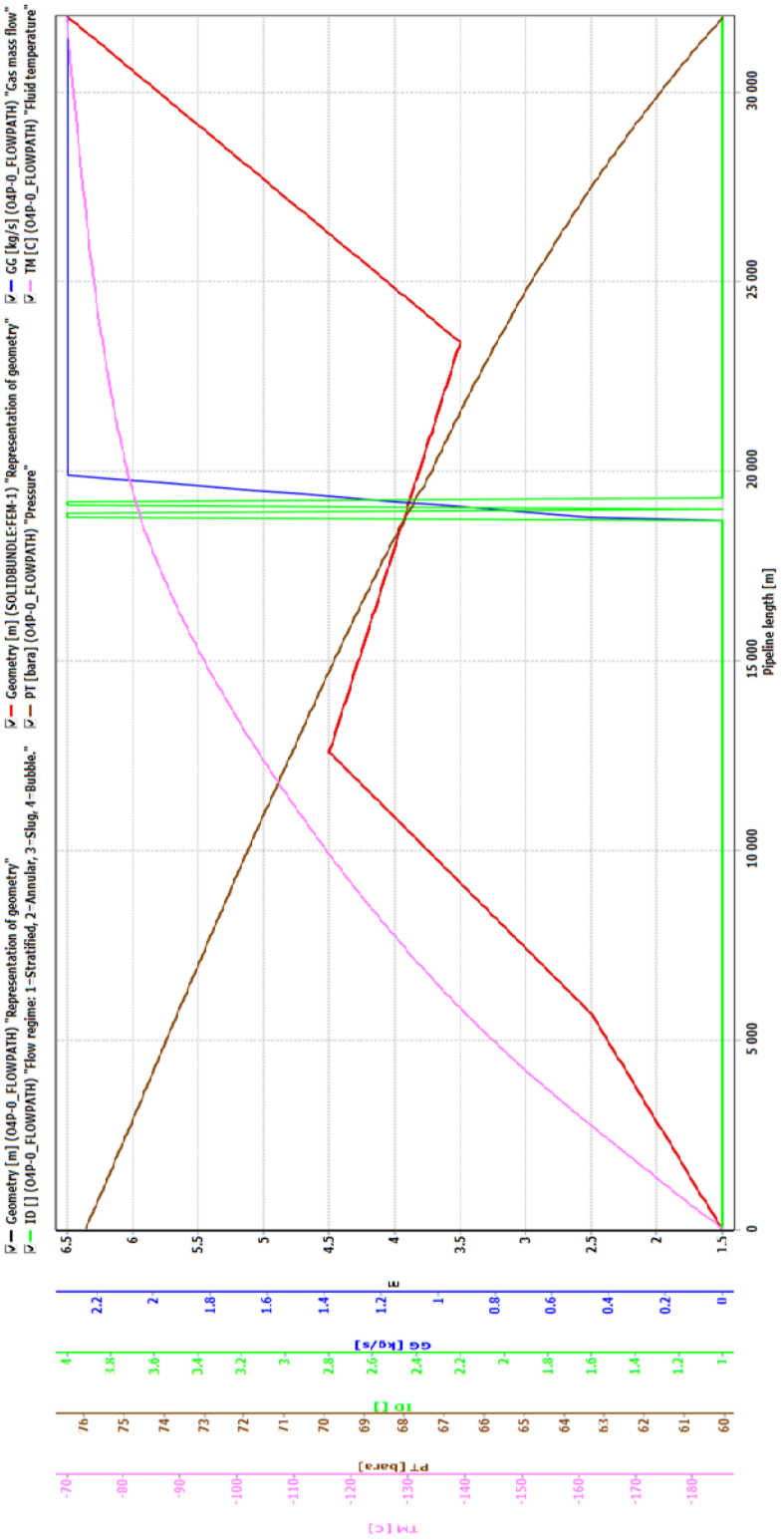

Figure 63: Results of hydraulic calculation with aerogel thermal insulation thickness 5 mm for 3rd above-ground line of LNG cryogenic pipeline

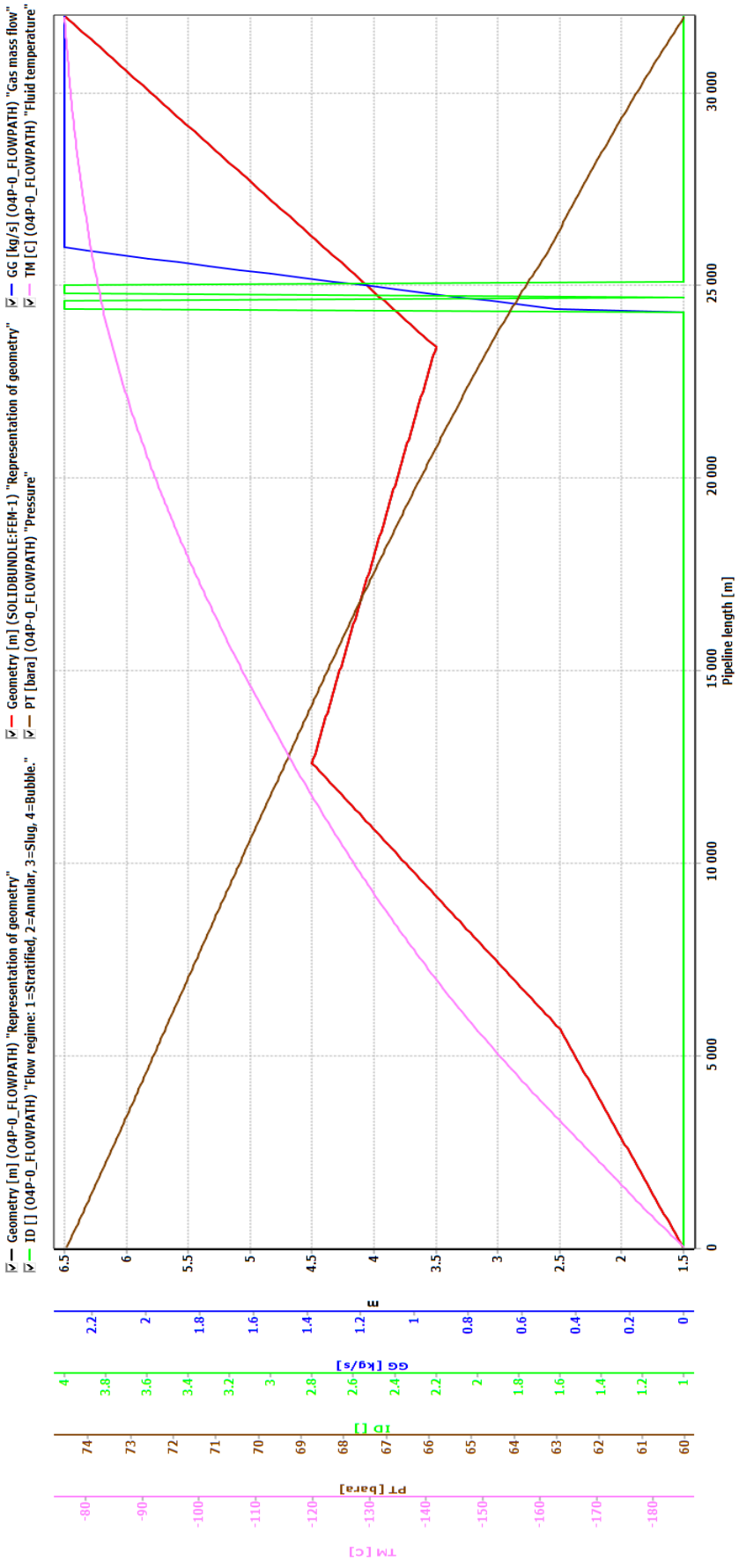

Figure 64: Results of hydraulic calculation with aerogel thermal insulation thickness 10 mm for 3rd above-ground line of LNG cryogenic pipeline

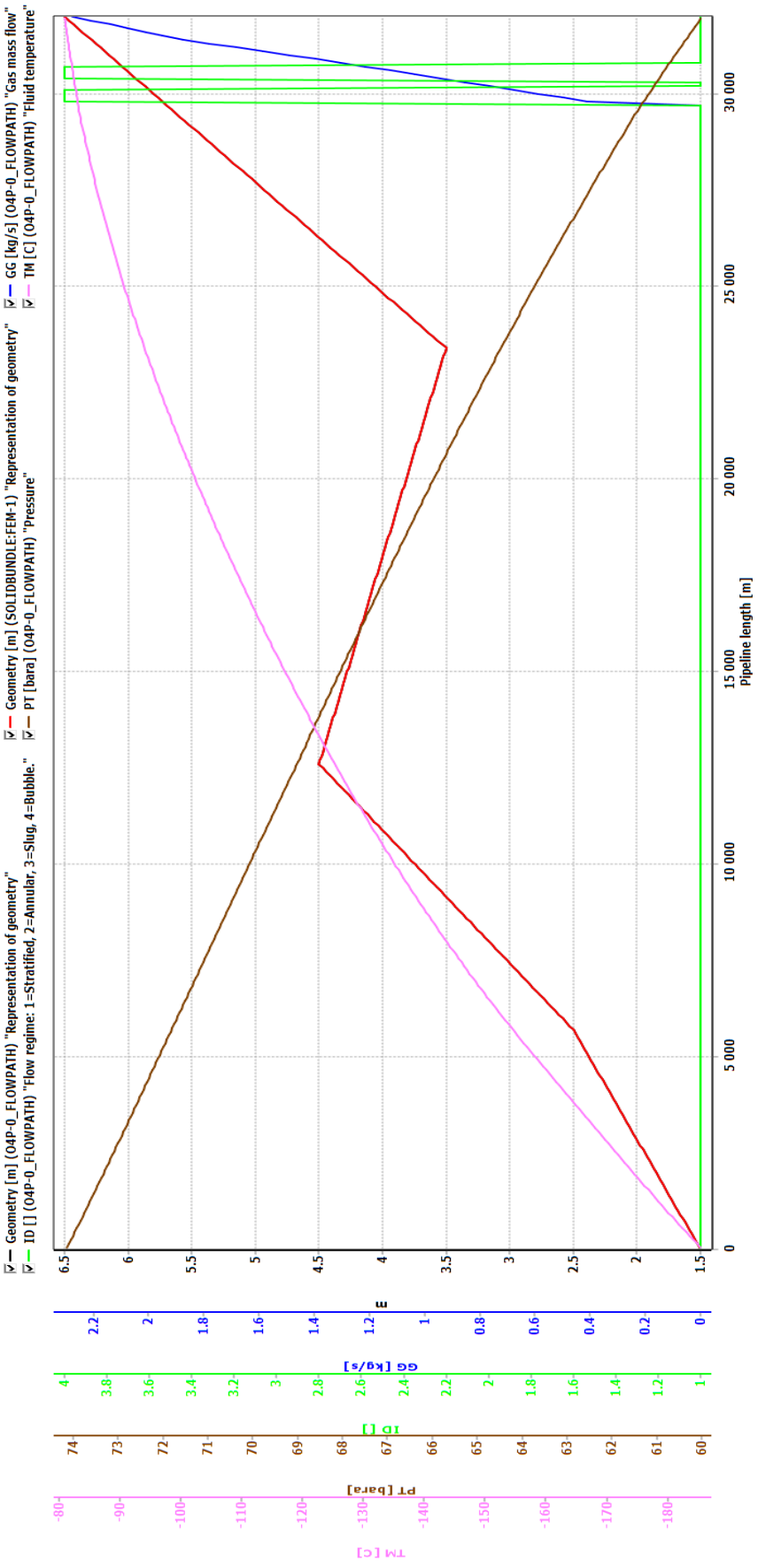

Figure 65: Results of hydraulic calculation with aerogel thermal insulation thickness 15 mm for 3rd above-ground line of LNG cryogenic pipeline

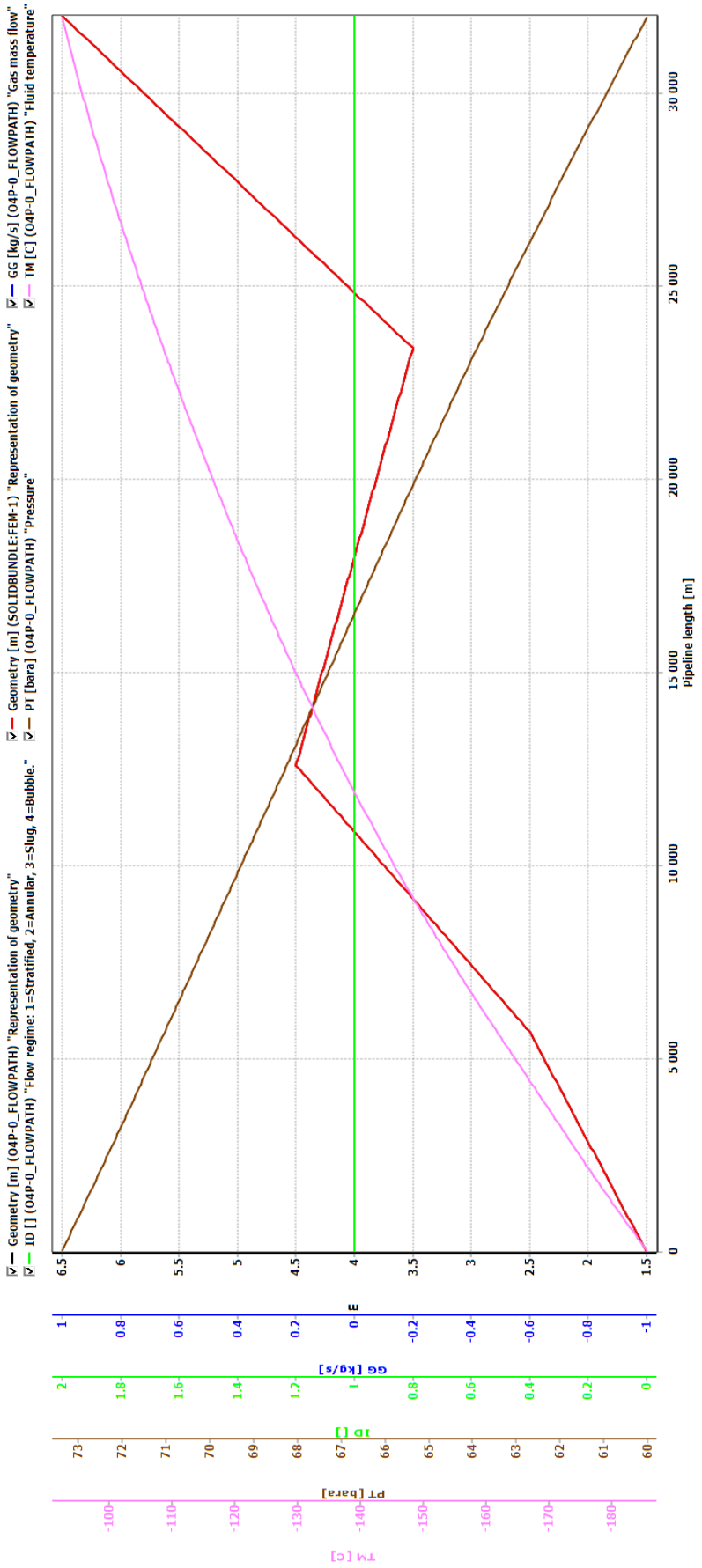

Figure 66: Results of hydraulic calculation with aerogel thermal insulation thickness 20 mm for 3rd above-ground line of LNG cryogenic pipeline

In this case, the initial and final parameters are P_1=7,3371 MPa, t_{in}=-185,531°C, P_2=6 MPa, t_{out}=–90°C at thermal insulation thickness 20 mm. The division of the above-ground part of the pipeline into 2 line sections (2nd and 3rd) was carried out from the following results: the construction of a single pipeline line will be extremely cost-effective since to ensure the maintenance of thermal balance, aerogel thermal insulation must be provided, the thickness of which exceeds the diameter of the pipeline by 1.5-2 times. The last line section is the underwater section, which is responsible for the transport of LNG to Japan. Calculation results are given in Figures 69-73.

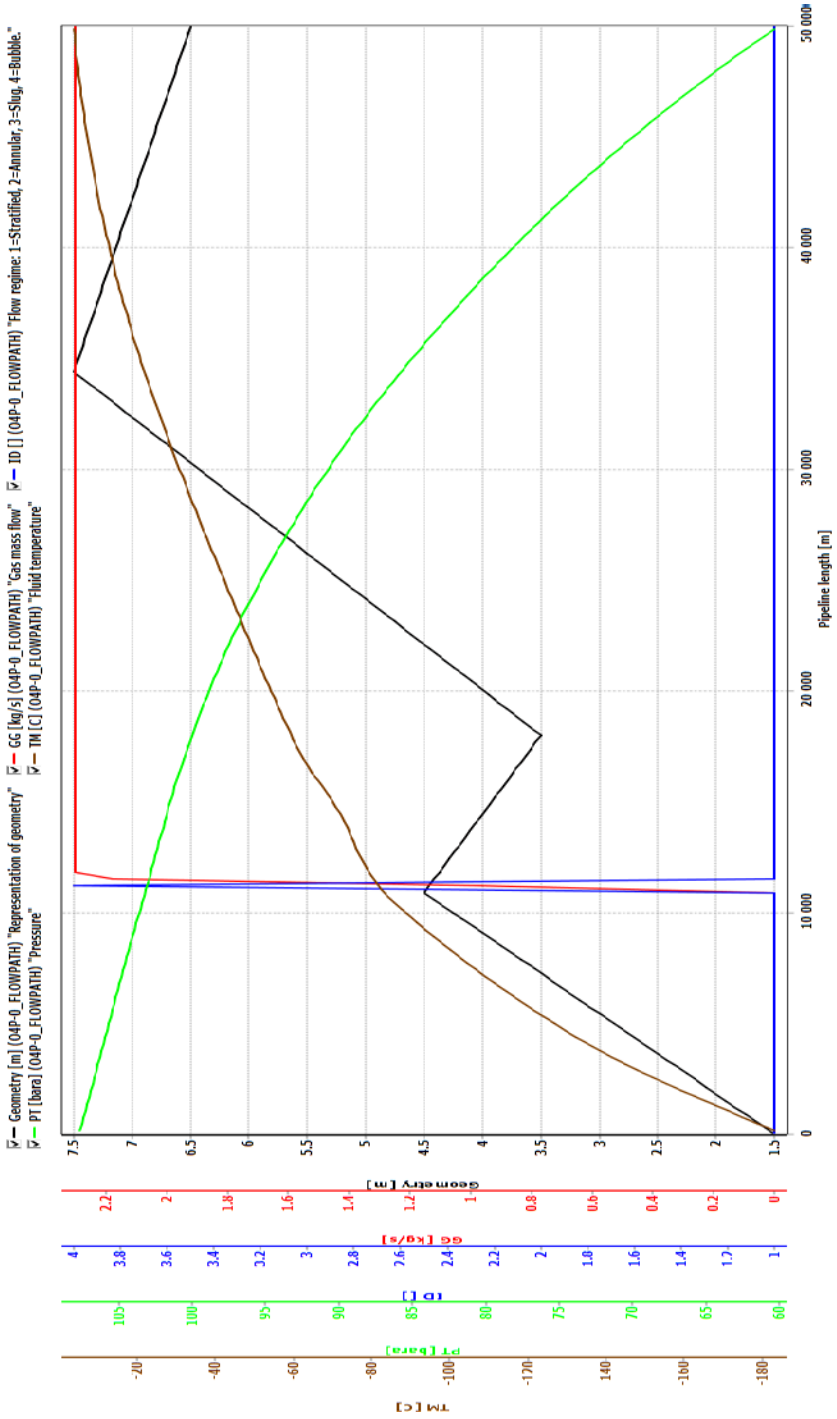

Figure 67: Results of hydraulic calculation with aerogel thermal insulation thickness 5 mm for 4th line of LNG cryogenic pipeline

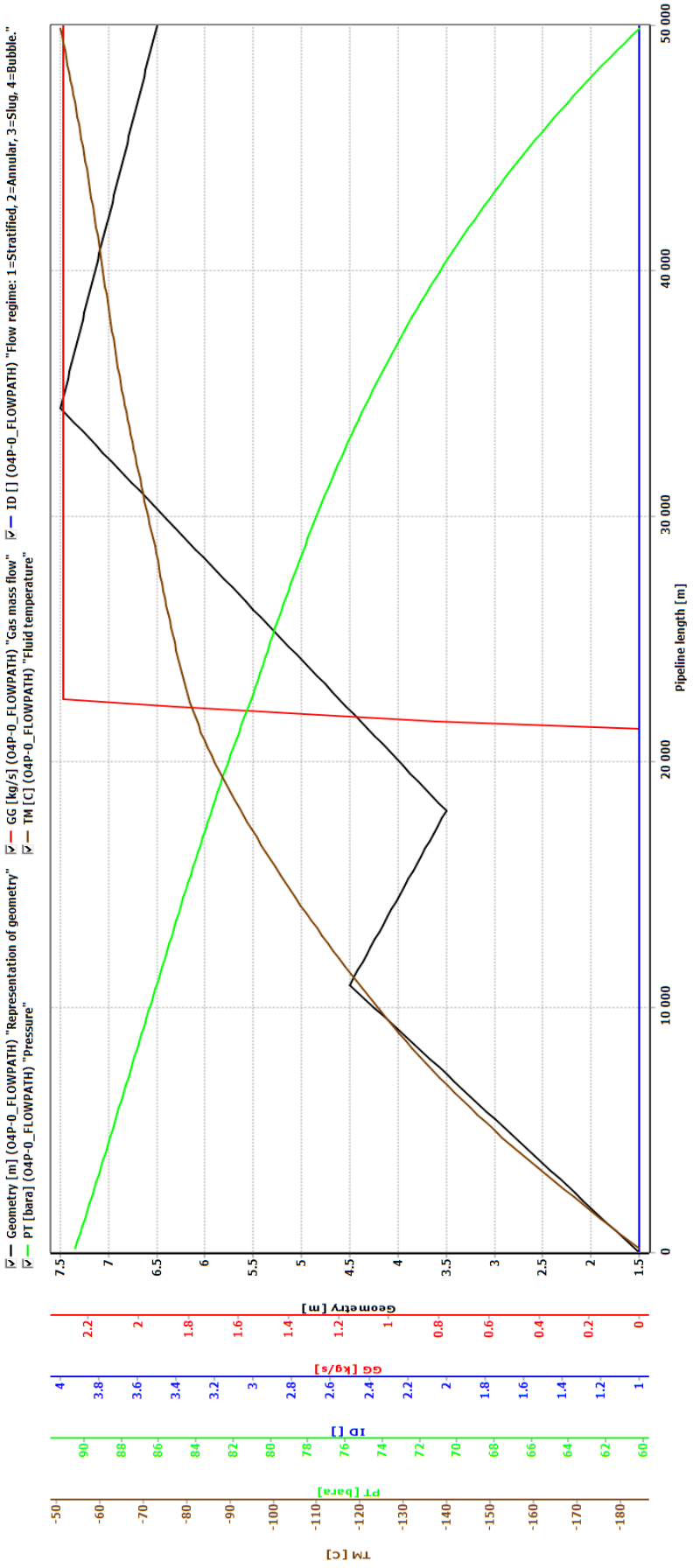

Figure 68: Results of hydraulic calculation with aerogel thermal insulation thickness 10 mm for 4th line of LNG cryogenic pipeline

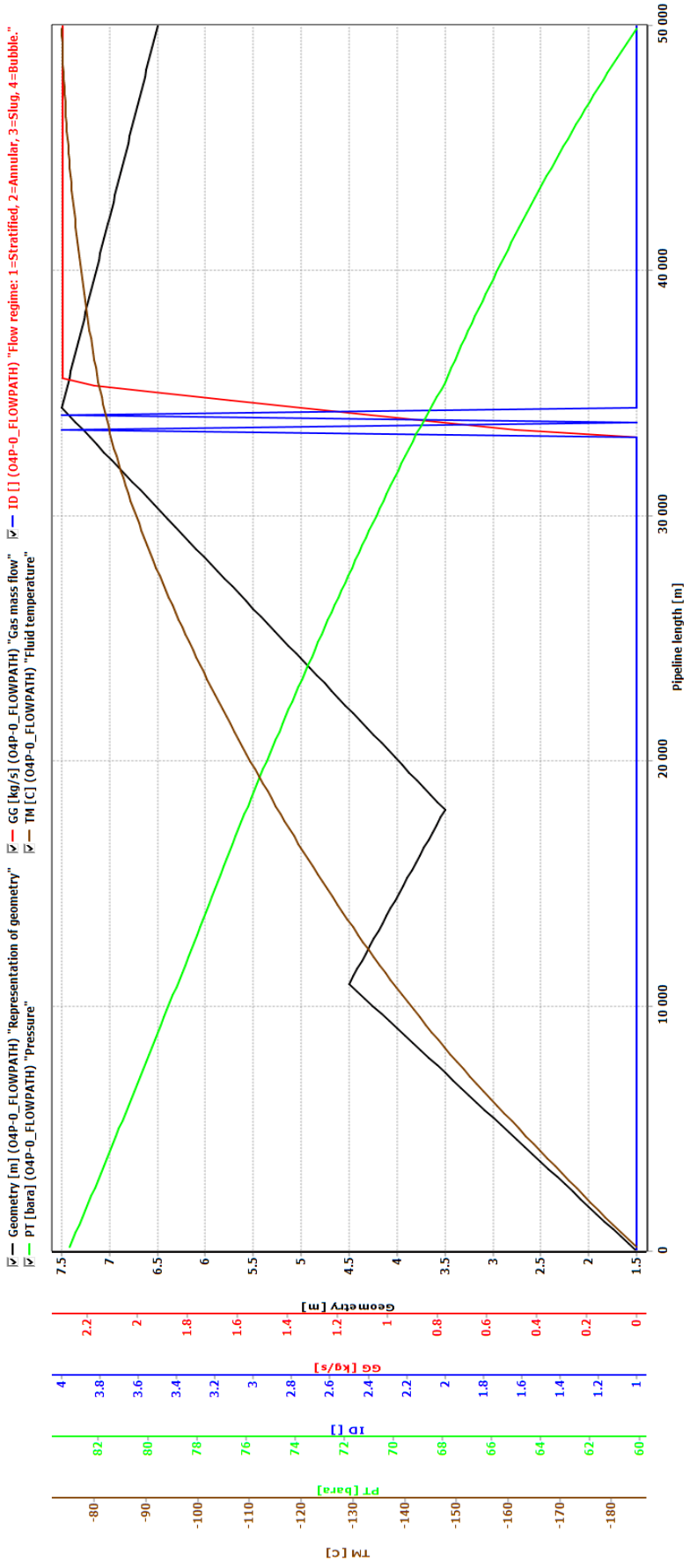

Figure 69: Results of hydraulic calculation with aerogel thermal insulation thickness 15 mm for 4th line of LNG cryogenic pipeline

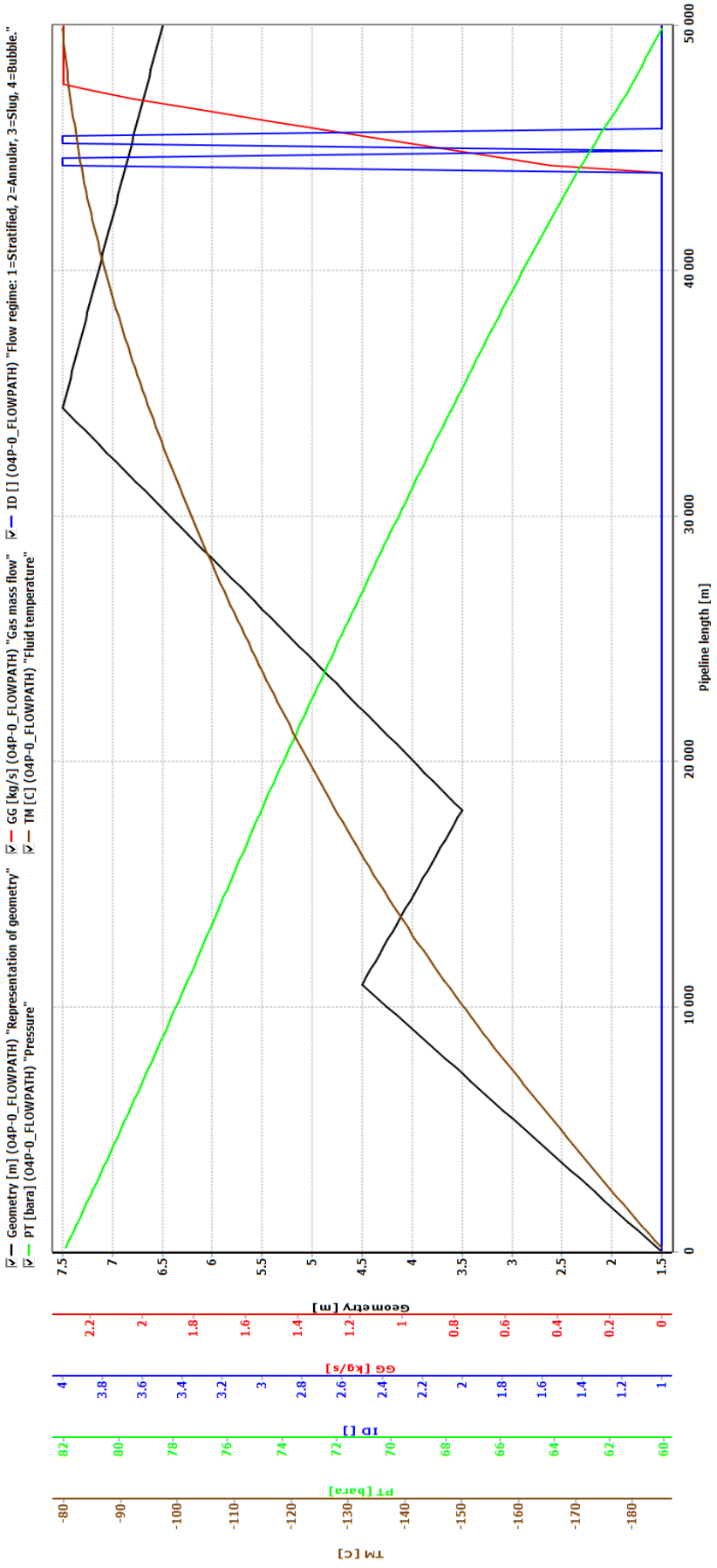

Figure 70: Results of hydraulic calculation with aerogel thermal insulation thickness 20 mm for 4th line of LNG cryogenic pipeline

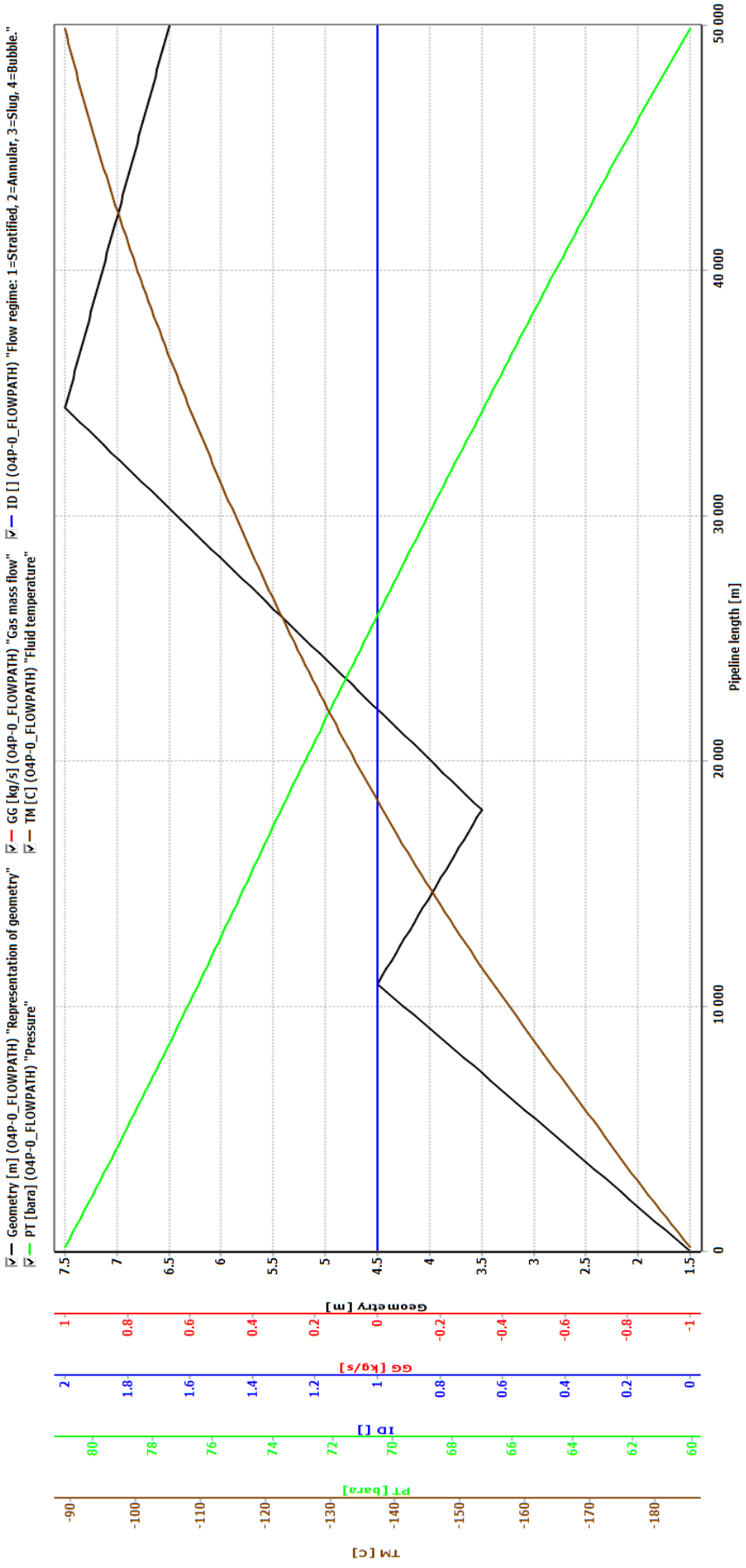

Figure 71: Results of hydraulic calculation with aerogel thermal insulation thickness 25 mm for 4th line of LNG cryogenic pipeline

From the results of the hydraulic calculation, it can be seen that sufficient thicknesses of thermal insulation are required to maintain the single-phase liquid flow, and since the aerogel is a new and expensive material, multilayer thermal insulation will be selected in the next item in the underground laying method.

5.3 Hydraulic calculation of underwater and underground sections of cryogenic pipeline with multilayer thermal insulation

Multilayer thermal insulation consists of the following layers: glass fiber layer, foam synthetic rubber layer, glass fiber layer, foam synthetic rubber layer, protective casing.

Underground laying will save the landscape of the area since in the future the state plans to expand the infrastructure of the southwestern part of Sakhalin to attract tourists there.

Hydraulic calculation for multilayer thermal insulation was carried out in the same way as above, the only difference was the separation of the thermal insulation layers when setting the thickness of the pipe wall. The results of hydraulic calculation of the required thermal insulation thickness are summarized in Table 13.

Table 13: Hydraulic Calculation Results Using Multilayer Thermal Insulation

№ section	P_1, MPa	P_2, MPa	T_{in}, °C	T_{out}, °C	$\delta_{isolation}$, mm
1 (underwater)	7,863	6	-185,8	-90	30 mm each layer
2 (underground)	7,285		-183,6		25 mm each layer
3 (underground)	7,197		-182,9		25 mm each layer
4 (underwater)	8,065		-187,3		30 mm each layer

The results of the hydraulic calculation show that in comparison with aerogel thermal insulation, the thickness of the multilayer thermal insulation exceeds its value by about 4 times.

Since the basic functionality of the program allows you to calculate the axial temperature distribution, you can track the transverse heat exchange for pipelines surrounded by solid medium (in this case, soil). To simulate temperature distributions, a FEMTherm package is provided in the OLGA software complex. Creating a model in this package will allow you to evaluate the effectiveness of the thermal insulation design, namely, to investigate whether there is a possibility of heat loss to the soil.

To begin, create a heat source as follows: Library→Add→Thermal Component and immerse the investigated pipeline in the soil, setting its characteristics. Figure 74 shows a screenshot of the initial data set.

The depth of 0.4 m is chosen conditional to obtain pictures on an adequate scale. If there are heat inflows, they will also appear at the specified depth, since the calculation temperature is indicated according to the initial data.

Then, specify the points at which the trend and profile will be drawn in the «Observation» tab. By setting the coordinates of interest, we select the necessary variables that will be calculated (in this case, TBUNXY, the temperature at a specific point in the object, was selected). The process of creating study points is given in Figure 75.

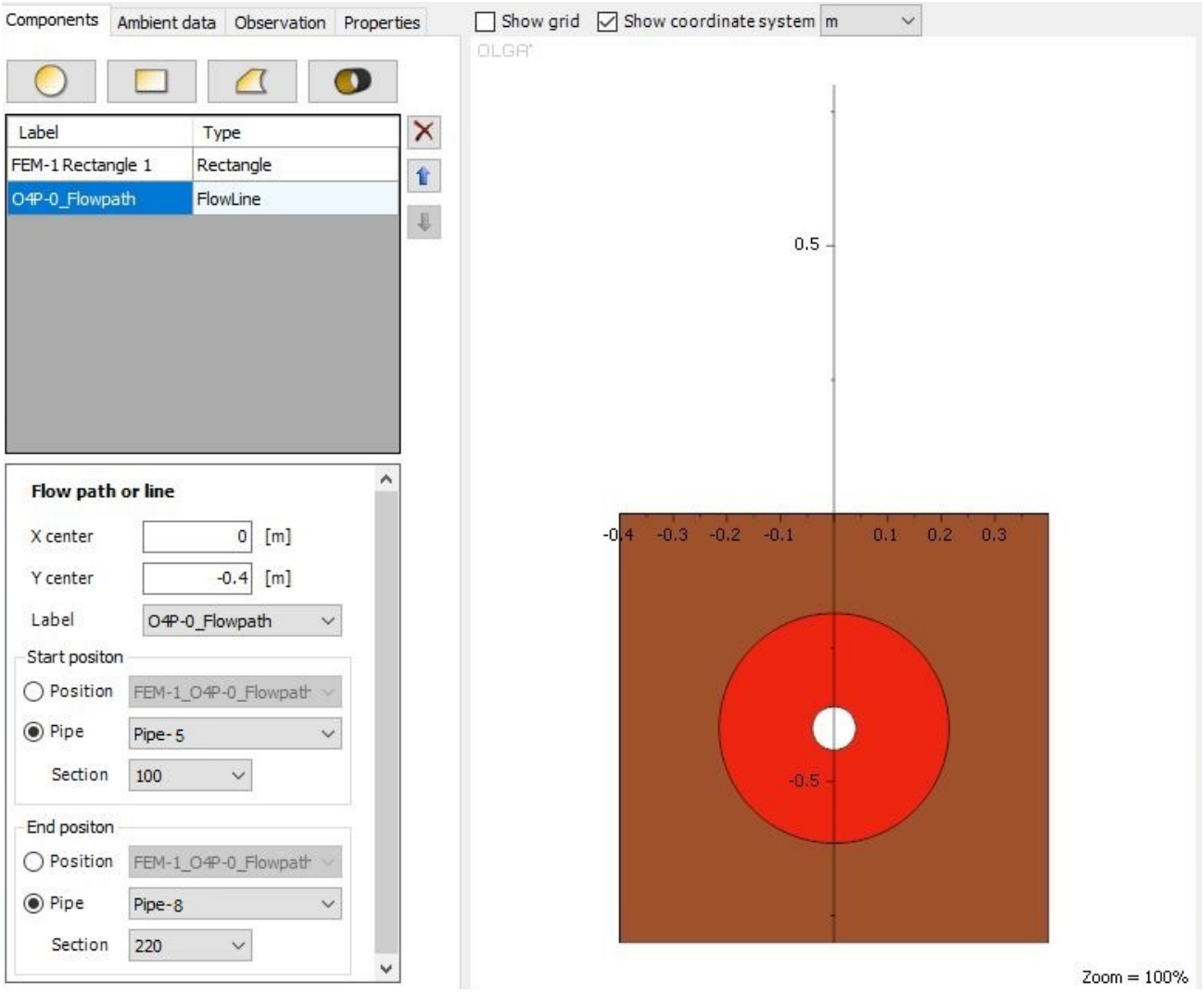

Figure 72: Set source data for the OLGA Schlumberger software package FEMTherm

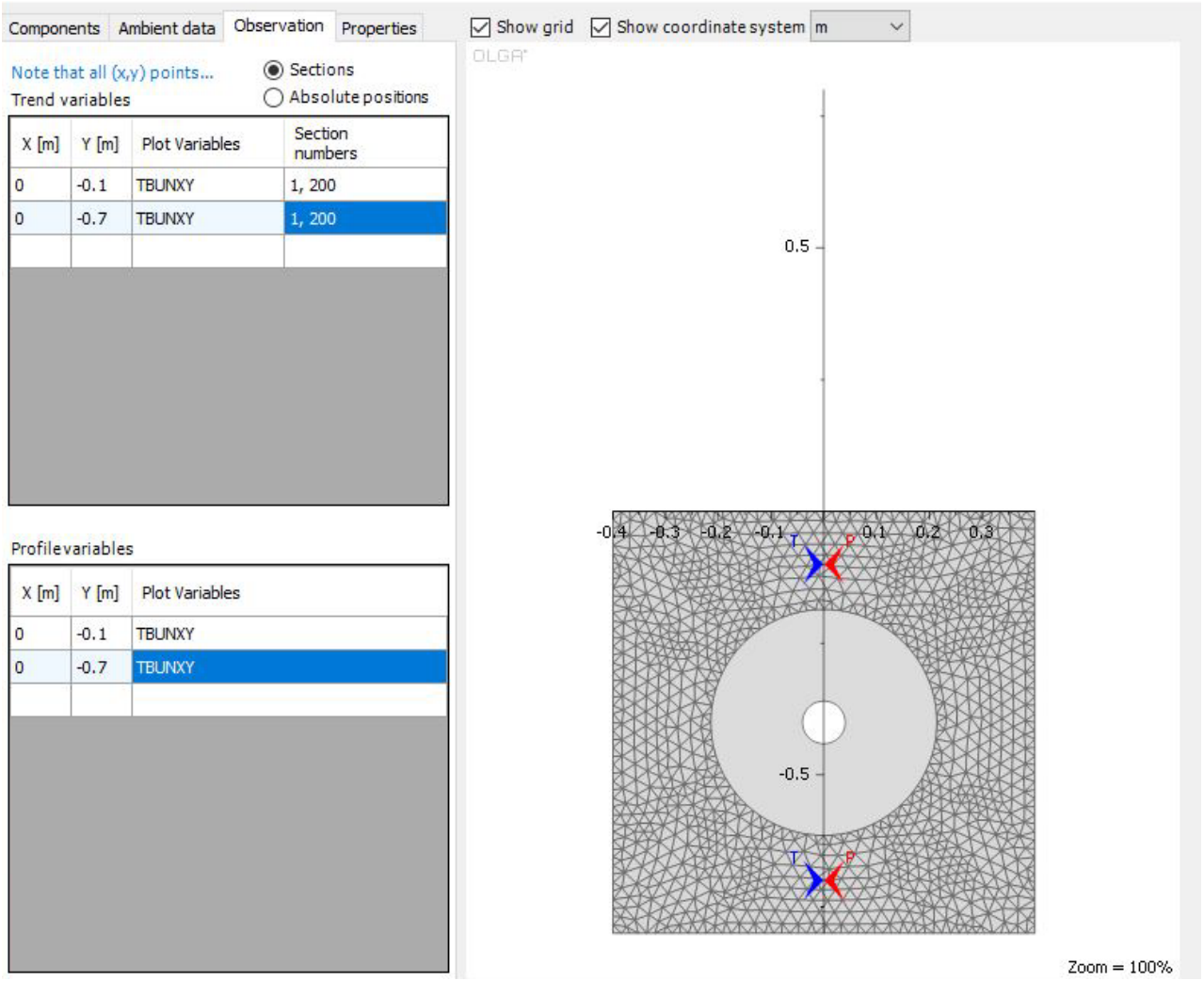

Figure 73: Creating Points for Trending and Profile Variables

The last step in the process of creating a file for further calculations is to create a grid that is generated for objects placed in a solid environment and designed to perform calculations in each specific grid "cell".

To complete the creation of the source file, the «Detailed Finite Element Results» function must be turned on and the resulting file in osi. format must be saved.

To display the results graphically through the OLGA command window, FEMThermViewer must be opened and a file with the desired extension must be selected. The results are shown in Figures 76-79, which show the temperature gradient over the length of the pipe over time.

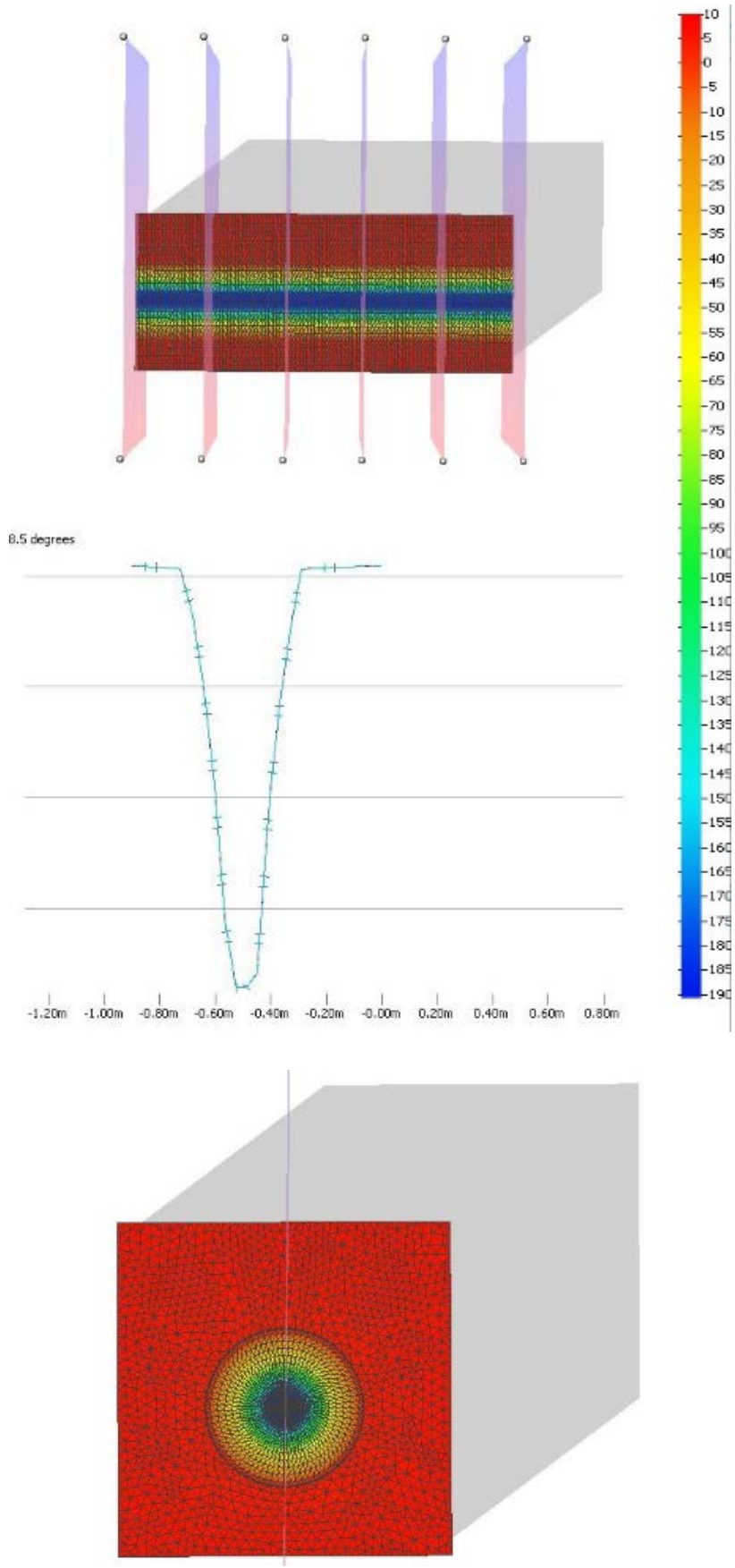

Figure 74: Initial Temperature Distribution (t=0 sec)

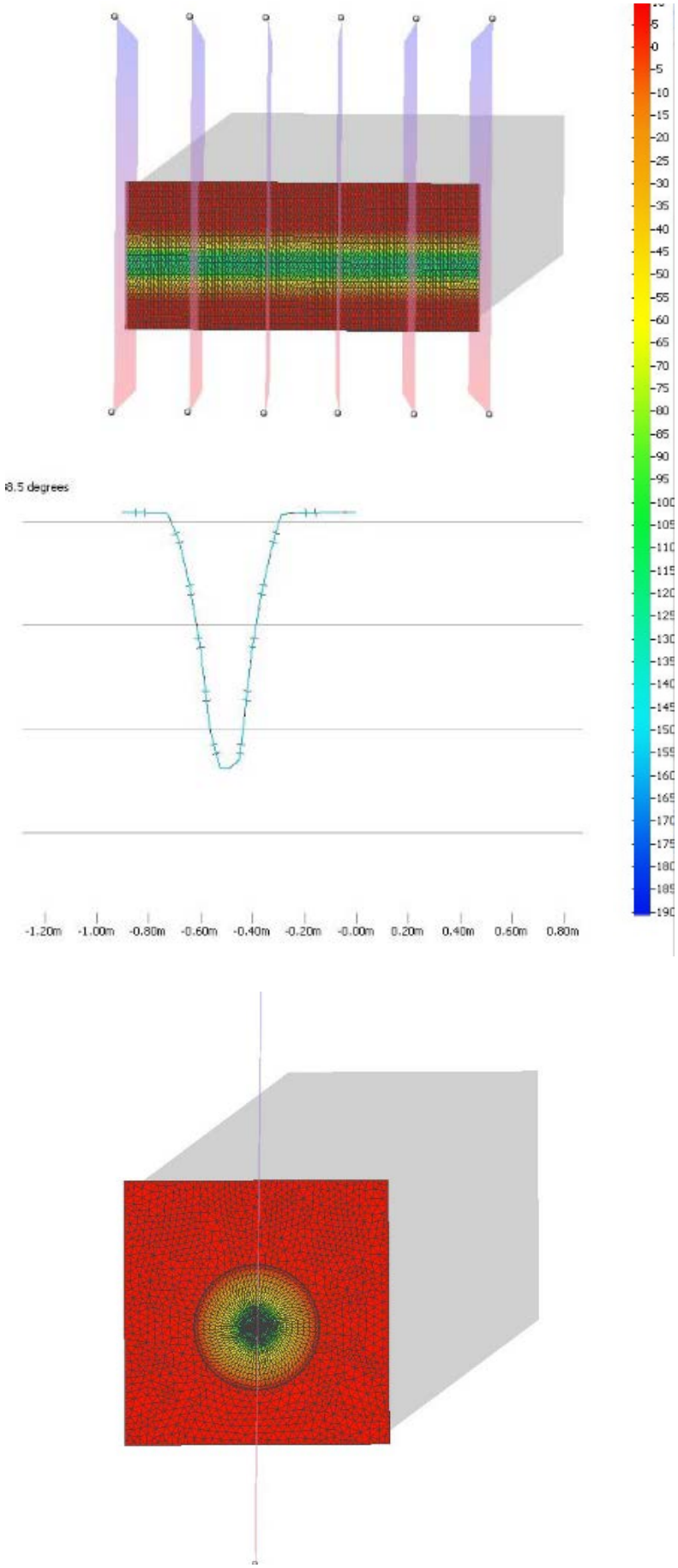

Figure 75: Temperature distribution at t=4 hour

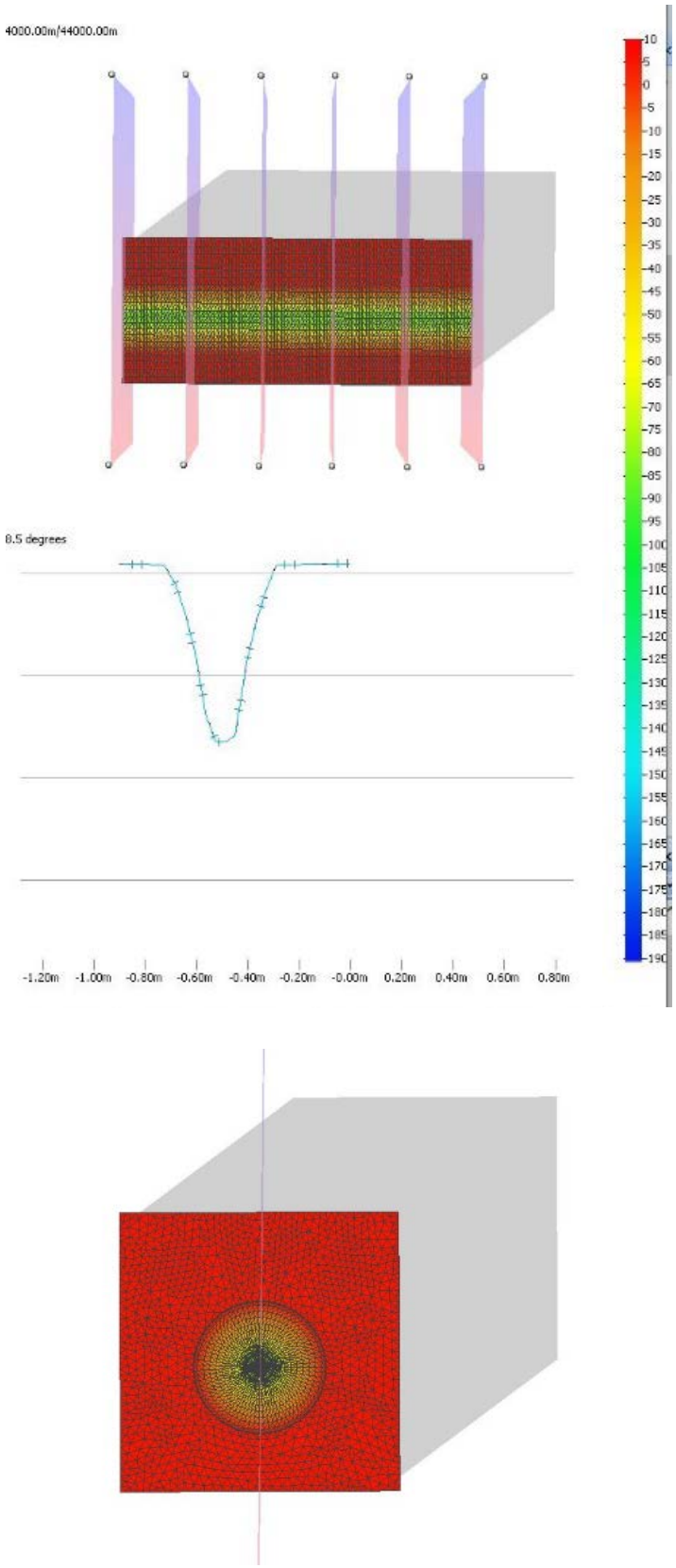

Figure 76: Temperature distribution after study time

By analyzing the temperature distribution graphs over time, it can be concluded that multilayer thermal insulation effectively insulates the cryogenic pipeline and does not cause any thermal effect on the surrounding soil.

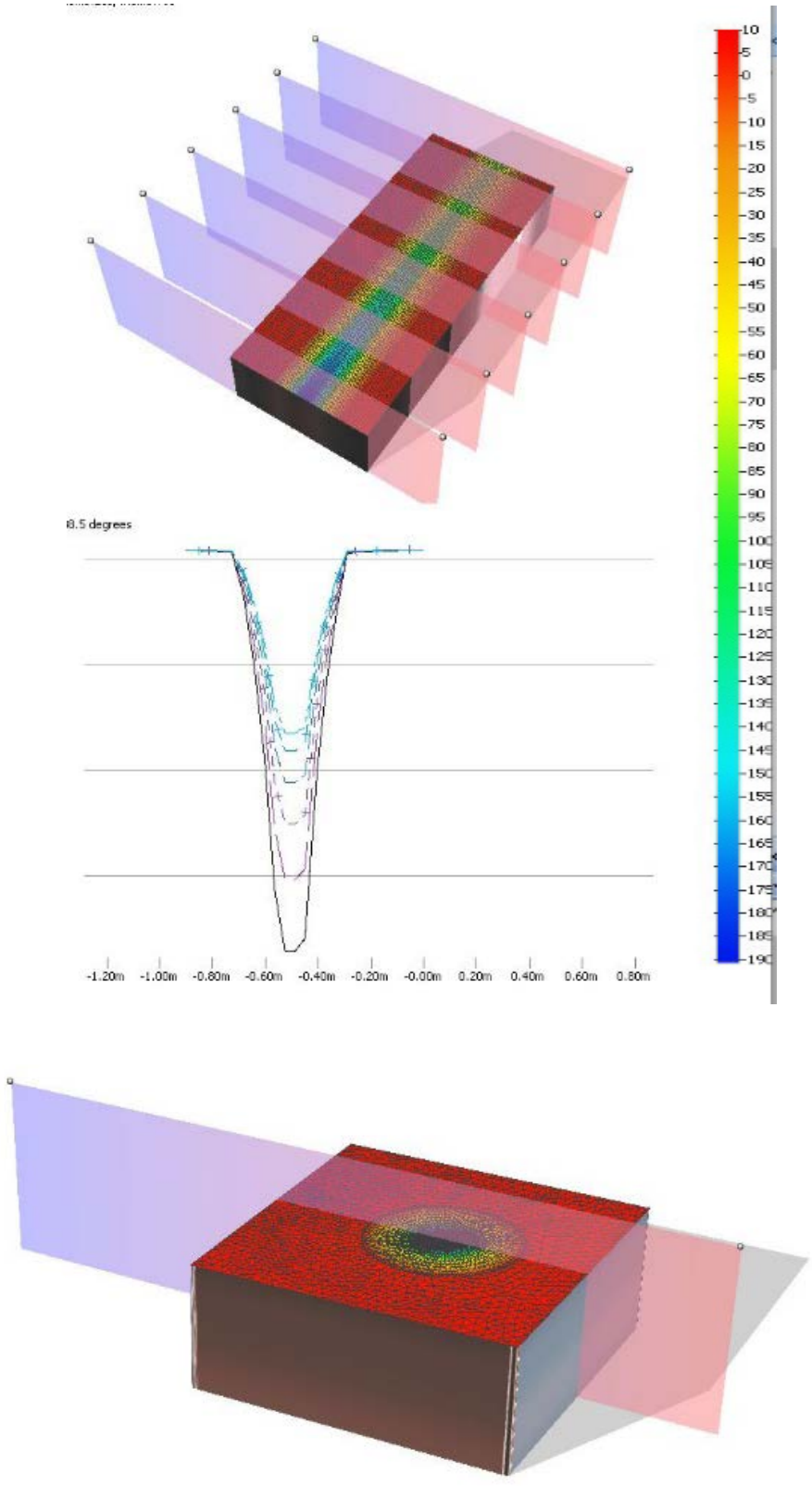

Figure 77: General distribution of temperature curves by pipeline depth in different sections

5.4 Practical Recommendations

Since at the moment there are no regulatory documents and methods for calculating the cryogenic pipeline, an analysis of the throughput capacity of several diameters at the calculated temperature and pressure parameters was carried out. The results were processed in Figures 80-83.

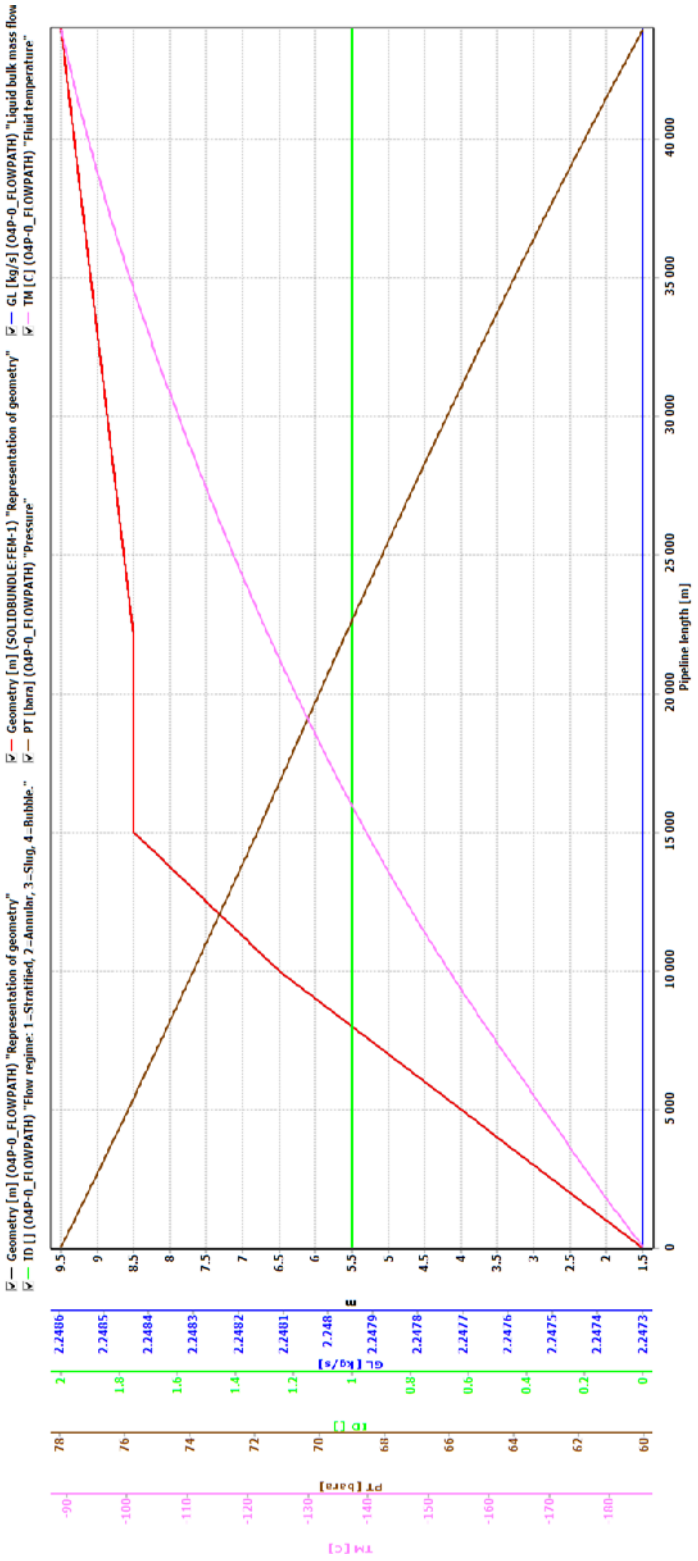

Figure 78: Maximum pipe capacity at outer diameter 140 mm

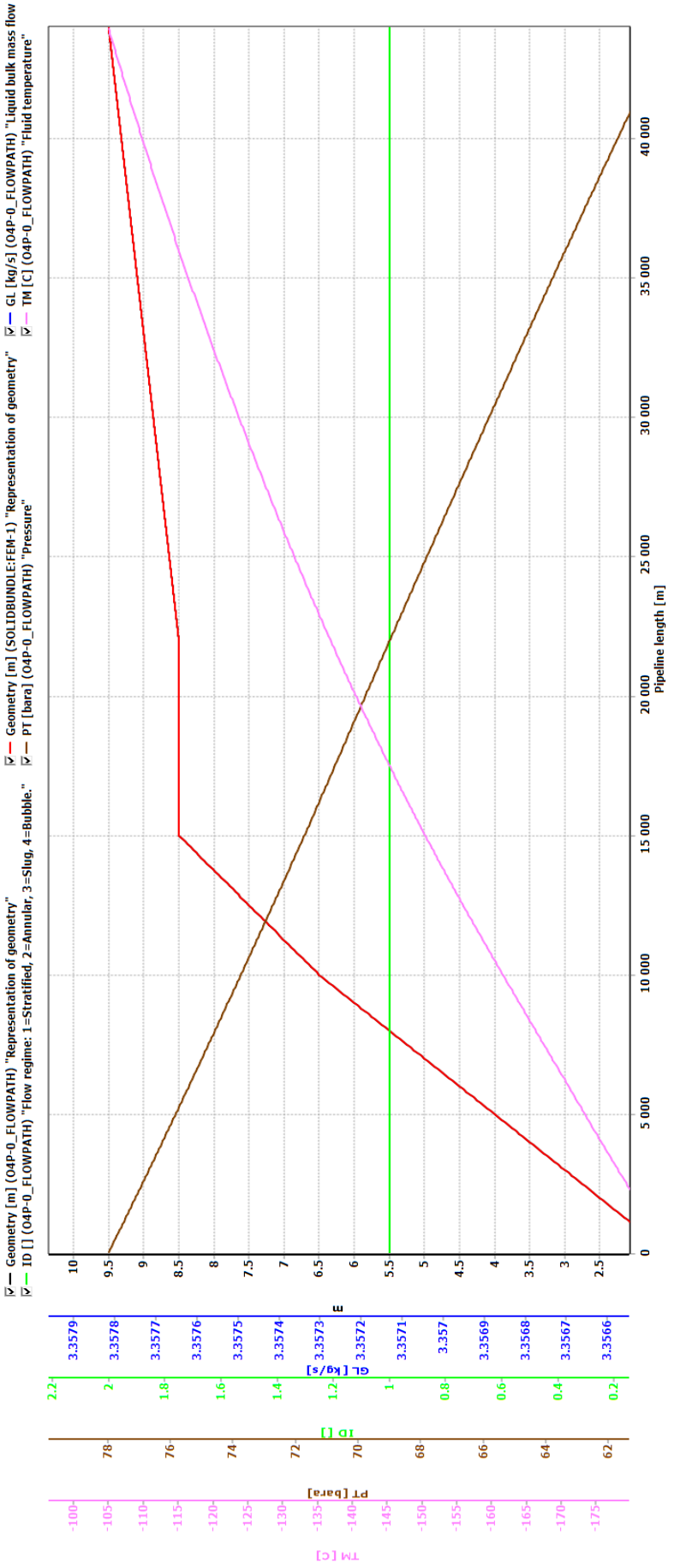

Figure 79: Maximum pipe capacity at outer diameter 114 mm

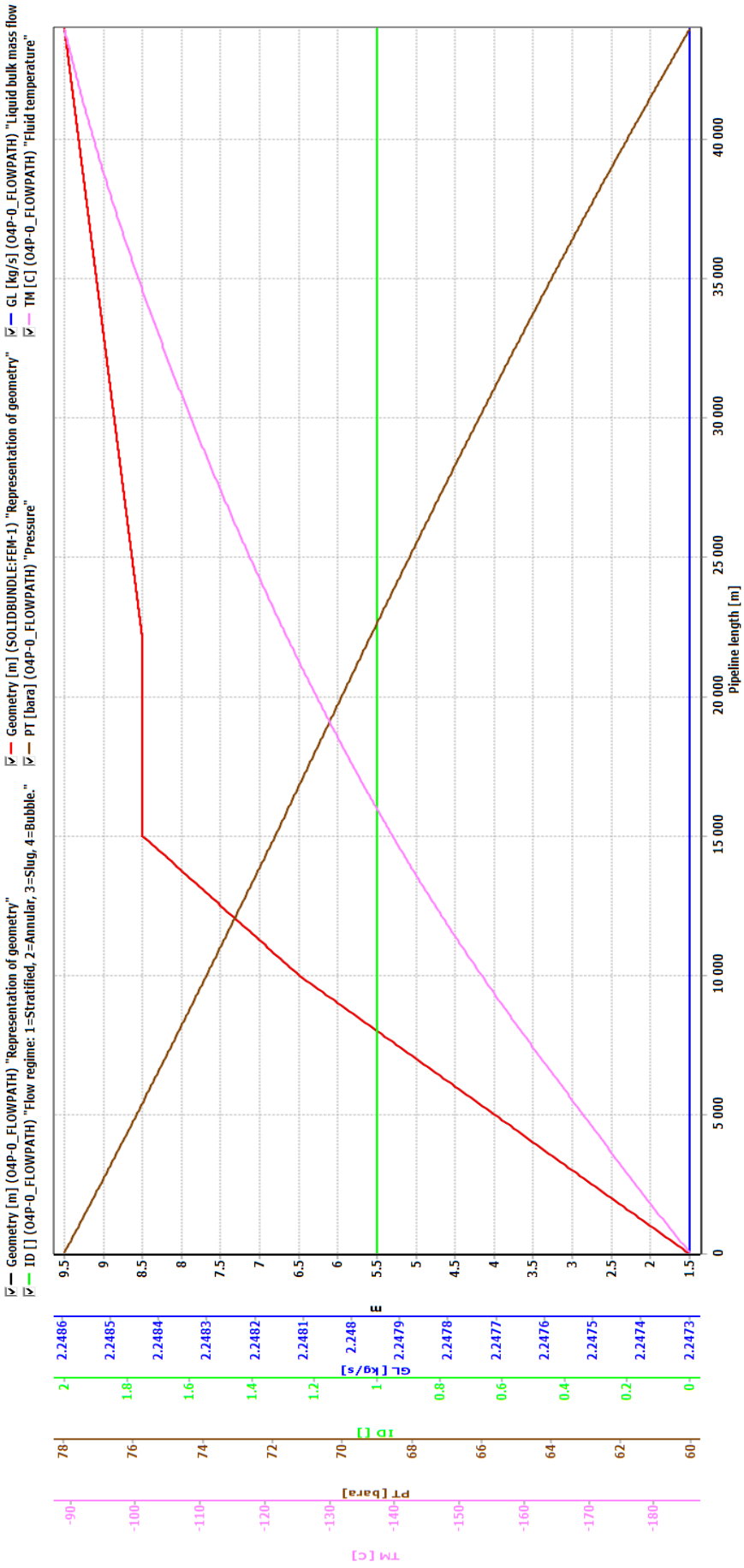

Figure 80: Maximum pipe capacity at outer diameter 101,4 mm

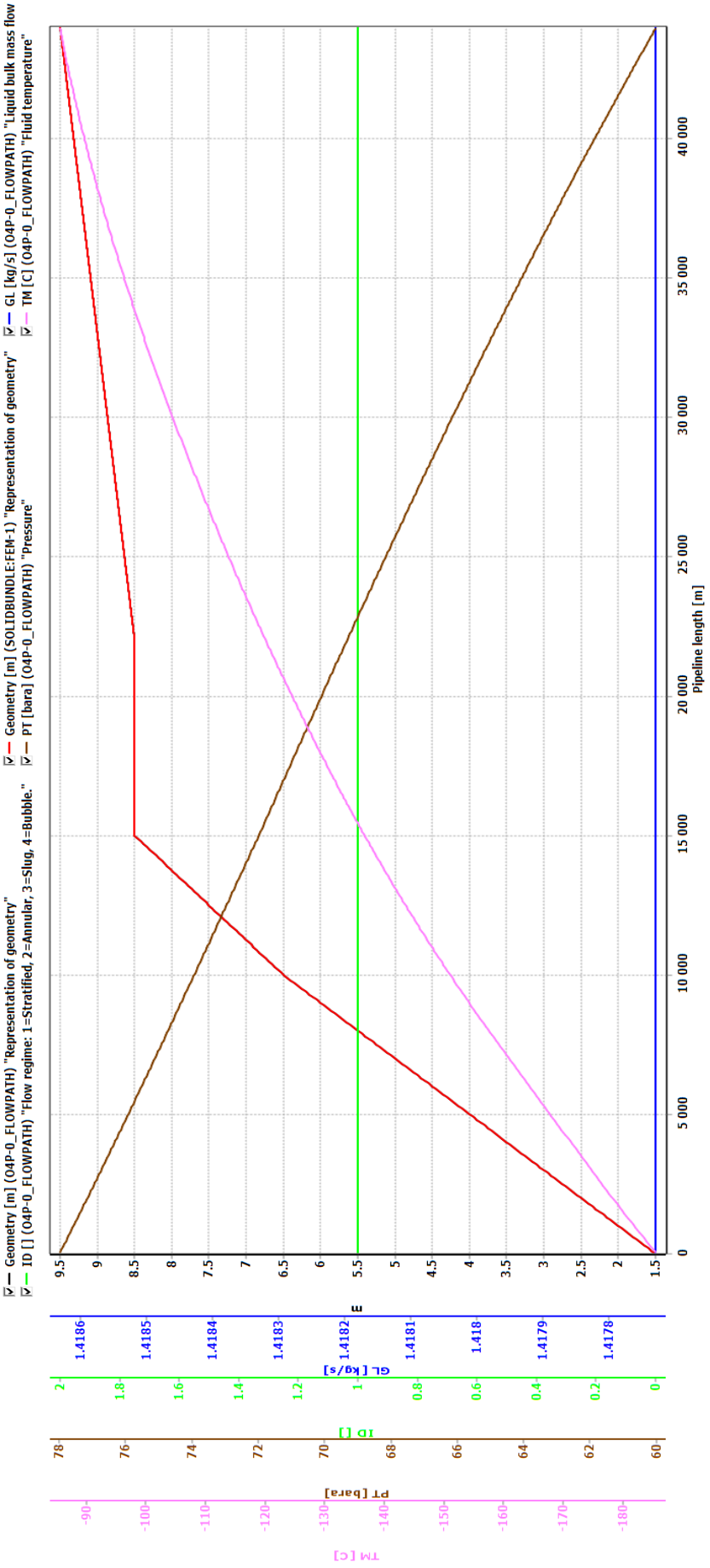

Figure 81: Maximum pipe capacity at outer diameter 88,5 mm

The maximum throughput for an outer diameter of 60 mm was also calculated. The calculation will allow us to have an idea of the choice of diameter depending on the production capacity and use the proposed methodology for calculating. The summary data is given in Table 14, with the values of internal diameter (with a selected wall thickness of 10 mm). Density data were taken from software calculations MultiFlash.

Table 14: Diameters for different volumes of natural gas transfer (can be used for lengths of sections 45 and close to this value, and pressure values close to P_1=7,8 MPa, P_2=6 MPa, ρ_{gas}=0,575486).

D_{in} (D_{out}), mm	Q_{OLGA}, kg/sec	Q`, kg/year	Q``, m^3/year	Q, m^3/year at standard conditions
40 (60)	0,588235	$17,6045 \cdot 10^6$	$30,5907 \cdot 10^6$	$8,00 \cdot 10^9$
55,5 (75,5)	0,956897	$30,1767 \cdot 10^6$	$52,4369 \cdot 10^6$	$13,72 \cdot 10^9$
68,5 (88,5)	1,417730	$44,7095 \cdot 10^6$	$77,6800 \cdot 10^6$	$20,32 \cdot 10^9$
81,3 (101,3)	2,247300	$70,8708 \cdot 10^6$	$123,1496 \cdot 10^6$	$32,21 \cdot 10^9$
94 (114)	3,356450	$105,8940 \cdot 10^6$	$183,9298 \cdot 10^6$	$48,11 \cdot 10^9$
120 (140)	6,456750	$203,6201 \cdot 10^6$	$353,82286 \cdot 10^6$	$92,72 \cdot 10^9$

6 Hydraulic calculation of gas pipeline

To formulate the resulting conclusions and carry out a detailed feasibility study of the project, it is necessary to carry out a hydraulic calculation of the gas pipeline with equal pumping volumes and length.

The pipeline diameter is determined based on pumping volumes and initial and final pressure parameters (P_1=7,48 MPa, P_2=5,1 MPa). For a given annual pumping volume, the outer diameter is proposed to be 1020 mm.

For the construction of the gas pipeline, a pipe made according to TU 14-3-1363-97 with steel grade 09GSF was accepted.

We define the value of the calculated metal resistance and wall thickness by the following formulas:

$$R_1 = \frac{R_1^n \cdot m}{k_1 \cdot k_n}, \quad \text{(Eq.55)}$$

$$\delta = \frac{n_p \cdot P_1 \cdot D_{out}}{2 \cdot (R_1 + n_p \cdot P_1)}, \quad \text{(Eq.56)}$$

Where R_1^n is the normative design resistance of the material (MPa) (R_1^n=588 MPa), m is the pipeline operating condition factor (m=0,9), k_1 is the metal reliability factor (k_1=1,34), k_n is the liability reliability factor (k_n=1,05), n_p is the internal pressure load reliability factor(n_p =1,1).

$$R_1 = \frac{588 \cdot 0,9}{1,34 \cdot 1,05} = 376,1 \text{ MPa},$$

$$\delta = \frac{1,1 \cdot 7,48 \cdot 1020}{2 \cdot (376,1 + 1,1 \cdot 7,48)} = 10,9 \text{ mm}$$

Accept standard pipe wall thickness δ=11 mm.

The inside diameter will be:

$$D_{in} = 1020 - 2 \cdot 11 = 998 \text{ mm},$$

Density, heat capacity, and viscosity of natural gas with 20% hydrogen content are accepted according to the program results MultiFlash:

$\rho = 0,5755 \text{ kg} / \text{m}^3, c_p = 2,499 \text{ kJ} / (\text{kg} \cdot \text{K}), \eta = 1,077 \cdot 10^{-5} \text{ Pa} \cdot \text{sec}.$

The molar mass of the mixture is determined by the formula:

$$M = \sum x_i \cdot M_i, \quad \text{(Eq.57)}$$

Gas constant, as well as pseudocritical temperature and pressure, are calculated by formulas:

$$R_{gas} = \frac{R_{un}}{M}, \quad \text{(Eq.58)}$$

$$T_{pc} = \sum x_i \cdot T_{pci} \quad \text{(Eq.59)}$$

$$P_{pc} = \sum x_i \cdot P_{pci} \quad \text{(Eq.60)}$$

Where x_i is the volume fraction of mixture components, T_{pci} is the pseudo critical temperature (K), P_{pci} is the pseudo critical pressure (MPa).

The relative density of gas through the air is equal to:

$$\rho_{\Delta} = \frac{\rho}{1{,}205}, \quad \text{(Eq.61)}$$

The daily capacity of the gas pipeline is calculated by the formula:

$$Q_{day} = \frac{Q}{365 \cdot 0{,}9}, \quad \text{(Eq.62)}$$

Then, by the method of successive approximations, it is necessary to find the values of the final pressure and temperature using the following algorithm. The coefficient of hydraulic resistance to friction is determined by Eq.29. The value of the average pressure in the linear section is determined by the following formula:

$$P_{avr} = \frac{2}{3} \cdot \left(P_1 + \frac{P_2}{P_1 + P_2} \right), \quad \text{(Eq.63)}$$

Pseudoreduced pressure and temperature are determined by formulas:

$$P_{pr} = \frac{P_{avr}}{P_{pc}}, \quad \text{(Eq.64)}$$

$$T_{pr} = \frac{T_{avr}}{T_{pc}}, \quad \text{(Eq.65)}$$

The compressibility factor of the gas is determined by the formula:

$$Z = 1 - A_1 \cdot P_{pr} + A_2 \cdot P_{pr}^2, \quad \text{(Eq.66)}$$

$$A_1 = -0,39 + \frac{2,03}{T_{pr}} - \frac{3,16}{T_{pr}^2} + \frac{1,09}{T_{pr}^3},$$

$$A_2 = 0,0423 - \frac{0,1812}{T_{pr}} + \frac{0,2124}{T_{pr}^2},$$

The average temperature is determined taking into account heat exchange with the environment and the Joule-Thomson coefficient. The Joule-Thomson coefficient is calculated as follows:

$$D_i = H_0 + H_1 \cdot P_{pr} + H_2 \cdot P_{pr}^2 + H_3 \cdot P_{pr}^3, \quad \text{(Eq.67)}$$

$$H_0 = 24,96 - 20,3 \cdot T_{pr} + 4,57 \cdot T_{pr}^2,$$

$$H_1 = 5,66 - \frac{19,92}{T_{pr}} + \frac{16,89}{T_{pr}^2},$$

$$H_2 = -4,11 + \frac{14,68}{T_{pr}} - \frac{13,39}{T_{pr}^2},$$

$$H_3 = 0,568 - \frac{2}{T_{pr}} + \frac{1,79}{T_{pr}^2},$$

Coefficient a_t is calculated by the formula:

$$a_t = \frac{K \cdot D_{in}}{L \cdot \rho_\Delta \cdot c_p \cdot 10^6}, \quad \text{(Eq.68)}$$

$$T_{avr} = T_{air} + \left(T_{gas} - T_{air}\right) \cdot \frac{1 - e^{-a_t \cdot L}}{a_t \cdot L} - D_i \cdot \frac{P_1^2 - P_2^2}{2 \cdot a_t \cdot L \cdot P_{avr}} \cdot \left[1 - \frac{1 - e^{-a_t \cdot L}}{a_t \cdot L}\right], \quad \text{(Eq.69)}$$

The final pressure is determined by the formula (Bykov et al., 2005):

$$P_{end} = \sqrt{P_1^2 - \frac{Q_{day}^2 \cdot \rho_\Delta \cdot \lambda \cdot Z \cdot T_{avr} \cdot L}{3,32 \cdot 10^{-6} \cdot D_{in}^5}}. \quad \text{(Eq.70)}$$

The results of successive approximations to determine the final parameters of the underground section of the gas pipeline are given in Table 11. The final temperature in this area is $T_{end} = 8,715\,^{o}C$.

Table 15:Results of hydraulic calculation of gas pipeline in the second linear section

	2nd and 3rd section of the gas pipeline (64 km) – underground	
	First approximation	Second approximation
Final pressure P_{end}, MPa	6,5086	6,709
Average pressure P_{avr}, MPa	6,969	7,065
Pseudoreduced temperature T_{pr}, K	1,758	1,77
Pseudoreduced pressure P_{pr}, MPa	1,723	1,747
Joule-Thomson coefficient D_i, K/MPa	2,816	2,766
a_t, km^{-1}	0,004277	0,004
Average temperature T_{avr}, K	290,66	290,94
Average compressibility factor Z	0,928	0,927
Reynolds number Re	27619280	28616270
Hydraulic resistance coefficient λ	0,010822	0,0108
Final pressure P_{end}, MPa	6,7091	6,7108
Relative pressure error	3%	-0,027%

The calculation of the underwater areas was carried out in the OLGA Schlumberger program, the results of which are given in Figures 46. The initial temperature in the area is 20°C, the final 7,581°C. The initial pressure in the gas pipeline is 7,3 MPa, final 6 MPa.

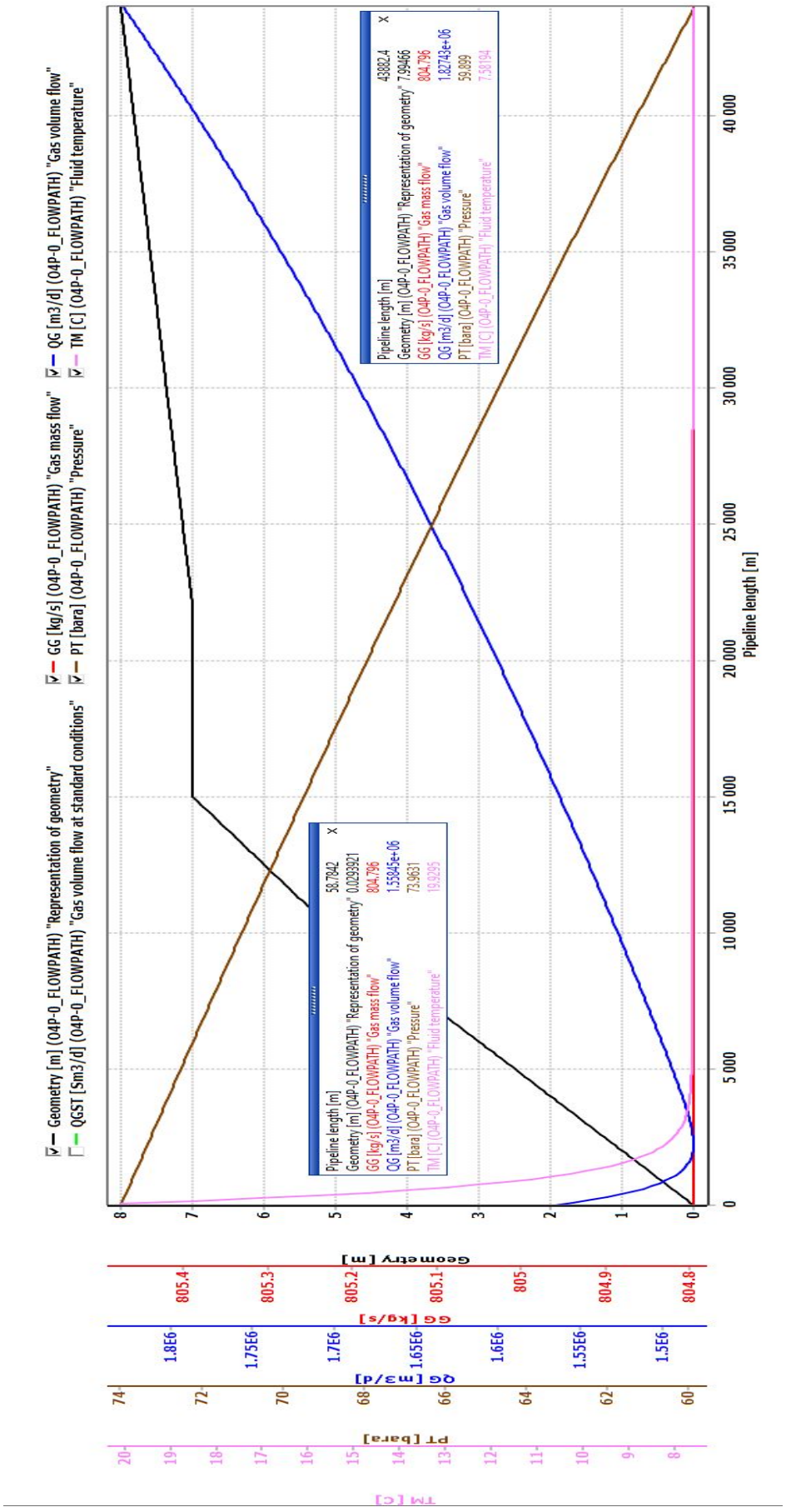

Figure 82: Hydraulic calculation of the 1st section of gas pipeline

7 LNG transport industry outlook

Since there is no accurate data for estimating total economic costs, the feasibility study will be based on the aggregated parameters, the main purpose of which will be to clearly show the percentage of costs for the construction of a gas pipeline and a cryogenic pipeline.

The following assumptions will be accepted: cooling costs are not taken into account, since it is possible to provide cooling at production facilities. Possible prospects for power generation will be given below. Also, the costs for construction of site facilities are assumed to be the same, since for the LNG pipeline, and for the gas pipeline, the same number of compressor (pump) stations is provided.

First, the metal capacity of the pipes shall be calculated according to the following formula:

$$B = \rho_{material} \cdot \pi \cdot D \cdot L \cdot \delta_{wall}, \quad \text{(Eq.71)}$$

Where $\rho_{material}$ is the metal density, kg/m^3.

$$B_{cryogenic} = 7920 \cdot 0,0755 \cdot \pi \cdot 159000 \cdot 0,01 = 2986889\ kg \approx 3000\ tons,$$

$$B_{gas\ pipeline} = 7850 \cdot 1,22 \cdot \pi \cdot (45000 \cdot 0,025 + 64000 \cdot 0,011 + 49000 \cdot 0,025) = 76822550\ kg = 76823\ tons$$

The metal capacity ratio is 25.61. This means that for the construction of a cryogenic pipeline, it is necessary to spend 25.61 times less material.

The ratio of gas pipeline diameters to LNG pipeline is:

$$\Delta = \frac{D_{gas\ pipeline}}{D_{cryogenic}} = \frac{1020}{75,5} = 13,51 \quad \text{(Eq.72)}$$

Total costs consist of capital costs (for cryogenic pipeline: cost of the pipeline and thermal insulation, for gas pipeline: pipe costs) and construction and installation works, which in turn include costs for logistics (30%), installation (30%), and land works (40%).

The capital costs for the construction of a cryogenic pipeline with a diameter of 75.5 mm with a wall thickness of 10 mm and a section length of 159 km will be calculated.

The cost of 1 ton of steel 12Ch18N10T the required diameter is 505000 rubles. (at the exchange rate of the Bank of Russia 1 USD=75,0893 RUB). Therefore, the cost of purchasing the material will be:

$$E_1^1 = 505000 \cdot 3000 = 1515\ \text{mln. rub.} = 20,17598\ \text{mln.\$} = 16,746\ \text{mln.}\ €$$

Thermal insulation costs will be calculated at the cost of Cryogel Z material, which, per 1 m^2 of material is 5227 rub.

The total area of thermal insulation is:

$$S = S_1 + S_2 + S_3 + S_4; \quad \text{(Eq.73)}$$

Where S_1, S_2, S_3, S_4 is the thermal insulation area in the 1st, 2nd, 3rd, and 4th section of the pipeline respectively (m).

$$S_1 = S_{out} - S_{in}, \quad \text{(Eq.74)}$$

Where S_{out}, S_{in} is the external and internal area according to the isolation thickness (m^2).

$$S_1 = \frac{\pi}{4} \cdot \left(0,0755 + 2 \cdot 0,025\right)^2 \cdot 45000 - \frac{\pi}{4} \cdot 0,0755^2 \cdot 45000 = 355,196\ m^2,$$

$$S_2 = S_3 = \frac{\pi}{4} \cdot (0,0755 + 2 \cdot 0,02)^2 \cdot 32000 - \frac{\pi}{4} \cdot 0,0755^2 \cdot 32000 = 192,014\ m^2,$$

$$S_2 = \frac{\pi}{4} \cdot \left(0,0755 + 2 \cdot 0,025\right)^2 \cdot 49000 - \frac{\pi}{4} \cdot 0,0755^2 \cdot 49000 = 386,769\ m^2,$$

$$S = 355,196 + 192,014 + 192,014 + 386,769 = 1125,993\ m^2,$$

$$E_1^2 = 1125,993 \cdot 5227 = 5,8856 \text{ mln. rub.} = 78381\$ = 65031€$$

Thus, the total capital cost for the construction of the cryogenic pipeline will be:

$$E_1 = 1515 + 5,8856 = 1520,8856 \text{ mln.rub.} = 20,0255 \text{ mln. \$.} = 16,622 \text{ mln.€}$$

Then, there is a calculation of the capital costs that need to be laid during the construction of the gas pipeline of the same length and volume of pumping. Thus, taking the cost of 1 ton of metal 09GSF equal to 87900 rub. for a wall, 11 mm thick, and 94700 for a wall 25 mm. Since the calculation is based on metal consumption, we take the average value of the cost equal to 91300 rub.

$$E_2 = 91300 \cdot 76823 = 7014 \text{ mln.rub.} = 93,42 \text{ mln. \$} = 77,54 \text{ mln.€}$$

To find the costs of construction and installation work during the construction of a cryogenic LNG pipeline, the task will be solved "bottom-up." As the basic cost of installation and construction works we will accept gas pipeline ICW. According to the accumulated practical experience, further calculations are carried out with the assumption that the cost of construction and installation work during the construction of the gas pipeline is approximately equal to capital costs. The ICW value for the LNG pipeline will then be refined by the found diameter ratio of 13.51 (to clarify the cost of land work) and the metal consumption of 25,61 (to clarify installation and logistics costs). For clarity, cost allocation is given in Table 16.

Table 16: Cost allocation

Cryogenic pipeline	Capital costs E_1 (50%) = 1520,8856 mln.rub.	
	ICW Y_1	Logistics $Y_{1.1}$
		Installation $Y_{1.2}$
		Land works $Y_{1.3}$
Gas pipeline	Capital costs E_2 (50%) = 7014 mln.rub.	
	ICW (50%) Y_2= 7014 mln.rub.	Logistics $Y_{2.1}$ (30%) = 2104,2 mln.rub
		Installation $Y_{2.2}$ (30%) = 2104,2 mln.rub.
		Land works $Y_{2.3}$ (40%) = 2805,6 mln.rub.

Logistics and installation costs will be:

$$Y_{1.1} = Y_{1.2} = \frac{2104,2}{25,61} = 82,163 \text{ mln. rub.} = 1,094 \text{ mln.\$=0,9083 mln.€}$$

The cost of land works will be:

$$Y_{1.3} = \frac{2805,6}{13,51} = 207,67 \text{ mln.rub=2,77 mln.\$=2,3 mln.€}$$

Total construction and installation costs for the construction of the cryogenic pipeline will be:

$$Y_1 = 82,163 + 82,163 + 207,67 = 372 \text{ mln.rub=4,95 mln.\$=4,112 mln.€}$$

And the total cost of building a cryogenic pipeline will be:

$$P_{R,E} = 1520,8856 + 372 = 1892,8856 \text{ mln.rub.} = 25,21 \text{ mln.\$=20,924 mln.€}$$

A more accurate calculation cannot be made at the moment, since the final cost will be influenced by inflation, which greatly increases the cost of imported equipment and the political situation (sanctions, etc.).

According to the calculations, it can be concluded that the design of a cryogenic pipeline is possible and technically feasible. Their effectiveness has been proven. However, since the economic calculation does not cover cooling and injection issues, an option will be considered to obtain electricity from a superconducting cryogenic cable that could supply both production needs and cooling and injection stations. Alternative energy sources are not considered as they are not capable of providing the required capacity on an industrial scale. The use of a superconductor also can be used for hydrogen production processes in the framework of

decarbonization projects. Currently, the production of hydrogen is possible in two ways: by burning natural gas or electricity obtained from gas combustion, or using alternative energy sources, it is proposed to consider using the effect of superconductivity, at which the electrical resistance will be zero when the cable reaches a certain temperature.

High-temperature DC superconductor (HTS) technologies reveal the full potential of useful action with a transmission line length of more than 100 km. The most common design includes a cryogenic cable installed inside the pipe through which the cryogenic liquid flows (for example, LNG, liquid nitrogen, etc.). The heat that the cable generates passes through the thermal insulation and heats the coolant (LN2). The diagram of the simplest superconductor transmission line is shown in Figure 84.

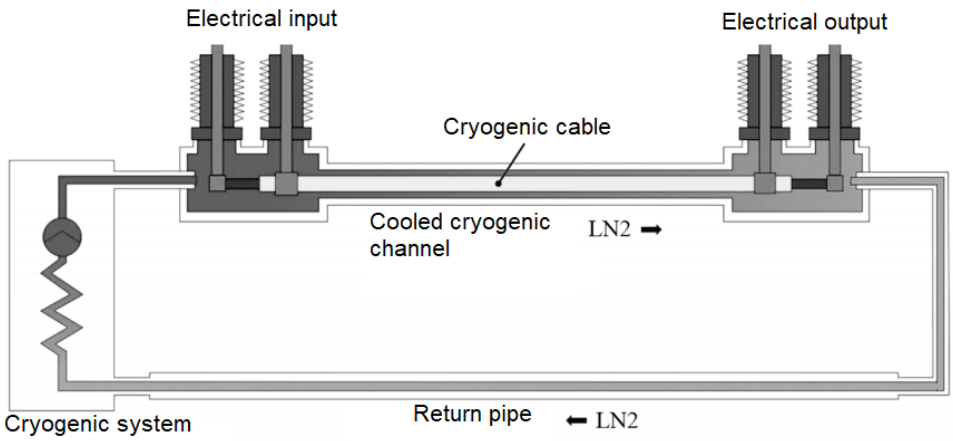

Figure 83: Diagram of the simplest transmission line with superconducting cable (Thomas et al., 2016)

The potential of using this technology as part of improving the transportation of LNG through cryogenic pipelines is huge since by supplying Japan with natural gas, Russia would receive electricity that would supply both retaining pumping stations, additional cooling stations, and electrolysis plants, the operation of which directly depends on electricity.

Figure 85 shows the configuration of cryogenic pipes. Since LNG temperatures are too high to maintain the superconductivity effect in the cable, it is proposed to use liquefied natural gas as cooling of the protective radiation shield. The need to use a radiation shield is caused by a decrease in the temperature gradient along the pipe, which creates favorable operating conditions. A similar experience has already been tested in Ishikari, Japan. More often, the superconducting cable is made of MgB_2.

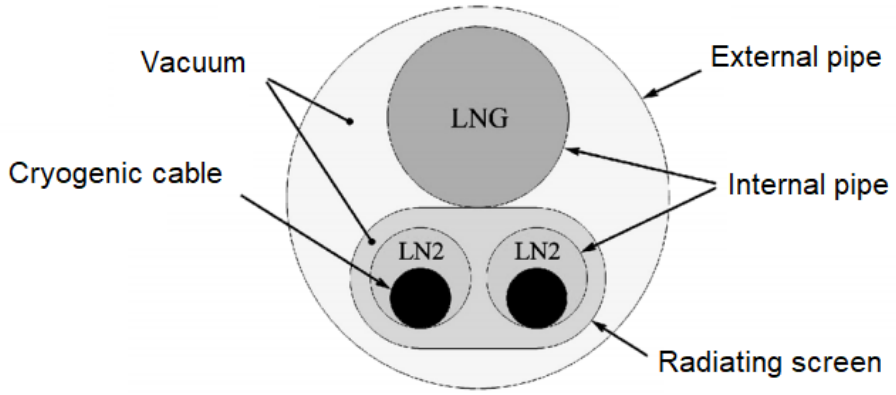

Figure 84: Configuration of HTS cable cooled by LN2 (LNG) with radiation shield (Yamaguchi et al., 2015)

Radiation protection can reduce heat losses, but is not able to completely solve the problem associated with cooling long superconducting cables. A large length requires a large amount of LNG transfer to cool the radiation shield. In addition to everything, the hydraulic resistance of cryogenic channels leads to high energy costs for pumping. Several methods of reducing hydraulic resistance are proposed:

- Modification of pipe surface properties;
- Change of pumped fluid properties.

The main effect is achieved by adding anti-turbulent additives that laminate the flow. To change the properties of the cryogenic liquid, the possibility of reducing the hydraulic resistance in the flows of the cryogenic shuga (mixture of crystals with the liquid phase) is considered.

8 Results

The results of this work are as follows. Firstly, analysis of existing literature shows that the LNG industry is well developed, however, existing product delivery methods can be improved. In situations where the laying of a gas pipeline is impractical due to difficult climatic or political conditions, and the delivery of LNG is too expensive due to huge distances, the possibility of using a cryogenic pipeline, the diameter of which will be several times smaller, is considered. Analyzing the existing literature, it can be seen that there are already ready-made technical solutions for the construction of pipelines and thermal insulation, in some countries, there is already experienced in the operation of small areas transporting liquefied hydrocarbons. However, an important aspect that slows down the development of this industry is the lack of a regulatory framework on which design can be carried out and which would fully cover the issues of safe operation and labor protection.

Chapter 3 set the goals and objectives of the project: to provide Japan with natural gas (LNG) directly from the liquefaction plant built as part of the Sakhalin-2 LNG «Prigorodnoye» project with a nominal capacity of 11.6 mln.tons/year, to the territory of Japan through a cryogenic pipeline with a total length of 159 km.

The main goal in Chapter 4 was to conduct a study on the influence of hydrogen on the physicochemical properties of natural gas (density, heat capacity, critical parameters), combustion parameters, and hydrate formation. As a result, the following results were formulated: the addition of hydrogen leads to a decrease in gas density by 15% and an increase in thermal conductivity and heat capacity by 18 and 13 percent, respectively, however, referring to existing studies in this field, the changes are not critical. It was also proved that hydrogen does not have a strong influence on the uniformity of combustion processes, since the Wobbe index calculated with the margin did not exceed the established regulatory standard. In addition, phase diagrams of hydrates were built to study the displacement of their curve, but the effect of introducing decarbonization on hydrate formation processes was not proven.

Chapter 5 was devoted to the hydraulic calculation of cryogenic pipeline and selection of thermal insulation based on aerogel for the above-ground area and multilayer thermal insulation for underground areas. With an outer diameter of 75.5 mm, the wall thickness was adopted 10 mm (to ensure safety). To maintain the liquefied state, the final pressure is 6 MPa. According to the calculation results, 20-25 mm aerogel or 100-120 mm multilayer thermal insulation is required to maintain single-phase flow. Also, for clarity, an analysis of the effectiveness of underground thermal insulation on the environment of the solid medium for heat losses was carried out. Also, upon completion of the hydraulic calculation of the cryogenic pipeline, a table was formed according to which, knowing the flow rate of natural gas, it is possible to select the diameter of the corresponding cryogenic pipeline.

In Chapter 6, a hydraulic calculation of the gas pipeline was carried out, the diameter of which was 1020 mm with a wall thickness of 11 mm. The calculation of the underground section was

carried out based on the existing calculation method, and, at an initial product temperature of 20°C and a pressure of 7.48 MPa, the final parameters will be 6.7 MPa and a temperature of 8.7°C. The calculation of the underwater area was carried out in the software complex from Schlumberger OLGA and at the same initial parameters, the final ones were 6 MPa and 7.58°C.

In the last chapter, economic indicators were calculated according to the enlarged methodology. It can be seen that the capital costs of an aerogel-insulated cryogenic pipeline (it was accepted to calculate the cost since there will be a representation of the maximum possible costs) are 78% less, and the calculated costs for construction and installation work, which were calculated from the ratio of metal capacities and diameters, are only 6% of the costs for construction and installation work during the construction of the gas pipeline. It should be borne in mind that the final economic effect will be significantly lower since the costs of intermediate cooling and pumping stations were not taken into account in the framework of this work, however, a scheme is proposed that will allow obtaining low-cost electricity - a superconductor. Exporting LNG to Japan through cryogenic pipelines, electricity will go backward, feeding additional cooling stations, retaining stations, as well as providing energy to electrolysis plants to produce hydrogen.

9 Conclusion

Even though the design of LNG pipelines causes a lot of debate about the rationality of its use, the industry does not stand still and every year, along with the growing needs of the world's population, it is increasingly difficult to export gas in the necessary amount. Many Asian countries, such as Japan, continue to burn coal and build new products on it, polluting the air, due to the lack of blue fuel. Therefore, to partially meet Japan's needs in LNG, a cryogenic pipeline was proposed, and the calculations proved that despite the many difficulties encountered both at the commissioning stage and at the operation stage, this task is technically feasible. Pipeline LNG transport is possible, which is confirmed by the hydraulic calculations carried out in the software complexes, the licensor of which is Schlumberger. The main aspect of safe transfer is effective thermal insulation, which will prevent rapid phase transition processes and allow for the maintenance of the required transfer parameters.

Also, as part of the decarbonization project, it was proposed to add pure hydrogen to the composition of natural gas, which was also possible based on the calculations of physicochemical and pumping parameters.

Undoubtedly, since the cryogenic LNG industry is uncharted and thermal insulation materials are expensive and difficult to access, expanding world practice may require both improving the existing state of the additional cooling, power generation, and thermal insulation technology industries, and creating completely new ones.

Cryogenic LNG transport is an excellent alternative to existing transport methods when pumping distances are small (as discussed in this paper, for example) and volumes are impressive. In such cases, piping is expensive and impractical, as well as transporting LNG by sea.

One way or another, every year progress does not stand still and, perhaps, someday cryogenic LNG transport will become more accessible, and all ambiguities will be successfully resolved.

References

1. A Bureau Veritas Group Company. 2015. Executive Summary of Environmental impact assessment for Dahej Nagothane ethane pipeline.
2. Aksyutin, O., Ishkov, A., Romanov, K., Teterevlev, R., Hloptsev, V., Kazaryan, V., Stolyarevskiy, A. 2017. Potential of methane-hydrogen fuel in the conditions of transition to a low-carbon economy. Gas industry, vol.1, pp. 82-85.
3. Aleksandrov, A. 1968. Issues in transport and use of natural gas in liquefied state. Moscow VNIIGAS, p.42.
4. Alekseeva, A., Natsievskiy, S. 2002. World experience in the application of thermal insulation based on foamed pearlite. Capital Design, vol.8, pp.42-46.
5. Anoshkin, A., Pospelov, A., Yakushev, R. 2014. Features of deformation and destruction of combined polymer pipes at low temperatures. Bringer PNIPU Mechanics, vol.2, pp. 5-28.
6. Arabadjan, A. 2015. Analysis and forecasting of gas demand in Japan. Eastern analytics, vol. 4, pp.166-169.
7. ASME B31.3-2008. Process piping. ASME code for pressure piping, B31.
8. ASME B31.4-2016. Pipeline transportation systems for liquids and slurries, B.31.
9. Babashov, V., Varrik, N., Karaseva, T. 2019.Application of aerogels for the heat insulation materials. Woks of WIAM, vol. 78, pp. 32-42.
10. Baranov, A., Sokolova, E. 2018.Storage and transportation of cryogenic liquids. Saint-Petersburg, Cryogenic pumps, vol.4, pp. 23-29.
11. Bleyher, E. 1977. Pipeline transportation of liquefied natural gas. Moscow VNIIE Gasprom, p. 63.
12. Bleyher, E., Vladimirov, A., Goldzberg, V. 1974. Hydraulic and thermal pipeline calculation for super cooled liquefied natural gas. NTS Transportation and storage of oil products and hydrocarbon raw materials, vol.10, pp.13-16.
13. Blinov, V., Kalinin, G., Kostiva, M., Mushnikov, S., Popov, V., Kharkov, A. 2003. Effect of nitrogen on corrosion and corrosion-mechanical properties of steel with martensite nitrogen structure. Moscow, Metals, vol. 4, pp.84-92.
14. Brusilovskiy, A. 2002. Phase transformations during development oil and gas fields. Moscow, Graal, 575 pages.
15. BS EN 1473:2007. Installation and equipment for liquefied natural gas – design of offshore installations.
16. Bykov, L., Mustafin, F., Rafikov, S., Nechval, A. 2005. Typical calculations for the construction and repair of gas and oil pipelines. Saint-Petersburg: Nedra.
17. CSA Z 275-18. Liquefied natural gas (LNG) – Production, storage and handling.
18. Davidson, Y., Farquharson, Y. 1955. Gas mixing in long pipes, second edition. Chemical Engineering Science.
19. Deason, D. Six-mile cryogenic system offshore Brunei loading platform. 1976. Pipe line ind., vol.38, №3, pp. 55-57.
20. Dierk, F., Andreas, Z. 2005. Patent US5789075A. Aerogel composites, process for production the same and their use.

21. Gadinova, S., Ponomareva, T. 2015. Economic relations between Russia and Asian countries: development prospects. Regional economy in the context of modernity, vol.9, pp.133-139.
22. Gaponova, D. 2017. Opportunities to supply Russian domestic LNG market. Bulletin of the faculty of management SPBGEU, vol.1, iss.1, pp.483-486.
23. Golubeva, I., Bakanev, I. 2015. LNG plant of the “Sakhalin-2” project (“Sakhalin Energy Investment Company LTD”). Refining and petrochemistry, vol.6, pp. 27-37.
24. GOST 32388-2013. Technological pipelines. Norms and methods for calculating strength, vibration and seismic effects.
25. GOST 32569-2013. Technological pipelines steel. Requirements for the device and operation on explosive and chemically hazardous productions.
26. GOST 5542-2014. Combustible gases for industrial and commercial purposes.
27. GOST R 56021-2014. Combustible natural liquefied gas. Fuel for internal engines combustion and power plants.
28. GOST R 56352-2015. Oil and gas industry. Production, storage and pumping of liquefied natural gas. General safety requirements.
29. Grigoriev, S., Porembskiy, V., Fateev, V., Samsonov, R., Kozlov, S. 2008. Hydrogen production by electrolysis of water: current state, problems and prospects. Alternative fuel vehicles, vol.3, iss.3, pp. 62-69.
30. Gurevich, G., Brusilovskiy, A. 1984. Phase state calculation reference and properties of gas condensate mixtures. Moscow: Nedra, 264 pages.
31. Ivanov, L., Anohin, A. 2019. Comparison of thermal insulation systems for LNG pipelines. Presented at the Russian Scientific Conference of Innovative development of LNG technologies, Moscow, 20.
32. Ivantsov, O. 1976. Pipes for low-temperature gas pipelines. Moscow, NIPIESU oil-gas-construction, p.25.
33. Jaesoek, R. 2008. Patent US6068882A. Flexible aerogel superinsulation and its manufacture.
34. Jan Willem van Gelder. 2003. The financing of the Camisea project. A research paper prepared for Focus on Finance.
35. Kaganer, M., Semenova, R., Glebova, L. 1962. Expanded pearlite sand as thermal insulation material for low temperature machines. Moscow, VNIIKIMASH, p.45.
36. Kalamars, C., Efstathiou, A. 2013. Hydrogen production technologies: current state and future developments. Pap.Enegy, vol.4, pp.20-35.
37. Kippers, M., Laat, Y., Hermkens, R. 2012. A small step into a hydrogen future. Kiwa Gas Technology, vol.1, pp.28-36.
38. Kopko, V. 2002. Thermal insulation of heating systems, second edition. Minsk, Tehnoprint, 160 pages.
39. Korshak, A., Nechval, A. 2005 Pipeline transportation of oil, oil products and gas. Study guide for the additional professional system education, Ufa: DesignPoligrapfService, 516 pages.

40. Koshelev, A., Yerin, O., Dorosheva, Yu. 2019. Low-temperature thermal insulation of tanks for storage and transportation of cryogenic products. Energy efficiency and energy saving in modern production and society, vol.2, pp. 119-122.
41. Kozachenko, S. 2017. Economic benefits from construction of the power of Siberia gas pipeline. E-SCIO, vol.11, iss.14, pp.48-55.
42. Liang, B., Wu H., Zhang, Y., Zheng, A. 2015. Patent CN204512801U. Vacuum insulation pipe.
43. Lyudeke, H., Kore, B., Pauli, K. 2015. Surge: causes, analysis and prevention methods. Water supply and sanitation technology, vol.8, pp.62-69.
44. Makaryan, I., Sedov, I., Nikitin, A., Artyunov, V. 2020. Modern approaches to obtain hydrogen from hydrocarbon raw materials. Scientific journal of the Russian society, vol.1, iss.24, pp. 50-68.
45. McKinnon, C., Offredi, M., Ollier, P. 2005. Camisea onshore loading system – design and construction of LPG pipelines. Presented at the 28th Annual Onshore Pipeline Technology Conference, Amsterdam.
46. Mnushkin, I., Nikitin, S. Patent RF №2018125984. 2018. Cryogenic pipeline, bulletin №13.
47. Motigin, A. 2015. Multimillion-dollar benefit from the use of screen-vacuum insulation in LNG infrastructure equipment. Gasworld, vol. 2, pp. 24-25.
48. Nazarova, M., Voronov, V., 2017. Comparative analysis of gas transportation by pipeline in liquid and gas states. Edition Neftegas.RU, issue №10.
49. Nechval, M., Novoselov, V. 1965. Experimental mixing process research with sequential pumping of gases, fourth edition. Proceedings of universities. Oil and gas.
50. Nechval, M., Yablonskiy, V. 1964. Effective ratio mixing with sequential pumping liquids and gases. Transportation and storage of oil and oil products.
51. NFPA 59A. Standard for the production, storage, and handling of liquefied natural gas.
52. Nikolaev, A., Dokukin, V., Voronov, V. 2015. Analysis of existing design procedures pumping mode LPG natural gas pipeline. Notes of the Mining Institute, issue №199, pp.357-359.
53. Nikolaev, V., Ganaga, S. 2011. Possible scales and effect of using wind power stations for the liquid gas production in Russia. Oil and gas business, vol. 6, pp. 463-470.
54. Odishariya, G., Odishariya, O. 1980. Studying of unsteady temperature conditions of heat-insulated gas pipelines. AN Energy and transport, vol.6, p.163.
55. OST 26-04-1221-75. Cryogenic pipelines.
56. Pavlov, N., Schippl, K. 2008. Characteristics of flexible cryogenic pipeline for liquid cryogenic products. Technical gases, vol.4, pp. 24-26.
57. Peng, D. 1976. A new two-constant equation of state. Ind. End. Chem. Fundamen., vol.15, pp.59-64.
58. Permyakov, V., Shvets, V. 2017. Rapid Phase Transition as a Potential Threat in LNG Transportation. Oil and gas, vol.2, pp.111-118.
59. Polozov, A., Zhmakin, V. 2005. Overcoming the two-phase flow of transported liquefied natual gas through a pipeline. Bulletin of BSTU im. V.G.Shukhova, vol.12, pp.58-61.

60. Ponomareva, T., Vasileva, Yu., Peskova, D., Eremenko, B., Vavilova, N. 2017. Problems of collection, preparation and transportation of oil and oil products, vol.1, iss.107, pp. 161-175.
61. Preobrazhenskiy, N. 1975. Liquefied natural gases. Saint-Petersburg: Nedra, 279 pages.
62. Process passports of the main apparatus of the LNG plant of the Sakhalin-2 project. 2006.
63. Rachevskiy, B. 2009. Liquefied hydrocarbon gases. Moscow, Oil and Gas.
64. RD-75.180.00-KTN-198.09 “Unified technological calculations of obfects of main oil pipelines and oil products”.
65. Safety Guide “Recommendations on construction and safe operation of technological pipelines”.
66. Safonov, V. 1977. Research of transient heat and hydrodynamic process related to launch and operation of pipelines for transport of chilled and liquefied natural gas. VNIIGAS.
67. Saidal, G., Krasnovskiy, K., Kotusov, S., Vasilieva, I. 2013. Patent RF №2532476. Cryogenic pipeline.
68. Sangeeta, R., Mukund, R. 2002. Patent US5306555A. Aerogel matrix composites.
69. Sarkisov, S., Smelik, A., Vdovichev, A. 2019. Thermal insulation analysis of LNG isothermal tanks. Actual issues in military-scientific researches, vol.4, pp.149-157.
70. Semenova, I. 2010. Electrolytic hydrogen production. Physical and chemical regularities, modern state and development prospects. Energy saving and water treatment, vol.3, iss.65, p. 15-21.
71. Serov, E., Korolkov, B. 1972. Dynamics of steam generators, third edition. Moscow, Energiya.
72. Sharifullin, A., Kantukov, R. 2015. Analysis of explosion hazard of a gas pipeline blow. Gas industry, vol. 5, pp.34-36.
73. Solodova, N., Cherkasova, E., Salakhov, I., Tutubalina, V. 2017. Hydrogen-the energy carried and the reagent. The technology of its receipt. Energy problems, vol.19, iss.11-12, pp. 39-50.
74. SP 18.13330.2011. Master plans industrial enterprises. Updated edition of SNiP II-89-80*.
75. SP 36.13330-2016. Trunk pipelines.
76. SP 240.1311500. LNG storages.
77. SP 326.1311500. Low-tonnage LNG production and consumption facilities.
78. Stepanian, C., Gould, G., Begag, R. 2011. Patent US7078359B2. Aerogel composite with fibrous batting.
79. Stetsenko, A., Nedzelsky, S., Naumenko, V. 2019. The effect of hydrogen on the properties of natural gas and the metrological characteristics of its metering systems. Experiments acheivements, vol.6, pp.45-50.
80. Sufiyanov, R. 2016. Obtaining hydrogen by electrolysis. Science synergy, vol.1, pp. 13-19.
81. Suleymanov, V., Safonov, V. 2017. Justification of operating parameters of technological pipelines of LNG complexes, taking into account the requirements of industrial safety in the event of water hummer. News of gas science, vol.1, p.84-87.
82. Technological flow diagram of an LNG plant Sakhalin-2 project. 2006.
83. Technological regulations of the “Sulfinol” plant Sakhalin-2 project. 2006.

84. Thomas, H., Marian, A., Chernyakov, A., Stueckrad, S., Salmieri, D., Rubbia, C. 2016. Superconducting transmission lines – Sustainable electric energy transfer with higher public acceptance. Renew. Sustain. Energy Rev., vol.55, pp.59-72.
85. Tsvetkov, P., Pritulyak, D. 2018. Comparative estimation of the cost of transportation of liquefied natural gas and pipeline gas. The north and the market: formation of the economic order, vol.6, iss.62, pp.30-43.
86. Ugryumov, O., Yarullin, R., Vasyukov, S. 2018. Electrolytic hydrogen: developing the technology of its generation and the key trends in perfecting its electrolysis. Technological university bulletin, vol.4, iss.21, pp. 128-138.
87. Vladimirov, A. 1975. Investigation of some issues of heat and hydraulic calculations of liquefied natural gas pipelines. Moscow bulletin, vol.4, pp. 20-23.
88. VNTP 51-1-88. Departmental norms technological design of installations for the production and storage of liquefied natural gas, isothermal storage and gas filling stations.
89. Voronov, V., Martynenko, Ya. 2017.The comparative analysis of single-phase and two-phase regimes of natural gas transportation by pipeline systems. International research kournal, vol. 4, iss. 4, pp. 28-34.
90. Yamaguchi, S., Koshizuka, H., Hayashi, K., Sawamura, T. 2015. Concept and design of 500 meter and 1000 meter DC superconducting power cables in Ishokari, Japan. IEEE Trans. Appl. Supercond., vol.25, iss.3.
91. Zamolodchikov, D. 2016. Forecasting global temperature growth in the 21st century based on a simple statistical model. Computer research and modeling, vol.8, iss.2, pp.379-390.
92. Zhizin, S., Timohov, V. 2019. Economical and geological aspects of the “Nord Stream-2”. Baltic region, vol.11, iss.3, pp.25-42. doi: 10.5922/2079-8555-2019-3-2.
93. https://en.wikipedia.org/wiki/Camisea_Gas_Project, assessed 01.10.2020.
94. http://hydrogeneurope.eu/wp-content/uploads/2017/01/20170109-HYDROGEN-COUNCIL-Vision-document-FINAL-HR.pdf, assessed 06.01.2021.
95. https://madmem.ru/raznoe/preimushhestvo-prirodnogo-gaza-pered-drugimi-vidami-topliva-3-kakie-preimushhestva-po-sravneniyu-s-drugimi-vidami-topliva-imeet-prirodnyj-gaz-dlya-kakix-celej-ispolzuetsya-prirodnyj-gaz-v.html, assessed 25.09.2020.
96. https://neftegaz.ru/tech-library/ekologiya-pozharnaya-bezopasnost-tekhnika-bezopasnosti/521106-dekarbonizatsiya-ekonomiki-i-energeticheskikh-sistem/, assessed 05.12.2020.
97. http://newchemistry.ru/letter.php?n_id=7949&cat_id=5&page_id=2, assessed 20.12.2020.
98. https://nsk.pulscen.ru/products/truba_1020kh10_17g1su_l_11_7_m_gost_20295_85_truby_svarnyye_dlya_magistralnykh_66498485, assessed 04.04.2021.
99. https://p.dw.com/p/3OGcU, assessed 05.02.2021.
100. https://prom.ua/p589105071-cryogelz-tolschina.html, assessed 04.04.2021.
101. https://ru.qaz.wiki/wiki/Error_function, assessed 25.10.2020.
102. http://vch.ru/event/view.html?alias=novatek_hochet_postroit_spg-terminal_pod_murmanskom, assessed 25.09.2020.
103. http://yamallng.ru/, assessed 25.09.2020.

104. https://yandex.ru/maps/?l=sat%2Cskl&ll=142.316956%2C45.870919&z=8, assessed 01.02.2021.
105. https://www.aerogel.com/products-and-solutions/product-documents/, assessed 20.10.2020.
106. https://www.bp.com/content/dam/bp/business-sites/en/global/corporate/pdfs/energy-economics/statistical-review/bp-stats-review-2020-full-report.pdf, assessed 20.09.2020.
107. https://www.cbr.ru/, assessed 03.04.2021.
108. https://www.cummins.com/new-power, assessed 05.01.2021.
109. http://www.gazpromexport.ru/presscenter/news/2503/, assessed 05.02.2021.
110. https://www.hydro.com/en/, assessed 05.01.2021.
111. https://www.intellinews.com/gazprom-s-power-of-siberia-gas-pipeline-to-china-is-finished-157956/, assessed 24.09.2020.
112. https://www.kommersant.ru/doc/4405401, assessed 23.09.2020.
113. https://www.naturalgasworld.com/japan-future-uncertainty-but-potential-upside-lng-condensed-68811, assessed 10.01.2021.
114. https://www.offshore-mag.com/subsea/article/16759840/france-subsea-pipeline-passes-cryogenic-tests-for-lng-transfer, assessed 01.10.2020.
115. https://www.popmech.ru/made-in-russia/249842-kak-sozdat-aerogel-novosibirskie-eksperimenty/, assessed 10.10.2020.
116. https://www.rostechsteel-perm.ru/goods/82043340-truba_nerzhaveyushchaya_75kh8_stal_12kh18n10t_gost_9941_81, assessed 03.04.2021.
117. https://www.rubaltic.ru/news/26032020-handelsblatt-poslednee-slovo-v-borbe-za-severnyy-potok-2-ostalos-za-nemetskim-regulyatorom/, assessed 25.09.2020.
118. http://www.sakhalinenergy.ru/media/library/ru/environmental/impact_assessment/lng/Project_Documentation_LNG_Jetty.pdf, assessed 01.02.2021.
119. https://www.un.org/ru/climatechange/paris-agreement, assessed 01.12.2020.

List of Tables

List of Figures

Abbreviations

AMC	Adiabatic Methane Conversion
API	American Petroleum Institute
DMD	Dahej Manufacturing Division
FPT	Fast Phase Transition
HPC	Hard Polymer Coating
HTH	High Temperature Heat exchanger
HTS	High Temperature Superconductor
ICW	Installation and Construction Works
LNG	Liquefied Natural Gas
NMD	Nagothane Manufacturing Division
PC	Production Complex
PR	Peng-Robinson
PRA	Peng-Robinson Advanced
RK	Redlich-Kwong
SVTI	Screen-Vacuum Thermal Insulation
SCAP	Short-Cycle Adsorption Process
TES	Tetraethyl silicate

Nomenclature

A	Turbulent diffusion coefficient [m^2/sec]
a	Van-der-Waals coefficient [-]
a_t	Shukhov length coefficient [km^{-1}]
B	Metal consumption [tons]
C_A	Displaced gas concentration [m]
C_B	Displacement gas concentration [m]
C_{sound}	Sound velocity [m/sec]
c	Heat capacity [kJ/(kg·K)]
c_p	Isobaric heat capacity [kJ/(kg·K)]
D_i	Joule-Thomson coefficient [K/MPa]
D_{in}	Internal diameter [m]
D_{isol}	External diameter with isolation [m]
D_{out}	External diameter [m]
D_t	Diffusion coefficient [m^2/sec]
E	Capital costs [mln. €]
F	Area of free cross-section [m^2]
F_1	Cross-section of the coolant [m^2]
G_d	Displacement gas mass flow [kg/sec]
G_g	Mass flow rate of the injected gas [kg/sec]
G_1	Mass flow rate of coolant [kg/sec]
g	Acceleration gravity [m^2/sec]
h_{snow}	Snow thickness [m]
h_0	Reduced depth of the pipeline axis [m]
Δh	Friction head loss [m]
K	Heat transfer coefficient [W/(m^2·K)]
k_n	Liability reliability factor [-]
k_1	Metal reliability factor [-]
L	Pipeline length [m]
M	Mole weight [mole]
m	Pipeline operating condition factor [-]
Nu	Nusselt number [-]
n	Number of cells [num.]
n_p	Internal pressure load reliability [-]
P	Total costs [mln.€]
P_{avr}	Average pressure [MPa]
P_{cr}	Critical pressure [MPa]
P_{pc}	Pseudocritical pressure [MPa]
P_{pr}	Pseudo reduced pressure [-]
P_s	Suction pump pressure [MPa]
$P_{st.cond.}$	Pressure at normal conditions [MPa]

P_1 Initial pressure [MPa]
P_2 End pressure [MPa]
P(x) Pressure in x point from coordinate system[MPa]
Pr Diffusion Prandtl criterion [-]
Q_L Lower heating value [MJ/m^3]
Q_m Volume flow rate of the pumping product [m^3/sec]
R Thermal resistance [m^2·°C/W]
R_{gas} Gas constant [J/mol·K]
R_{un} Universal gas constant [J/mol·K]
R_1 Resistance of material [MPa]
R_1^n Normal designing resistance of material [MPa]
Re Reynolds number [-]
r Radial coordinate [m]
S Insulated area [m^2]
SG Specific gravity [-]
St Stanton criterion [-]
T Temperature of isothermal flow [K]
T_{cr} Critical fluid temperature [K]
T_{end} End temperature [K]
T_{in} Initial temperature [K]
T_{pc} Pseudocritical temperature [K]
T_{pr} Pseudo reduced temperature [K]
T_{soil} Soil temperature [K]
$T_{st.cond.}$ Temperature at standard conditions [K]
t_{avr} Average temperature [°C]
t_{wall} Pipeline wall temperature [°C]
U Correction for heating due to internal friction [-]
W_{index} Wobbe index [MJ/m^3]
W_1 Coolant flow velocity [MJ/m^3]
X Axial coordinate [m]
x_i Volume fractions of i-component [-]
Y Installation and construction works cost [mln.€]
Z Compressibility coefficient [-]
Шу Shukhov parameter [-]
Ф Integral of probability [-]

α_1 Internal heat transfer coefficient [W/(m^2·K)]
α_2 External heat transfer coefficient [W/(m^2·K)]
α_{air} Air heat transfer coefficient [W/(m^2·K)]
Δ_e Equivalent roughness [-]
δ Wall thickness [m]
δ_{is} Isolation thickness [m]

η_i Numerical coefficient [-]

$\bar{\nu}$ Average coefficient of kinematic viscosity [N·sec/m^2]

λ Thermal conductivity of gas [W/(m·K)]

λ_{is} Thermal conductivity of the isolation material [W/(m·K)]

λ_{metal} Thermal conductivity of the pipeline material [W/(m·K)]

λ_{snow} Thermal conductivity of snow [W/(m·K)]

λ_{soil} Thermal conductivity of soil [W/(m·K)]

$\tilde{\lambda}$ Coefficient of hydraulic resistance of friction [-]

ρ_g Injected gas density [kg/m^3]

ρ_l Coolant density [kg/m^3]

τ Flow resistance time [sec]

τ_0 Time of the pipeline filling [sec]

ϑ Average linear velocity [m/sec]

ω Pitzer factor [-].